



Transportation Pooled Fund Program



CRASH TESTING AND EVALUATION OF THE 12 FT PINNED F-SHAPE TEMPORARY BARRIER

by

Nauman M. Sheikh
Associate Transportation Researcher

Roger P. Bligh, P.E.
Research Engineer

and

Wanda L. Menges
Research Specialist

Contract No. T4541-AB
Report/Test No. 405160-3-1/2a
Date of Test: 09-19-2006/11-15-2008

Sponsored by
**Roadside Safety Research Program Pooled Fund
Study No. TPF-5(114)**

April 2008
(Revised 2012-09-04)

**TEXAS TRANSPORTATION INSTITUTE
THE TEXAS A&M UNIVERSITY SYSTEM
COLLEGE STATION, TEXAS 77843**

DISCLAIMER

The contents of this report reflect the views of the authors who are solely responsible for the facts and accuracy of the data, and the opinions, findings and conclusions presented herein. The contents do not necessarily reflect the official views or policies of the State of Alaska Department of Transportation and Public Facilities, California Department of Transportation, Louisiana Department of Transportation and Development, Minnesota Department of Transportation, Tennessee Department of Transportation, Texas Department of Transportation, Washington State Department of Transportation, the Federal Highway Administration, The Texas A&M University System, or Texas Transportation Institute. This report does not constitute a standard, specification, or regulation. In addition, the above listed agencies assume no liability for its contents or use thereof. The names of specific products or manufacturers listed herein does not imply endorsement of those products or manufacturers.

KEY WORDS

Temporary barriers, F-shape barriers, concrete median barriers, pinned barriers, anchored barriers, restrained barriers, crash testing, roadside safety

1. Report No.		2. Government Accession No.		3. Recipient's Catalog No.	
4. Title and Subtitle CRASH TESTING AND EVALUATION OF THE 12 FT PINNED F-SHAPE TEMPORARY BARRIER				5. Report Date April 2008 (rev 2012-09-04)	
				6. Performing Organization Code	
7. Author(s) Nauman M. Sheikh, Roger P. Bligh, and Wanda L. Menges				8. Performing Organization Report No. 405160-3-1	
9. Performing Organization Name and Address Texas Transportation Institute The Texas A&M University System College Station, Texas 77843-3135				10. Work Unit No. (TRAIS)	
				11. Contract or Grant No. T4541-AB (405160-0003)	
12. Sponsoring Agency Name and Address Washington State Department of Transportation Transportation Building, MS: 47372 Olympia, Washington, 98504-7372				13. Type of Report and Period Covered Test Report: February – September 2006	
				14. Sponsoring Agency Code	
15. Supplementary Notes Research Study Title: Anchored Temporary Concrete Barrier Systems for Limited Deflections Name of Contacting Representative: Dick Albin					
16. Abstract <p>During bridge replacement or repair operations, restrained temporary concrete barriers are often used to protect motorists from extreme drop-offs at the edge of bridge decks. There are a few restrained temporary concrete barrier designs that have been crash tested for this application. Among the existing designs, most require through the deck bolting, anchor bolts, or other restraining features. Such designs are usually difficult to install, inspect, and remove in the field. Furthermore, some of these designs result in significant damage to thin bridge decks.</p> <p>Under this project, a new restraining design that limits lateral deflections of F-shaped precast concrete barrier was developed through a program of finite element simulation analysis and full-scale vehicle crash testing. This design uses the pins to restrain the barriers in a manner that is easy to install, inspect, and remove. It also minimizes damage to bridge decks or concrete pavements and no through the deck bolting is required. The design uses steel pins which are simply dropped into inclined holes that pass through the toe of the barrier and continue a short depth into the bridge deck or concrete pavement underneath.</p> <p>The new F-shaped pinned-down barrier successfully passed <i>NCHRP Report 350</i> Test Level 3 requirements. The maximum permanent and dynamic barrier deflections measured in the crash test were 5.76 inches (483 mm) and 11.52 inches (293 mm), respectively.</p>					
17. Key Words Temporary barriers, F-shape barriers, concrete median barriers, pinned barriers, anchored barriers, restrained barriers, crash testing, roadside safety			18. Distribution Statement Copyrighted. Not to be copied or reprinted without consent from Sponsor.		
19. Security Classif.(of this report) Unclassified		20. Security Classif.(of this page) Unclassified		21. No. of Pages 118	22. Price

SI* (MODERN METRIC) CONVERSION FACTORS

APPROXIMATE CONVERSIONS TO SI UNITS

Symbol	When You Know	Multiply By	To Find	Symbol
LENGTH				
in	inches	25.4	millimeters	mm
ft	feet	0.305	meters	m
yd	yards	0.914	meters	m
mi	miles	1.61	kilometers	km
AREA				
in ²	square inches	645.2	square millimeters	mm ²
ft ²	square feet	0.093	square meters	m ²
yd ²	square yard	0.836	square meters	m ²
ac	acres	0.405	hectares	ha
mi ²	square miles	2.59	square kilometers	km ²
VOLUME				
fl oz	fluid ounces	29.57	milliliters	mL
gal	gallons	3.785	liters	L
ft ³	cubic feet	0.028	cubic meters	m ³
yd ³	cubic yards	0.765	cubic meters	m ³
NOTE: volumes greater than 1000 L shall be shown in m ³				
MASS				
oz	ounces	28.35	grams	g
lb	pounds	0.454	kilograms	kg
T	short tons (2000 lb)	0.907	megagrams (or "metric ton")	Mg (or "t")
TEMPERATURE (exact degrees)				
°F	Fahrenheit	5 (F-32)/9 or (F-32)/1.8	Celsius	°C
ILLUMINATION				
fc	foot-candles	10.76	lux	lx
fl	foot-Lamberts	3.426	candela/m ²	cd/m ²
FORCE and PRESSURE or STRESS				
lbf	poundforce	4.45	newtons	N
lbf/in ²	poundforce per square inch	6.89	kilopascals	kPa

APPROXIMATE CONVERSIONS FROM SI UNITS

Symbol	When You Know	Multiply By	To Find	Symbol
LENGTH				
mm	millimeters	0.039	inches	in
m	meters	3.28	feet	ft
m	meters	1.09	yards	yd
km	kilometers	0.621	miles	mi
AREA				
mm ²	square millimeters	0.0016	square inches	in ²
m ²	square meters	10.764	square feet	ft ²
m ²	square meters	1.195	square yards	yd ²
ha	hectares	2.47	acres	ac
km ²	square kilometers	0.386	square miles	mi ²
VOLUME				
mL	milliliters	0.034	fluid ounces	fl oz
L	liters	0.264	gallons	gal
m ³	cubic meters	35.314	cubic feet	ft ³
m ³	cubic meters	1.307	cubic yards	yd ³
MASS				
g	grams	0.035	ounces	oz
kg	kilograms	2.202	pounds	lb
Mg (or "t")	megagrams (or "metric ton")	1.103	short tons (2000 lb)	T
TEMPERATURE (exact degrees)				
°C	Celsius	1.8C+32	Fahrenheit	°F
ILLUMINATION				
lx	lux	0.0929	foot-candles	fc
cd/m ²	candela/m ²	0.2919	foot-Lamberts	fl
FORCE and PRESSURE or STRESS				
N	newtons	0.225	poundforce	lbf
kPa	kilopascals	0.145	poundforce per square inch	lbf/in ²

*SI is the symbol for the International System of Units. Appropriate rounding should be made to comply with Section 4 of ASTM E380.
(Revised March 2003)

ACKNOWLEDGMENTS

This research project was performed under a pooled fund program between the State of Alaska Department of Transportation and Public Facilities, California Department of Transportation (Caltrans), Louisiana Department of Transportation and Development, Minnesota Department of Transportation, Tennessee Department of Transportation, Texas Department of Transportation and Washington State Department of Transportation, and the Federal Highway Administration. The authors acknowledge and appreciate their guidance and assistance.

Roadside Safety Research Pooled Fund Committee CONTACTS

Revised February 2008

ALASKA

Elmer E. Marx, PE
Technical Engineer II
State of Alaska Department of
Transportation and Public Facilities
3132 Channel Drive
Room 100
Juneau, AK 99801
(907) 465-6941
elmer_marx@dot.state.ak.us

Clint Adler, P.E.
Research Engineer
Alaska Department of Transportation and
Public Facilities
Research and Technology Transfer
2301 Peger Road
Fairbanks, AK 99709
(907) 451-5321
Clint_adler@dot.state.ak.us

Kurt Smith, P.E.
Statewide Traffic & Safety Engineer
Alaska Department of Transportation &
Public Facilities
3132 Channel Drive
Juneau, AK 99801-7898
(907) 465-6963
kurt_smith@dot.state.ak.us

CALIFORNIA

John Jewell, P.E.
Caltrans
Office of Materials and Infrastructure
Division of Research and Innovation
5900 Folsom Blvd
Sacramento, CA 95819
(916) 227-5824
(916) 227-5856
john_jewell@dot.ca.gov

Gary Gauthier, PE
Caltrans
Sr. Roadside Safety Engineer
Office of Materials and Infrastructure
Division of Research and Innovation
1101 R St.
Sacramento, CA 95814
Gary_Gauthier@dot.ca.gov

LOUISIANA

Paul Fossier
Bridge and Structural Design Section
P.O. Box 94245
Baton Rouge, LA 79084-9245
(225)379-1323
PaulFossier@dotd.louisiana.gov

Harold “Skip” Paul
Associate Director, Research
Louisiana Transportation Center
4101 Gourrier Ave.
Baton Rouge, LA 70808
(225) 767-9102
spaul@louisiana.gov.dotd

MINNESOTA

Michael Elle, P.E.
Design Standards Engineer
Minnesota Department of Transportation
395 John Ireland Blvd, MS 696
St. Paul, MN 55155
(651) 296-4859
michael.elle@dot.state.mn.us

James Klessig, Pooled Fund Manager
Minnesota Department of Transportation
Office of Investment Management
Research Services Section
395 John Ireland Blvd, MS 330
St. Paul, MN 55155
Jim.klessig@dot.state.mn.us

TENNESSEE

Jeff Jones
Director, Design Division
Tennessee Department of Transportation
Suite 1300
James K. Polk State Office Building
Nashville, TN 37243-0348
(615) 741-2221
Jeff.C.Jones@state.tn.us

Nancy W. Sartor
Manager, Office of Research
Suite 900
James K. Polk State Office Building
Nashville, TN 37243-0334
(615) 741-5789
Nancy.Sartor@state.tn.us

TEXAS

Mark A. Marek
Design Division
Texas Department of Transportation
125 East 11th Street
Austin, TX 78701-2483
(512) 416-2653
MMAREK@dot.state.tx.us

Charmaine Richardson
CRICHARD@dot.state.tx.us

WASHINGTON

Dick Albin, Chair
Assistant State Design Engineer-NW Region
Washington State Department of
Transportation
(360) 705-7451
AlbinD@wsdot.wa.gov

Rhonda Brooks, Research Manager
Washington State Department of
Transportation
P.O. Box 47372
Olympia, WA 98504-7372
(360) 705-7945
Brookrh@wsdot.wa.gov

FEDERAL HIGHWAY ADMINISTRATION

Martin Hargrave
U.S. Department of Transportation
Federal Highway Administration
Turner-Fairbanks Highway Research Center
Mail Code: HRDS-04
6300 Georgetown Pike
McLean, VA 22101
(202) 493-3311
Martin.Hargrave@fhwa.dot.gov

TEXAS TRANSPORTATION INSTITUTE

D. Lance Bullard, Jr., P.E.
Associate Research Engineer
Safety and Structural Systems Division
Texas Transportation Institute
Texas A&M University System
College Station, TX 77843-3135
(979) 845-6153
L-Bullard@tamu.edu

C. Eugene Buth, Ph.D., P.E.
Senior Research Engineer
Safety and Structural Systems Division
Texas Transportation Institute
Texas A&M University System
College Station, TX 77843-3135
(979) 845-6159
G-Buth@tamu.edu

Roger P. Bligh, Ph.D., P.E.
Associate Research Engineer
Safety and Structural Systems Division
Texas Transportation Institute
Texas A&M University System
College Station, TX 77843-3135
(979) 845-4377
RBligh@tamu.edu

TABLE OF CONTENTS

<u>Section</u>	<u>Page</u>
CHAPTER 1. INTRODUCTION	1
INTRODUCTION	1
BACKGROUND	1
OBJECTIVES/SCOPE OF RESEARCH	2
CHAPTER 2. DESIGN AND SIMULATION ANALYSIS	5
EVALUATION OF EXISTING BARRIER SYSTEMS.....	5
Barrier Profile	5
Barrier Length.....	7
Joint Gap and Connection Details.....	7
NCHRP Report 350 Crash Testing.....	8
BARRIER SYSTEM SELECTION.....	8
PINNED-DOWN DESIGN FOR WSDOT NJ-PROFILE BARRIER.....	8
WSDOT PINNED BARRIER ANALYSIS	10
WSDOT PINNED BARRIER ANALYSIS WITH MODIFIED MODEL	17
ANALYSIS OF THE NEW PINNED F-SHAPED CONCRETE BARRIER	21
CHAPTER 3. TESTING PARAMETERS	27
TEST FACILITY.....	27
TEST CONDITIONS.....	27
EVALUATION CRITERIA	27
CHAPTER 4. CRASH TEST 405160-3-1 (<i>NCHRP REPORT 350</i> TEST NO. 3-11)	29
TEST ARTICLE – DESIGN AND CONSTRUCTION.....	29
TEST VEHICLE.....	35
WEATHER CONDITIONS.....	35
IMPACT DESCRIPTION	35
DAMAGE TO TEST ARTICLE	35
VEHICLE DAMAGE.....	41
OCCUPANT RISK FACTORS.....	41
ASSESSMENT OF TEST RESULTS	41
CHAPTER 5. CRASH TEST 405160-3-2a (<i>NCHRP REPORT 350</i> TEST NO. 3-11).....	47
TEST ARTICLE – DESIGN AND CONSTRUCTION.....	47
TEST VEHICLE.....	58
WEATHER CONDITIONS.....	58
IMPACT DESCRIPTION	58
DAMAGE TO TEST ARTICLE	61
VEHICLE DAMAGE.....	61
OCCUPANT RISK FACTORS.....	61
ASSESSMENT OF TEST RESULTS	68
CHAPTER 6. SUMMARY AND CONCLUSIONS.....	71

TABLE OF CONTENTS (CONTINUED)

<u>Section</u>	<u>Page</u>
REFERENCES	75
APPENDIX A. CRASH TEST PROCEDURES AND DATA ANALYSIS	77
ELECTRONIC INSTRUMENTATION AND DATA PROCESSING	77
ANTHROPOMORPHIC DUMMY INSTRUMENTATION.....	78
PHOTOGRAPHIC INSTRUMENTATION AND DATA PROCESSING	78
TEST VEHICLE PROPULSION AND GUIDANCE.....	78
APPENDIX B. TEST VEHICLE PROPERTIES AND INFORMATION	79
APPENDIX C. SEQUENTIAL PHOTOGRAPHS	85
APPENDIX D. VEHICLE ANGULAR DISPLACEMENTS AND ACCELERATIONS	91

LIST OF FIGURES

	<u>Page</u>
Figure 2.1. Initial configuration with 55-degree drop-pin angle.	9
Figure 2.2. Drop-pin and longitudinal rebar location with the 55-degree drop-pin angle.....	9
Figure 2.3. Finite element model barrier segments in the initial WSDOT pinned-barrier model.	11
Figure 2.4. FE model of the drop-pins in the initial WSDOT pinned-barrier model.	12
Figure 2.5. Pin-and-loop connection model in the initial WSDOT pinned barrier model.....	12
Figure 2.6. Initial FE system model of the WSDOT pinned barrier.....	13
Figure 2.7. Results of initial simulation analysis of WSDOT pinned down barrier.....	14
Figure 2.8. Simulation results indicate high vehicle climb.....	14
Figure 2.9. Barrier segment with maximum roll.....	15
Figure 2.10. Failure of the concrete around the drop-pin at the joint of impact.....	16
Figure 2.11. Regions of the barrier that incorporate concrete failure.....	17
Figure 2.12. Barrier reinforcement modeled in regions with concrete material failure.	17
Figure 2.13. Changes to the barrier model.....	18
Figure 2.14. Modified full-system model of the WSDOT barrier.	19
Figure 2.15. Increased barrier rotation in modified WSDOT model (left) versus old model (right).	20
Figure 2.16. Lifting of the barrier observed in the test and simulation results.....	20
Figure 2.17. Vehicle climb comparison. Modified WSDOT simulation (left), old simulation (right), and crash test (top).	21
Figure 2.18. Changes in barrier reinforcement.	22
Figure 2.19. Modified barrier reinforcement for crash testing.	23
Figure 2.20. Barrier model for the new pinned-down F-shaped barrier.	23
Figure 2.21. System model for the new pinned-down F-shaped barrier.....	24
Figure 2.22. Simulation results of the new pinned-down F-shaped barrier when placed at the edge of the deck.....	24
Figure 2.23. Vehicle climb observed in WSDOT barrier (left) and the new pinned-down barrier (right).....	25
Figure 2.24. Maximum barrier roll in WSDOT barrier (left) and the new pinned-down barrier (right).....	25
Figure 2.25. Barrier lift observed in the WSDOT simulation (left) is improved in new design (right). (Vehicle not shown).....	25
Figure 2.26. Barrier rotation comparison with the barrier placed on edge (left) and barrier placed at a 6-inch offset (right).....	26
Figure 4.1. Details of the pinned F-shape barrier – layout.	30
Figure 4.2. Details of the pinned F-shape barrier – detail A.....	31
Figure 4.3. Details of the pinned F-shape barrier – cross section.....	32
Figure 4.4. Details of the pinned F-shape barrier – rebar.	33
Figure 4.5. Pinned F-shape barrier prior to testing.	34
Figure 4.6. Vehicle/installation geometrics for test 405160-3-1.	36
Figure 4.7. Vehicle before test 405160-3-1.	37

LIST OF FIGURES (CONTINUED)

	<u>Page</u>
Figure 4.8. Vehicle trajectory path after test 405160-3-1.....	38
Figure 4.9. Installation after test 405160-3-1.....	39
Figure 4.10. Concrete failure around the upstream drop-pin of the forth barrier segment after test 405160-3-1.....	40
Figure 4.11. Vehicle after test 405160-3-1.....	42
Figure 4.12. Summary of results for <i>NCHRP Report 350</i> test 3-11 on the pinned F-shape barrier.	43
Figure 5.1. Details of the pinned F-shape barrier – installation layout.....	48
Figure 5.2. Details of the pinned F-shape barrier – Section A-A.	49
Figure 5.3. Details of the pinned F-shape barrier –segment detail.	50
Figure 5.4. Details of the pinned F-shape barrier – cross section.....	51
Figure 5.5. Details of the pinned F-shape barrier – barrier details.	52
Figure 5.6. Details of the pinned F-shape barrier – pin placement.....	53
Figure 5.7. Details of the pinned F-shape barrier – rebar placement.....	54
Figure 5.8. Details of the pinned F-shape barrier – rebar details.....	55
Figure 5.9. Details of the pinned F-shape barrier – pin details.....	56
Figure 5.10. Pinned F-shape barrier prior to testing.	57
Figure 5.11. Vehicle/installation geometrics for test 405160-3-1.	59
Figure 5.12. Vehicle before test 405160-3-1.	60
Figure 5.13. Vehicle trajectory path after test 405160-3-1.....	62
Figure 5.14. Installation after test 405160-3-1.....	63
Figure 5.15. Deformed drop-pins after test 405160-3-1.....	64
Figure 5.16. Vehicle after test 405160-3-1.....	65
Figure 5.17. Interior of vehicle for test 405160-3-1.	66
Figure 5.18. Summary of results for <i>NCHRP Report 350</i> test 3-11 on the modified pinned F-shape barrier.....	67
Figure B1. Vehicle properties for test 405160-3-1.....	79
Figure B2. Vehicle properties for test 405160-3-2a.	82
Figure C1. Sequential photographs for test 405160-3-1 (rear view).	85
Figure C2. Sequential photographs for test 405160-3-1 (overhead and frontal views).....	86
Figure C3. Sequential photographs for test 405160-3-2a (overhead and frontal views).....	88
Figure C4. Sequential photographs for test 405160-3-2a (rear view).	90
Figure D1. Vehicle angular displacements for test 405160-3-1.	91
Figure D2. Vehicle longitudinal accelerometer trace for test 405160-3-1 (accelerometer located at center of gravity).....	92
Figure D3. Vehicle lateral accelerometer trace for test 405160-3-1 (accelerometer located at center of gravity).....	93
Figure D4. Vehicle vertical accelerometer trace for test 405160-3-1 (accelerometer located at center of gravity).....	94
Figure D5. Vehicle longitudinal accelerometer trace for test 405160-3-1 (accelerometer located over rear axle).....	95

LIST OF FIGURES (CONTINUED)

	<u>Page</u>
Figure D6. Vehicle lateral accelerometer trace for test 405160-3-1 (accelerometer located over rear axle).....	96
Figure D7. Vehicle vertical accelerometer trace for test 405160-3-1 (accelerometer located over rear axle).....	97
Figure D8. Vehicle angular displacements for test 405160-3-2a.	98
Figure D9. Vehicle longitudinal accelerometer trace for test 405160-3-2a (accelerometer located at center of gravity).....	99
Figure D10. Vehicle lateral accelerometer trace for test 405160-3-2a (accelerometer located at center of gravity).....	100
Figure D11. Vehicle vertical accelerometer trace for test 405160-3-2a (accelerometer located at center of gravity).....	101
Figure D12. Vehicle longitudinal accelerometer trace for test 405160-3-2a (accelerometer located over rear axle).....	102
Figure D13. Vehicle lateral accelerometer trace for test 405160-3-2a (accelerometer located over rear axle).....	103
Figure D14. Vehicle vertical accelerometer trace for test 405160-3-2a (accelerometer located over rear axle).....	104

LIST OF TABLES

	<u>Page</u>
Table 2.1. Design features of concrete barrier systems from participating states.	6
Table 6.1. Performance evaluation summary for <i>NCHRP Report 350</i> test 3-11 on the pinned F-shape temporary barrier.....	73
Table 6.2. Performance evaluation summary for <i>NCHRP Report 350</i> test 3-11 on the modified pinned F-shape temporary barrier.....	74
Table B1. Exterior crush measurements for test 405160-3-1.	80
Table B2. Occupant compartment measurements for test 405160-3-1.....	81
Table B3. Exterior crush measurements for test 405160-3-2a.	83
Table B4. Occupant compartment measurements for test 405160-3-2a.....	84

CHAPTER 1. INTRODUCTION

INTRODUCTION

Bridge replacement and repair projects often require the use of phased bridge construction techniques to maintain traffic operation during construction. An important safety requirement is to use temporary concrete barriers to protect motorists from extreme drop-offs that may exist at the edge of bridge decks during such projects. Since very limited space is available during these operations, ordinary temporary concrete barriers must be restrained to limit lateral deflections in the event of an impact from an errant vehicle. There are few restrained temporary concrete barrier designs that have been crash tested to provide limited deflection requirements. Among the restraining or anchoring mechanisms currently available, most designs require through the deck bolting, anchor bolts, or other constraining straps. Through the deck bolting is difficult to achieve in the field and can result in significant damage to thin bridge decks. Similarly, the use of anchor bolts requires adhesive bonding, which complicates barrier installation, inspection, and removal procedures. An easy to install restraining mechanism that limits lateral deflections of concrete barriers, while minimizing damage to the bridge deck is needed.

BACKGROUND

In 1993, Texas Transportation Institute (TTI) developed a limited-slip portable concrete barrier connection for Texas Department of Transportation (TxDOT) that passed the *NCHRP Report 350* evaluation criteria.⁽¹⁾⁽²⁾ This connection was developed for 30 ft TxDOT portable concrete barriers (PCB) placed on bridge decks and/or concrete pavements. Four steel pins, 1.25 inches in diameter and 20.5 inches in length, were inserted into holes drilled through each of the barriers. The pins were inclined at an angle of approximately 40 degrees from the ground and were installed from one side of the barrier only. A TL-3 crash test for this system resulted in maximum static and dynamic deflections of 9.6 inches and 15.6 inches, respectively.

In 2002, Midwest Roadside Safety Facility developed an anchored system for the F-shaped Iowa barrier.⁽³⁾ This design incorporated a double steel strap that attached to the pin-and-loop connection and anchored to the deck using 19-mm anchor bolts at the traffic and the field side of the barrier. When tested with a one-foot offset from the deck edge, the barrier had a dynamic deflection of 3.15 feet. One of the barriers was deflected off the deck edge but remained supported by the steel straps. The vehicle was successfully redirected, but had a relatively high climb.

In 2002, MwRSF developed a tie-down system for attaching Iowa H-section steel barriers to bridge decks.⁽⁴⁾ Four angle brackets were welded to the base of each steel barrier and anchored to the concrete bridge deck by passing anchor bolts through the holes in the angle brackets. The maximum static and dynamic deflections measured during crash testing were 9.5 inches and 12.5 inches, respectively.

In 2003, MwRSF developed a concrete bridge deck tie-down for Kansas temporary barriers.⁽⁵⁾ Three anchor bolts were passed through the holes in the barrier and fastened to the bridge deck on the traffic side of the barrier. The maximum static and dynamic deflections were 3.5 inches and 11.3 inches, respectively.

TTI has previously researched the staking of Oregon Department of Transportation's (DOT) pin-and-loop pre-cast PCB (FHWA Contract DTFH61-97-C-00064).⁽⁶⁾ A detailed analytical analysis was performed to examine the behavior of the stakes under different stake angles and friction coefficients. Analytical analysis was also performed to examine the strength of the staking configuration. Based on these analyses, optimum stake inclination angle, appropriate stake length, and barrier concrete load capacity levels were suggested.

OBJECTIVES/SCOPE OF RESEARCH

The primary objective of this research was to develop a limited deflection pinned concrete barrier that meets NCHRP Report 350 Test Level 3 requirements and limits dynamic deflection to accommodate restricted space requirements in a work zone. The barrier was required to have a safety shape profile ('F' or New Jersey) and a segment length between 12.5 to 15 feet. It was also required that the barrier be easy to install and cause minimum damage to bridge decks.

The participating states of the pooled fund program initially desired to have a design that works in conjunction with the portable concrete barrier designs being used by most of the participating states. A preliminary evaluation of all barrier designs was conducted and Washington State DOT's pin-and-loop New Jersey profile barrier was identified as the design likely to result in greatest vehicle instability and lateral deflection during impact. It was argued that a restraint mechanism which performs adequately for this design, will work acceptably for the designs being used by the other participating states.

Based on the review of previously developed designs for restraining temporary concrete barriers to bridge decks and pavements, the researchers adopted the pinned-down approach rather than the bolted-down approach. This approach has many inherent advantages such as the ease of installation and removal, and the elimination of through the deck bolting. A finite element model of the WSDOT barrier was developed and impact simulations were performed to assist in the development of an appropriate pinned-down design for this barrier. Simulation results prior to crash testing showed that due to the NJ profile of the barrier and rotation induced during impact, high vehicle climb was expected and the test results would be marginal. However, since this design offered the most flexibility in applying the pinned design to barriers used by the participating states, the states decided to proceed with a full-scale crash test. The WSDOT pinned-down barrier was subsequently crash tested, but failed to meet the design requirements due to excessive rotation of the barriers and excessive vehicle climb.

A second phase of the analysis was performed to develop a new pinned-down temporary concrete barrier design, which did not necessarily incorporate all of the existing barrier designs of the participating states. The researchers performed a detailed evaluation of crash test results

to make necessary modifications to the barrier design. The profile of the new pinned-down barrier was changed from NJ to F-shaped. Barrier connections were modified among other changes, to provide better resistance to barrier roll.

The crash test analysis of the WSDOT pinned-barrier suggested that the role of concrete failure was significant in barrier performance. Therefore, in the second phase of the analysis, the finite element model of the WSDOT pinned-barrier was modified to include concrete material failure. Simulation analyses were performed to validate the updated model against the crash test and to determine parameters for concrete modeling for use in the analysis of the new pinned-down barrier design.

Using this concrete modeling approach, simulation analyses for the new barrier were performed. The results of the analysis showed significant improvement in barrier performance compared to the WSDOT pinned-down design. A successful crash test was subsequently performed with the new F-shaped pinned-down concrete barrier design.

Details of the evaluation of existing barrier designs among the participating states, along with the details of the design and simulation analyses are presented in Chapter 2. Chapter 3 presents a description of the testing parameters. Crash testing results are presented in chapter 4 and 5. Conclusions emanating from this research are presented in chapter 6.

CHAPTER 2. DESIGN AND SIMULATION ANALYSIS

Based on the review of previously developed designs for restraining temporary concrete barriers to bridge decks and concrete pavements, the researchers adopted the pinned-down rather than the bolted-down approach. Pinned-down design has several advantages over bolted-down design. Use of drop-pins greatly simplifies the installation deployment, barrier inspection, and removal process. When the system is used on asphalt pavement rather than a concrete bridge deck or pavement, the only modification required would be to increase the embedment depth of the drop-pins. Thus, the same design can be used without much modification to the barriers. Under the current project, however, the researchers have focused on the use of barriers on concrete bridge decks and concrete pavements. Use of the pinned-down concept on asphalt pavement will require additional analysis and testing.

The participating states of the pooled fund program initially expressed interest in having a drop-pin configuration that worked with the temporary concrete barrier designs already in use in their respective state. However, there were many variations between the existing designs of these states. The researchers suggested developing the restraining mechanism for the barrier design that was expected to result in the largest lateral deflection and vehicular instability. A restraint mechanism that performs successfully for such a design would be expected to perform adequately for other less critical designs being used by the participating states. The researchers thus evaluated the design details of the temporary concrete barriers of the participating states to identify the design that is likely to result in largest lateral deflection and highest degree of vehicular instability on impact. After a careful evaluation of several design aspects, the researchers selected Washington DOT's NJ-profile pin-and-loop barrier system as the design to use in the initial design and analysis effort. Following are the details of the evaluation and selection.

EVALUATION OF EXISTING BARRIER SYSTEMS

Table 2.1 compares several design aspects of the temporary concrete barriers from all participating states. Design aspects evaluated included the profile of the barrier, length of the barriers, connection gap between adjacent barriers, configuration of connection loops, details of the connecting pin, and whether the system was previously crash tested according to the *NCHRP Report 350* criteria or not.

Barrier Profile

The profile of the barrier (whether F-shape or New Jersey) effects vehicle stability during impact. The New Jersey profile is known to result in higher vehicle climb compared to the "F" profile. Once the lateral movement of the barriers is restricted by anchoring the system, the barriers tend to rotate under vehicle impact loads, providing a ramping effect to the vehicle. Under these conditions, NJ profile becomes more critical due to its tendency to induce higher vehicle climb. Thus concrete barrier designs of Washington, Tennessee, and California, which use the New Jersey profile, were considered more critical.

Table 2.1. Design features of concrete barrier systems from participating states.

State	Barrier Profile	Barrier Length	Connection Gap	Connection Loops	Loops Diameter	Loops Type	Connecting Pin Restraint	Connecting Pin Diameter	Connecting Pin Material	NCHRP Report 350 Crash Tested
WA	NJ	10' or 12.5'	0.25"	2 sets of 2 loops	5/8"	wire rope	no	1"	A36	Yes
MN	F	12.5'	3.5"	2 sets of 3 loops	3/4"	smooth bar	optional/no	1.25"	A36	Yes
TN	NJ	10' or 20'	2.25"	2 sets of 2 loops	3/4"	smooth bar	yes	1.25"	A307 Grade C	Yes
LA	F	15'	1"	2 sets of 3 loops	3/4"	smooth bar	no	1"	ASTM A449	Yes
AK	F	12.5'	1"	2 sets of 3 loops	3/4"	smooth bar	no	1"	ASTM A449	Yes
CA	NJ	20'	2"	2 sets of 2 loops	3/4"	smooth bar	no	1.25"	-	Yes
TX	F	30' or 10'	0"	cross-bolt connection	N/A	N/A	N/A	N/A	N/A	Yes

Barrier Length

Length of the barrier segments has an effect on the lateral deflection of the system. Smaller segment length results in a larger system deflection when compared to longer segment length. This is due to the fact that for a fixed installation length, a system with smaller barrier segments results in greater number of barrier-to-barrier connections, which increases the overall deflection due to rotations at additional connections. It can be seen from Table 1 that all states use 12.5 ft or longer barriers, with the exception of Washington, Texas, and Tennessee, which in addition to using 12.5 ft, 30 ft, and 20 ft barriers, respectively, also have a 10 ft barrier in their standards. It should be noted that the 10 ft Texas system is only used for maintenance operations. The research team learned from TNDOT that even though Tennessee uses the 10 ft long barriers, their use of this segment length is significantly less (approximately 20%) compared to the 20 ft long barriers. Tennessee DOT also had plans to shift to 12.5 ft barrier length for their pinned barrier design. So even though a barrier length of 10 ft is more critical, it is used in only a small percentage of installations among the participating states. Therefore, a 12.5 ft barrier length was selected as the critical length for this research.

Joint Gap and Connection Details

Several design features related to barrier connections were compared as shown in table 2.1. These included the gap between faces of adjacent barriers, configuration of the connection loops, loop diameters, presence of a restraint on the connection pin, pin and loop material properties, etc.

The gap between the face of adjacent barriers is an important parameter. A larger gap permits greater free rotation at these connections prior to the adjacent barrier faces bearing against one another and providing resistance to further rotation. In case of a vehicular impact on an unrestrained free standing barrier system, the pin and loop connection will rotate freely until the toes of the adjacent barrier faces bear against each other and pull the loops in tension. In the context of a drop-pin restraint, a larger joint gap implies that during the initial lateral deflection and free joint rotation period, most of the load will be taken up by the drop-pins, thus making larger gaps more critical. Of the barrier systems compared, Minnesota's design has the largest connection gap (3.5 inch) followed by Tennessee (2.25 inch) and California (2.0 inch).

Another factor that effects the overall lateral deflection of the barrier systems is the configuration of the connection loops. There are two types of configurations that exist in the designs evaluated. These are connections with "two sets of two loops" and connections with "two sets of three loops." Of these two configurations, "two sets of two loops" is more critical as it provides less pull out resistance for the connection pin. Hence the designs for Washington, Tennessee, and California are considered more critical in this regard.

Additionally, it should be noted that Washington uses wire loops with smaller 5/8 inch diameter as opposed to the 3/4 inch diameter smooth bar loops used by the Tennessee and California designs. Similarly, the connecting pin used by the Washington design is a 1-inch diameter unrestrained pin as opposed to the 1.25 inch diameter pin used by Tennessee and

California designs. Therefore, even though the connection gap for Washington is less than some of the other barriers, these aspects make the Washington design more critical.

NCHRP Report 350 Crash Testing

All evaluated designs were either previously crash tested according to *NCHRP Report 350* criterion or were adopted from a design that was crash tested according to this criterion. Thus, there were no concerns about any one of the free-standing barrier systems requiring such compliance. It was noted that the vehicle in the test of the Washington design experienced significant climb and roll.

BARRIER SYSTEM SELECTION

Considering factors mentioned above, Washington DOT's 12.5 ft NJ profile barrier was selected as the most critical design for use in the development of a pinned-down system. Being the more critical system, a pinned-down design developed for it was expected to perform adequately for the rest of the barrier systems used by the participating states.

PINNED-DOWN DESIGN FOR WSDOT NJ-PROFILE BARRIER

Based on review of previously developed designs for anchoring temporary concrete barriers to bridge decks and concrete pavements, the research team had proposed to adopt the drop-pin approach rather than the bolted-down approach for anchoring temporary barriers. The new design was expected to be similar to the limited-slip portable concrete barrier design that TTI developed for Texas DOT in 1993 ⁽¹⁾. Lateral movement of the barrier was restricted using steel pins that passed through holes drilled into the concrete barriers and the underlying concrete bridge deck or pavement. These pins were at an angle of approximately 40 degrees from the ground, with the bottom end coming out of the barrier at the centerline of its cross-section. In this type of drop-pin design, it is important that the pins pass over at least one longitudinal rebar inside the barrier. This ensures that if concrete in the vicinity of a pin fails and spalls off during vehicular impact, the rebar will engage the drop-pin and provide additional restraint against lateral movement.

On evaluating barrier cross-sections and reinforcement details of all participating states, the researchers was found that using same pin angle as the Texas design would require modifications to rebar details of TN, AK, LA and MN designs. These modifications would be required to ensure the drop-pins pass over at least one longitudinal rebar inside the barrier. To eliminate the need for barrier modification by the majority of participating states, the researchers increased the drop-pin angle to 55 degrees (see figure 2.1). Evaluating barrier cross-sections and rebar designs of participating states indicated that, except Minnesota, no state would require modification to its current rebar details. Even for Minnesota, the nature of the modification was minor. Figure 2.2 shows the scaled half-profile of each state's barrier and the position of the pin inside the barrier. The location of the longitudinal rebar is also shown in the figure. The

drop-pin angle of 55 degrees is currently being used by Oregon DOT and was also adopted by Alaska DOT. However, the impact performance of this practice has not been evaluated with full-scale crash testing.

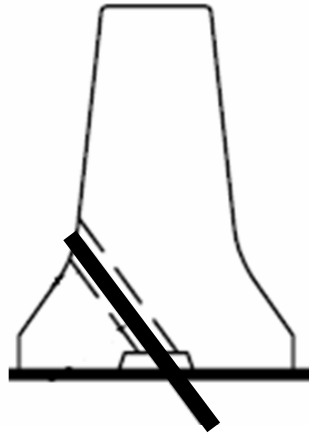


Figure 2.1. Initial configuration with 55-degree drop-pin angle.

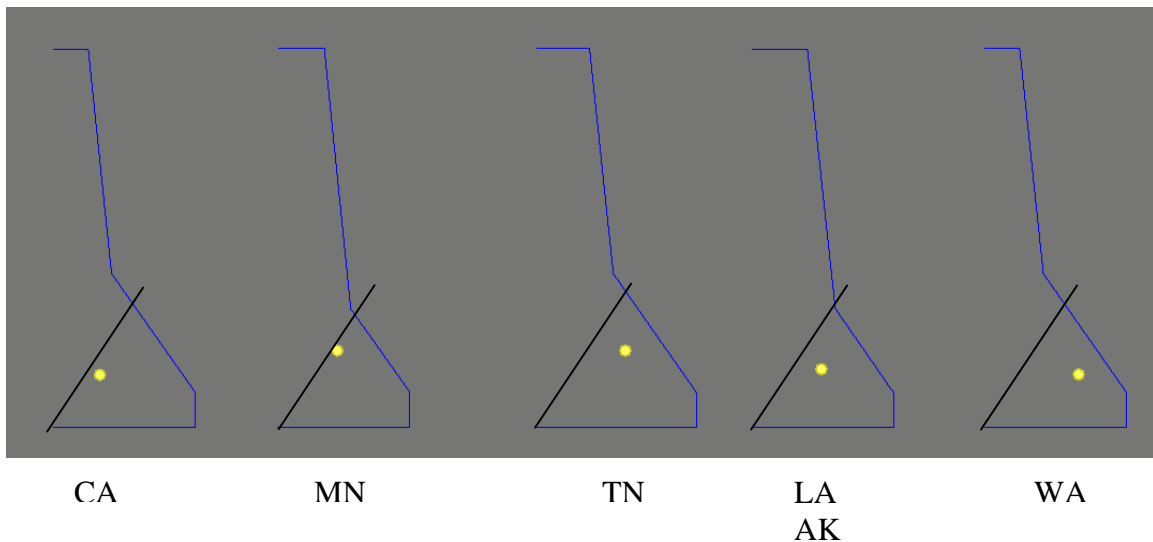


Figure 2.2. Drop-pin and longitudinal rebar location with the 55-degree drop-pin angle.

Thus to incorporate existing reinforcement details of most participating states, a drop-pin orientation of 55 degrees was selected. The initial configuration incorporated two drop-pins per barrier segment, located 22 inches from each edge of the barrier. The initial diameter of the drop-pins was 1-inch. The initial embedment depth of the pins inside the concrete ground was 6 inches when measured vertically.

WSDOT PINNED BARRIER ANALYSIS

The research team used numerical simulations to lead the design effort to develop the drop-pin configuration for the temporary concrete barriers. Numerous research studies have successfully utilized simulation codes to simulate vehicle handling, vehicle impacts with roadside objects, and vehicle encroachments over roadside geometric features such as slopes, ditches, and driveways. In these studies, researchers have utilized varying levels of vehicle model sophistication ranging from simple lumped masses, springs and dampers, to detailed finite element representations using many thousands of elements. All simulation codes have their limitations, and they all incorporate different levels of assumptions or approximations. It was considered crucial that the simulation code(s) selected for use in this project be capable of accurately modeling relevant characteristics of the vehicle, the concrete barrier, and the interactions between them.

The decision to choose the explicit finite element code LS-DYNA for this project was based on several reasons including:

1. The availability of vehicle models that correspond to *NCHRP Report 350* design test vehicles – mainly the 2000P vehicle. This vehicle model has been used for roadside safety applications for several years, and its fidelity and limitations are reasonably understood.
2. The ability to model the roadside device with a high degree of fidelity including: the barrier geometry (which affects the interaction between the vehicle and barrier), the mass and inertial properties of the barrier (which affect the kinetic behavior of the barrier), and the material properties (which affect the deformation of the device).
3. The ability to model contact-impact problems. LS-DYNA has a very extensive set of contact definitions that fit several impact-contact scenarios. Contact definitions having the option of including frictional sliding are well suited to modeling the dynamic interaction between a vehicle and roadside barrier.

In order to evaluate the initial drop-pin configuration for the free standing WSDOT precast concrete barrier, a full-scale finite element model of the barrier was developed. The concrete barrier segments were modeled using the an NJ profile with the top width of the barrier maintained at 6 inches and the segment length maintained at 12.5 ft (both of which are WSDOT standards). The barrier segment model was assigned the mass density of concrete, which makes the total mass of the barrier model equivalent to that of the actual barrier segment.

The finite element (FE) mesh for the barrier model, shown in figure 2.3, was comprised of solid elements. Most of the elements were assigned elastic material properties while the ends of the barriers were assigned rigid material properties. A friction coefficient of 0.4, as determined from barrier pull tests on a concrete pavement, was used between the barrier and the ground. The ground surface was modeled using rigid shell elements. Regions where the drop-pins were to pass through the ground surface were modeled using solid element blocks. The elements in these blocks were modeled using elastic material representation with properties

of the concrete in compression. Thus a complete concrete deck was not modeled to reduce model size. The drop-pins in the model did not pass through explicit holes in the barriers or the concrete deck. Instead, thin cylindrical sleeves comprised of elastic shell elements were used to define a contact between the drop-pins and the holes in the barriers and the concrete deck, as shown in figure 2.4. The elastic cylindrical sleeves were 0.5 mm in thickness and were constrained to move with the barrier (or the blocks representing the concrete deck) using the `CONSTRAINED_LAGRANGE_IN_SOLID` constraint in LS-DYNA. The drop-pins was assigned material properties of ASTM A36 steel. The initial diameter of the drop-pins and the holes were 1 inch and 1.5 inches, respectively.

The model of the pin-and-loop connection between adjacent barriers is shown in figure 2.5. The loops were constrained to the rigid ends of the barriers. The connecting pins, drop-pins, and the loops were modeled using beam elements. To establish a robust contact between the beam elements and the surrounding parts, a cylindrical mesh of shells was modeled around the beam elements. The nodes of the shell elements were constrained to move with the nodes on the beam elements using nodal rigid-body constraints. The shell elements were assigned NULL material type, which has no stiffness of its own and thus only acts as a contact surface for the beam elements. This type of modeling technique is used to avoid using solid elements for modeling the cylindrical parts. Using solids elements for relatively smaller diameter pins results in a large number of small size elements, which in turn reduces the computational time-step and significantly increases the time required to complete each simulation.

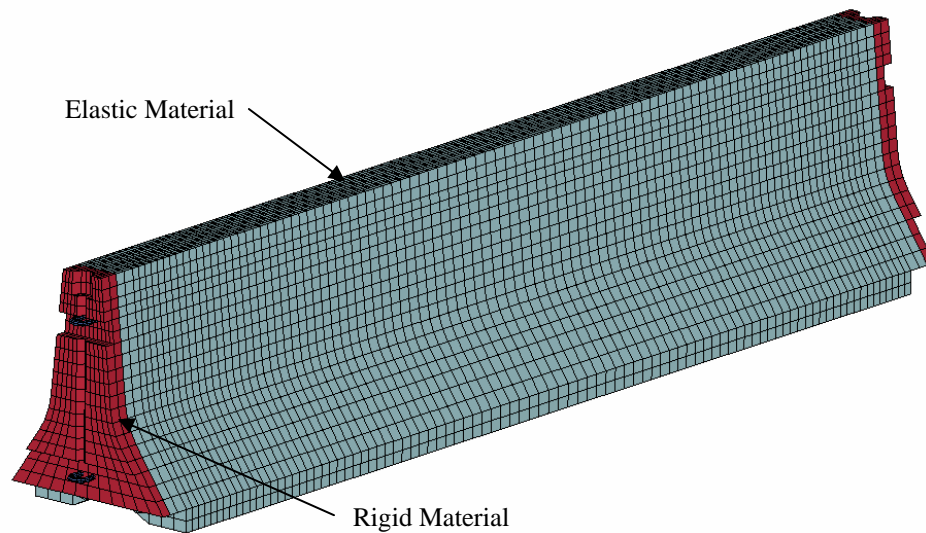


Figure 2.3. Finite element model barrier segments in the initial WSDOT pinned-barrier model.

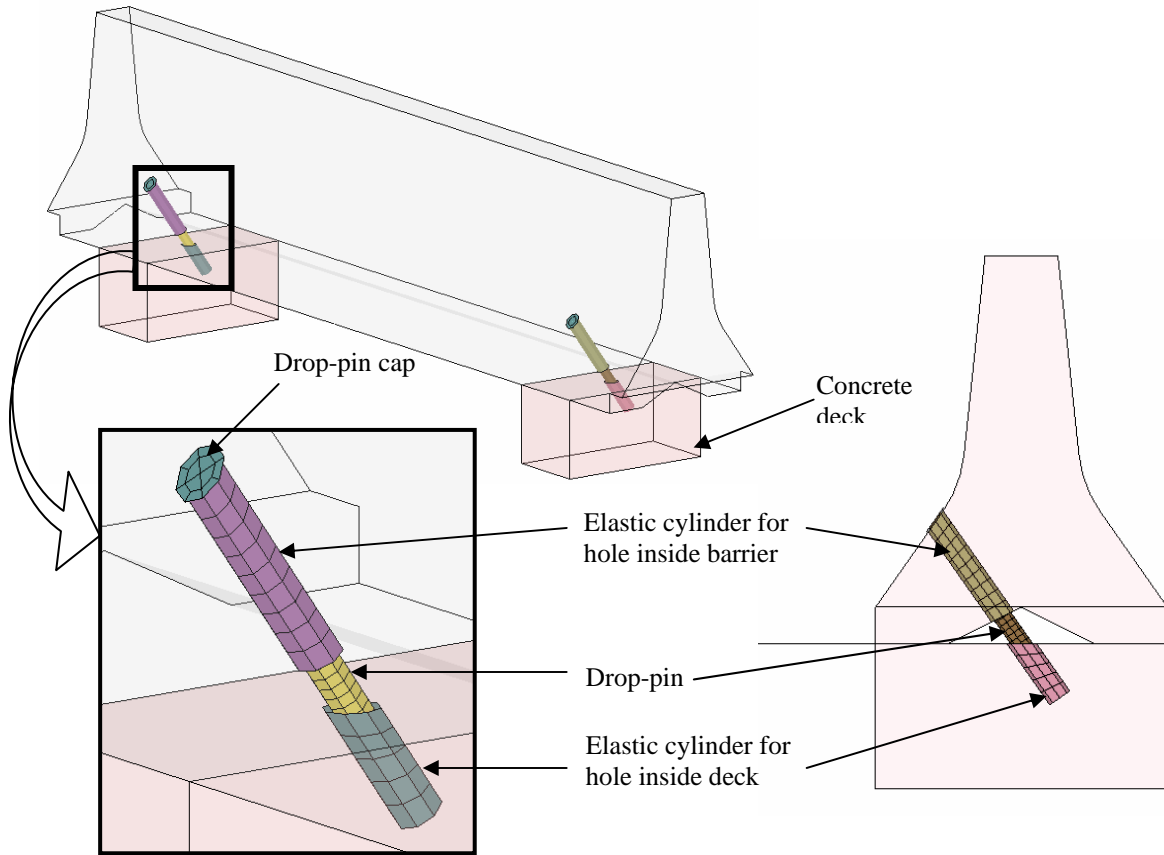


Figure 2.4. FE model of the drop-pins in the initial WSDOT pinned-barrier model.

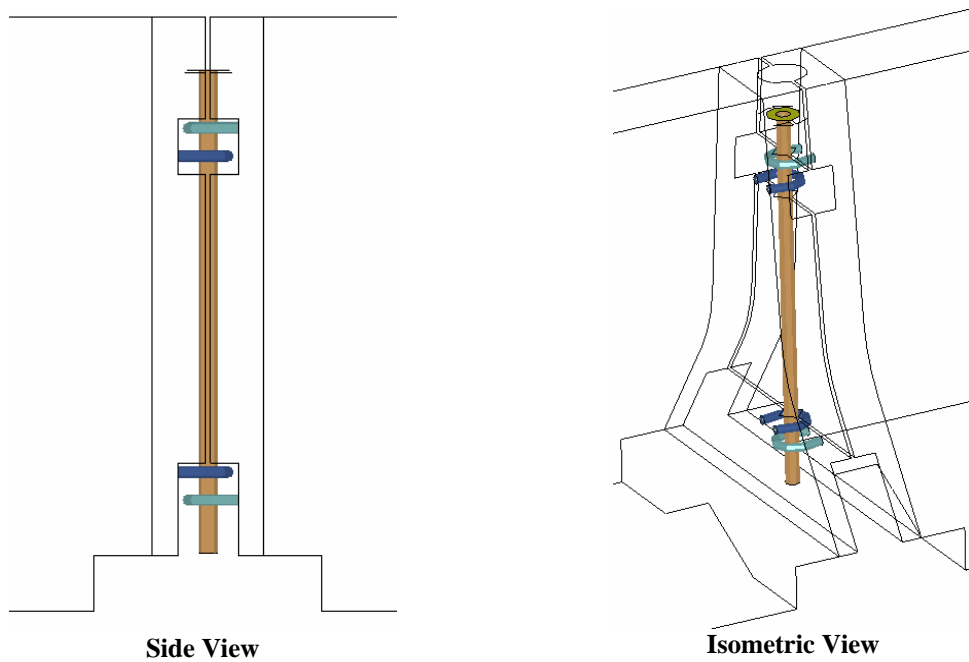


Figure 2.5. Pin-and-loop connection model in the initial WSDOT pinned barrier model.

It should be noted that the failure of the concrete was not included in this initial model. This implied that the results of the simulation represented a lower bound estimate of the overall barrier system deflection and barrier roll. If significant concrete fracture and spalling occurs at the ends of one or more barrier segments, or around the drop-pins during an actual impact, additional joint rotation or barrier roll can occur. This in turn can increase barrier deflection and vehicle instability and climb. With these aspects of the model understood, valuable design and performance information can be gleaned from the simulation results.

The full system model of the WSDOT pinned barrier is shown in figure 2.6. The simulation replicated Test Designation 3-11 of *NCHRP Report 350*. This test involves a 4409 lb (2000 kg) pickup truck impacting the barrier at a speed of 62.2 mi/h (100 km/h) and an angle of 25 degrees. This test is considered to be the critical test for evaluating the structural integrity of the drop-pin configuration and the maximum dynamic deflection of the barrier. A total of eight barrier segments were modeled to provide a barrier length of 100 ft. The vehicle model impacted the barrier system 4 ft upstream of the joint between the 3rd and the 4th barrier segment as shown in figure 2.6.

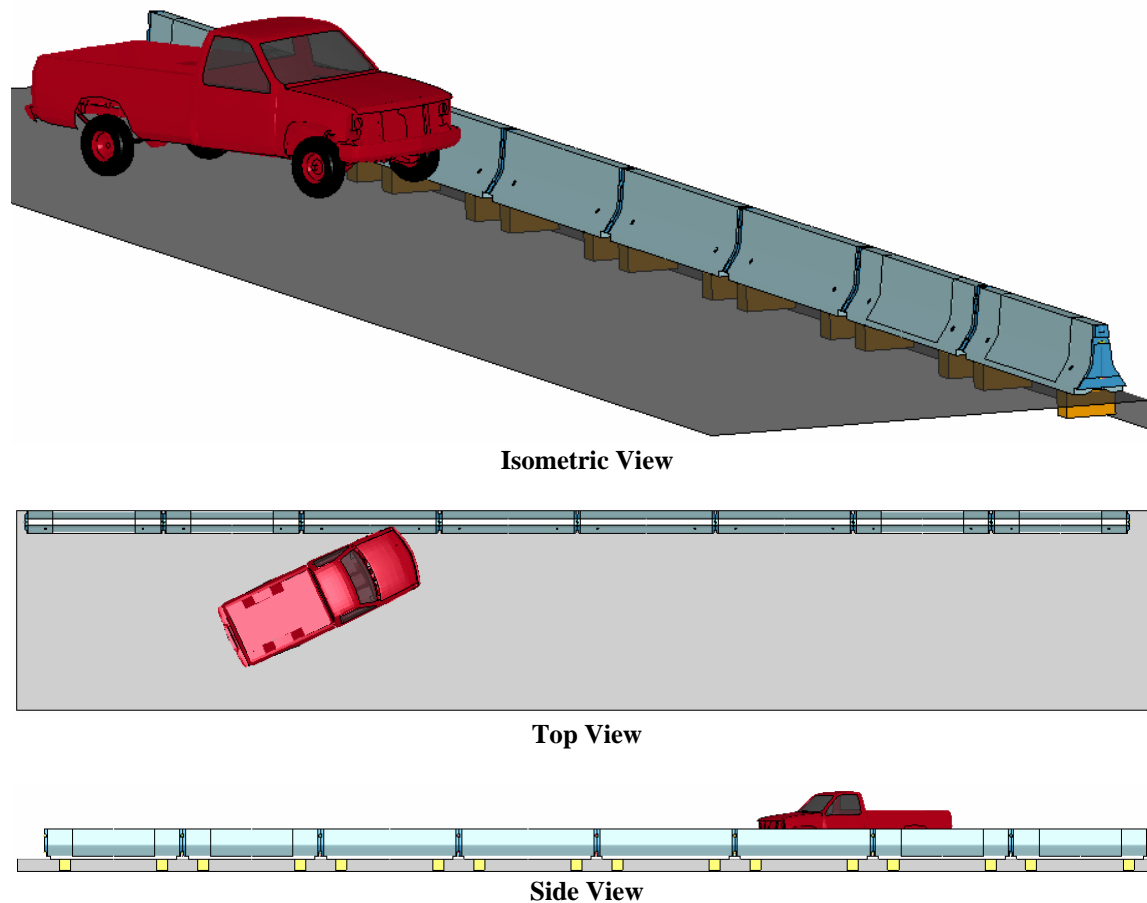


Figure 2.6. Initial FE system model of the WSDOT pinned barrier.

Simulation Results

Simulation results from this initial configuration showed high lateral deflection of the barriers due to high deformations in the drop-pins and the tolerance in the holes for the drop-pins. Based on the results of this initial drop-pin configuration, another simulation was performed after increasing the diameter of the drop-pins by 0.5 inches and decreasing the tolerance inside the holes by 0.25 inches. The new diameters for the drop-pins and the holes were 1.5 inches and 1.75 inches, respectively.

Figure 2.7 and 2.8 show the results of the simulation analysis. Simulation results indicated that the vehicle was redirected after impact and was expected to stay upright after redirection. However, the vehicle exhibited significant climb during redirection and the impacted barriers showed significant roll due to the impact. Figure 2.9 shows the maximum roll exhibited by the impacted barrier segment. The high climb of the vehicle can be partially attributed to the NJ profile of the barriers, which inherently results in greater vehicle instabilities. It is also attributed to the approximately 15 degrees of roll induced in the barriers during impact. The overall lateral deflection of the barriers was 7 inches.

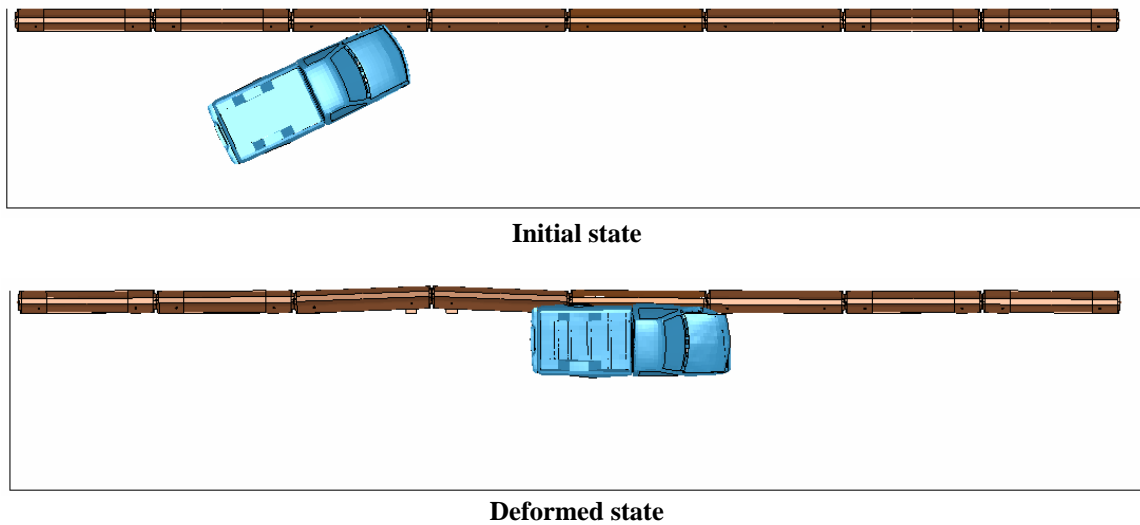


Figure 2.7. Results of initial simulation analysis of WSDOT pinned down barrier.

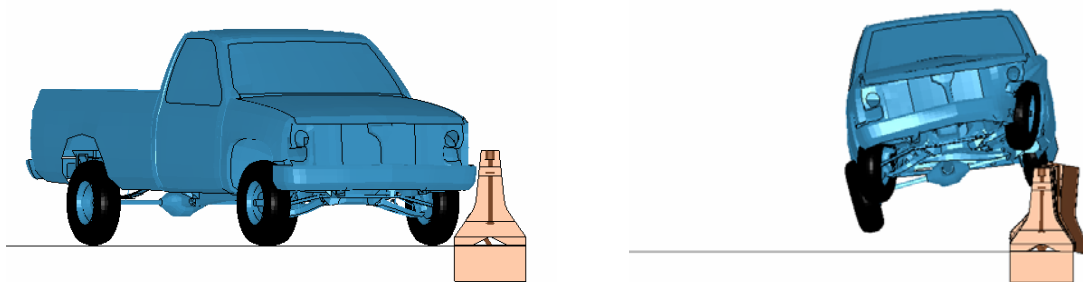


Figure 2.8. Simulation results indicate high vehicle climb.

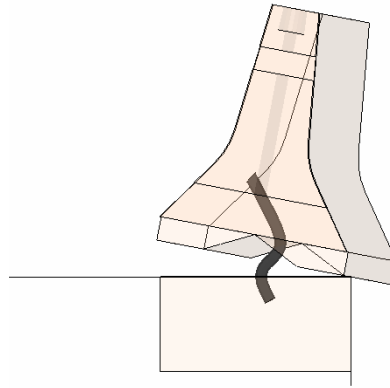


Figure 2.9. Barrier segment with maximum roll.

As previously discussed, to save computational time while performing iterative design simulations, the simulation results did not incorporate concrete failure in material model used for the modeling the barrier segments. Thus, the predictive simulation results were considered lower bound estimates of vehicle stability and barrier performance. The amount of vehicle climb and barrier roll was expected to increase in the test if the concrete around the drop-pins or the barrier faces were to spall off or fail. Based on these considerations, it was concluded that the results of the simulation did not indicate a definite pass and were therefore termed marginal. However, since this configuration offered the most flexibility in applying the drop-pin design to barriers used by all participating states, the states decided to proceed with a full-scale crash test. If the results of the test were successful, the design could be used by all participating states. If, however, the test was to be unsuccessful, further analysis would be conducted to develop a pinned-down barrier which meets the design criteria, but does not necessarily adapt to all existing state barrier designs.

A crash test was subsequently performed with the above mentioned pinned configuration, but it failed to meet the *NCHRP Report 350* criteria. Concrete around one of the drop-pins failed catastrophically as shown in figure 2.10. The drop-pin initially caught on to the longitudinal rebar, but slipped off after bending the pin-cap, which resulted in high barrier roll and vehicle climb. The barrier then dropped off the edge of the deck and as it rotated, causing more rotation and lift in the adjacent upstream barriers, which also eventually dropped off the deck. Details of the crash testing are presented in Chapter 4.



Figure 2.10. Failure of the concrete around the drop-pin at the joint of impact.

Analysis of the crash test results also indicated that even though concrete damage at the ends of adjacent barrier segments was moderate, it was enough to reveal some portions of the wire-rope loops that ran into the barrier. Since the wire-rope loops do not have any significant torsional stiffness of their own, the exposed wire-rope resulted in additional rotation of the barrier segments relative to each other. Thus, it was noted that instead of using the wire-rope connection, the new design should incorporate connections with loops made of round stock steel.

It was also observed that once the barriers started to roll, the drop-pins pulled out of the concrete pavement without significant resistance. Reducing the drop-pin angle relative to the ground was expected to offer more resistance to the drop-pin pullout. Welding a thicker pin cap to the top of the drop-pins was also expected to help grab on to the longitudinal rebar in case of concrete failure in the vicinity of the drop-pins. It was also noted that further finite element analysis for the barrier design should incorporate concrete material failure as it can significantly affect the outcome of the crash test.

Once the evaluation of the crash test results was completed, further analysis was performed to complete the pinned barrier design by modifying design parameters such as the pin angle, barrier profile, barrier connection, etc, as discussed above. The analysis was performed in two steps. In the first step, the existing model of the WSDOT pinned barrier was modified to better capture the failure behavior observed in the test. Concrete material failure was incorporated in the model among other changes. In the second step, the analysis was performed for the new pinned-down barrier design using modeling techniques incorporated in the modified WSDOT pinned barrier model. Details of these further analysis are presented next.

WSDOT PINNED BARRIER ANALYSIS WITH MODIFIED MODEL

TTI researchers made several modifications to the finite element model of the previously tested WSDOT pinned-down barrier. The objective of these modifications was to improve the correlation between the crash test and simulation results.

Modifications were made to capture some of the concrete failure that was observed in the test. The failure was incorporated using the Continuous Surface Cap Model (CSCM) (*MAT_CSCM) in LS-DYNA materials library. Inclusion of the concrete failure significantly increases the size of the model and the computational time required to complete the simulations. To reduce model size, concrete failure was only incorporated in regions that exhibited failure in the crash test. These regions were the ends of the adjacent barriers at two joints immediately downstream of the impact, and the concrete in the vicinity of the drop-pins. Figure 2.11 highlights the regions of the barriers that included concrete failure. The reinforcement of the barrier was also modeled in these regions as shown in figure 2.12. Portion of the rebar inside the concrete material was constrained using LAGRANGE_IN_SOLID constraints between the rebar and the concrete material.

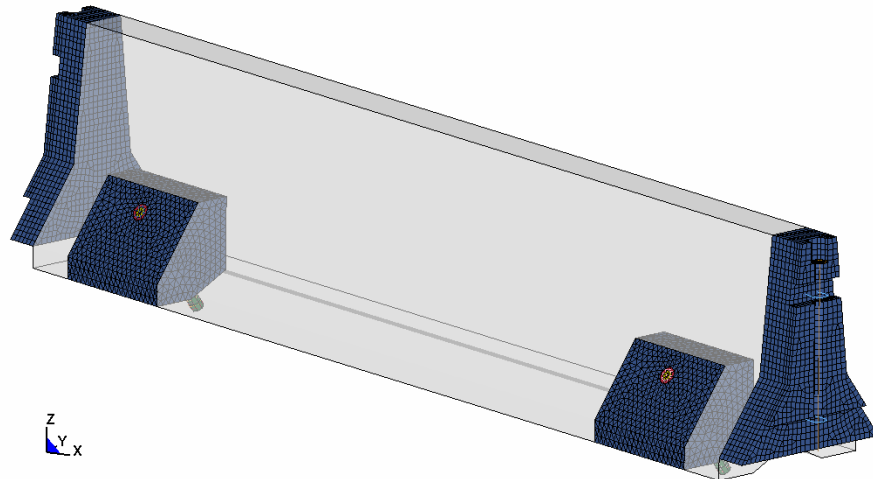


Figure 2.11. Regions of the barrier that incorporate concrete failure.

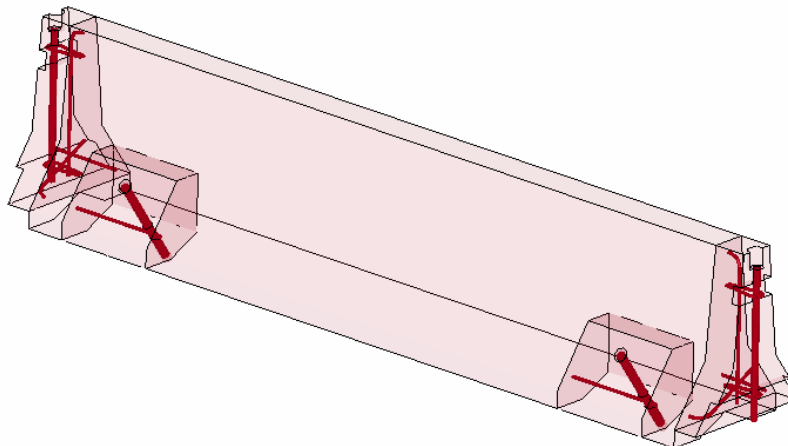


Figure 2.12. Barrier reinforcement modeled in regions with concrete material failure.

The wire-rope loops were comprised of beam elements that passed a certain distance inside the regions of the barrier where concrete material failure was incorporated (see figure 2.13). This was done to account for barrier rotation resulting from wire-rope loops that were exposed once the concrete failed in their vicinity. To allow for proper stress distribution in the concrete material around the drop-pins, the holes for passing the drop-pins were explicitly modeled as shown in figure 2.13.

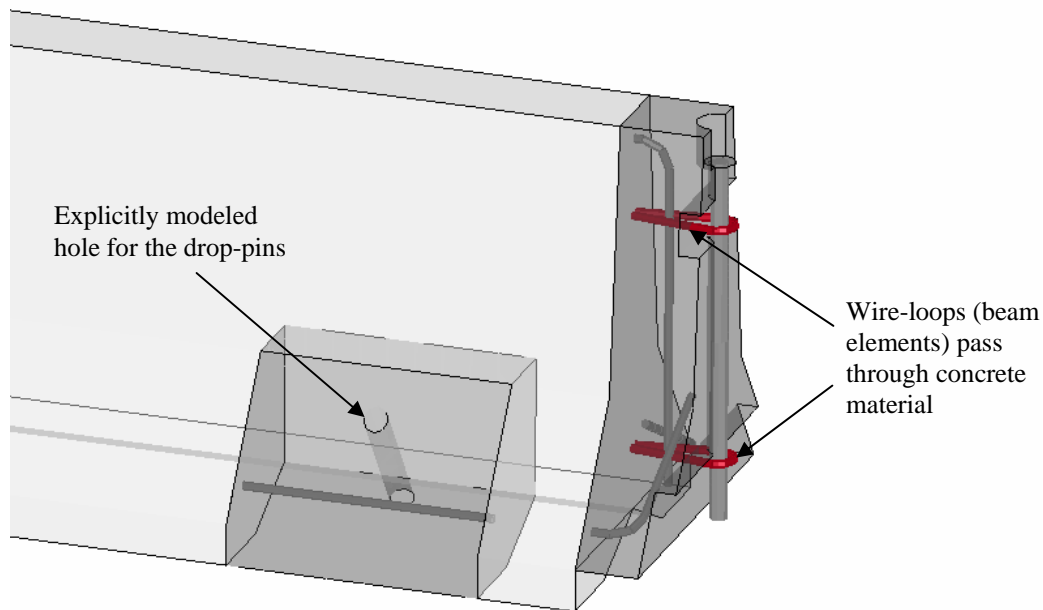


Figure 2.13. Changes to the barrier model.

The modified full system model of the WSDOT pinned barrier is shown in figure 2.14. The simulation replicated Test Designation 3-11 of *NCHRP Report 350*, which involves a 4409 lb (2000 kg) pickup truck impacting the barrier at a speed of 62.2 mi/h (100 km/h) and an angle of 25 degrees. A total of eight barrier segments were modeled to provide a barrier length of 100 ft (30.48 m). The vehicle model impacted the barrier system 1.2 meters upstream of the joint between the 3rd and the 4th barrier as shown in figure 2.14.

Several iterations were performed on the properties of the concrete material model to calibrate failure in the simulations to some of the failure observed in the test. The failure of concrete material in the finite element model occurred through erosion of elements that achieve a certain threshold of concrete damage and plastic strain. Thus the element erosion/material failure using the CSCM concrete material model is not completely independent of the mesh size used in the model. Several iterations of the erosion parameters were performed to improve correlation between simulation and test results.

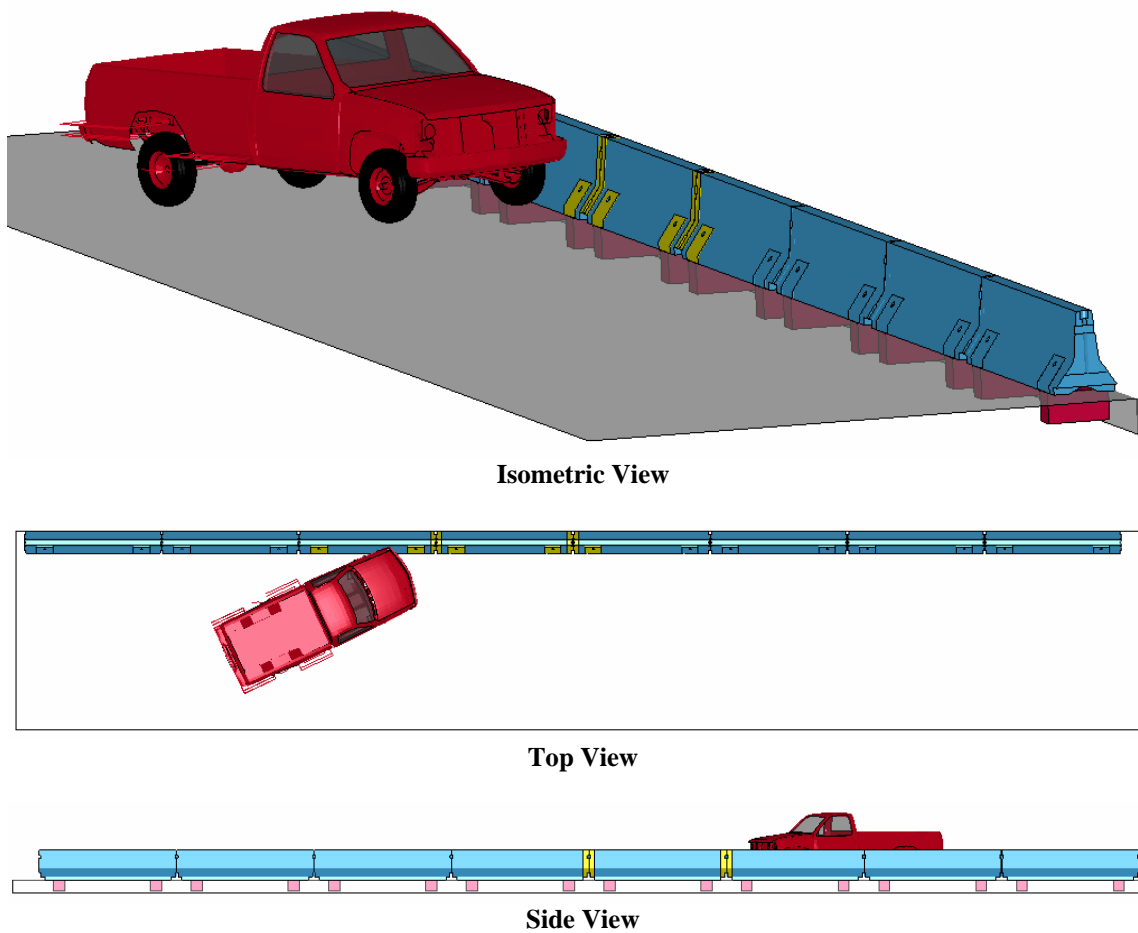


Figure 2.14. Modified full-system model of the WSDOT barrier.

Simulation Results

With the inclusion of concrete material failure at barrier faces and by modifying the properties wire-rope connection details, the relative rotation between adjacent barrier segments was improved compared to the previous model (see figure 2.15). In the crash test, the barriers upstream of the impact point showed a tendency to lift up without much resistance from the pins. This tendency was captured in the modified model as shown in figure 2.16). Similarly, the vehicle had significant climb in the test. The modified finite element model showed an increased climb of the vehicle compared to the previous model, as shown in figure 2.17.

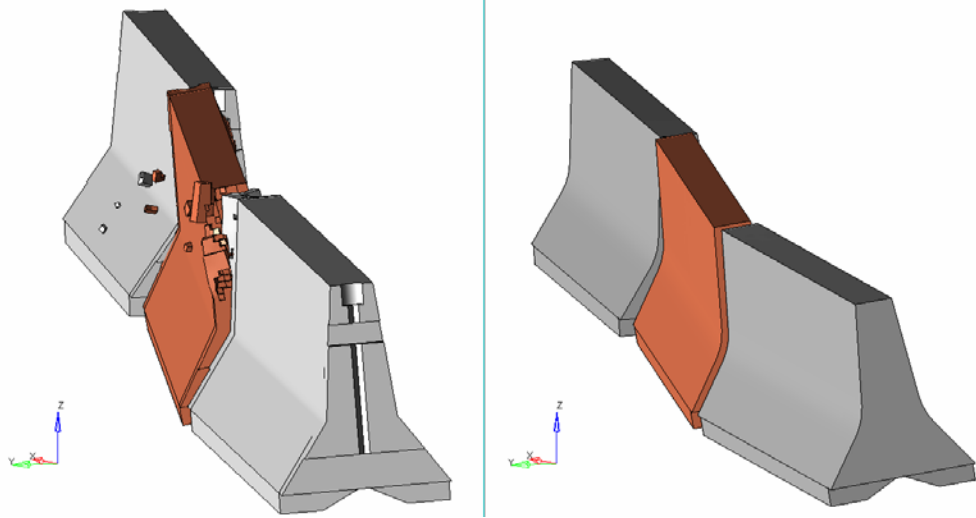


Figure 2.15. Increased barrier rotation in modified WSDOT model (left) versus old model (right).

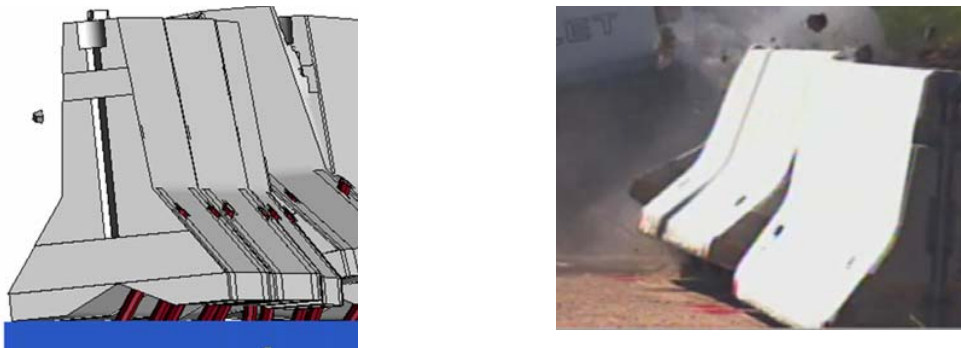


Figure 2.16. Lifting of the barrier observed in the test and simulation results.



Figure 2.17. Vehicle climb comparison. Modified WSDOT simulation (left), old simulation (right), and crash test (top).

While significant improvements to the finite element model of the WSDOT pinned barrier were made, a complete agreement with crash test results was not achieved within the limited resources allocated for the effort. The simulation results showed some failure in the concrete region around the drop-pin, but the catastrophic failure observed in the test was not replicated. This, in turn, influenced the degree of barrier roll and vehicle climb. Nonetheless, the overall model behavior was significantly improved and provided higher confidence in the use of simulation for analysis of the new pinned-down barrier system.

ANALYSIS OF THE NEW PINNED F-SHAPED CONCRETE BARRIER

Using the information gleaned from the results of the WSDOT pinned barrier crash test, the researchers developed a new pinned barrier design that adequately anchors the barriers, but does not necessarily accommodate all of the existing barrier designs of the participating states.

The design effort addressed factors that had a negative affect on barrier performance in the WSDOT pinned barrier crash test. The NJ profile of the barrier, which causes high vehicle climb, was changed to the more stable F-shape profile. After evaluating connection details of crash tested barrier designs, the researchers selected Oregon DOT's pin-and-loop concrete barrier as the basis for the new pinned-down configuration. This barrier design has been adopted by Alaska and Louisiana Departments of Transportation, both of whom are members of the pooled fund. The basic profile and connection details of Oregon DOT's F-shaped pin-and-loop barrier were retained. The barrier connection incorporates "two sets of the three loops" made of $\frac{3}{4}$ -inch diameter smooth bar steel. The connecting pin is 1-inch in diameter and the gap between adjacent barrier segments is also 1-inch. The length of the barrier segments is 12.5-ft.

The drop-pin design incorporated two drop-pins per barrier segment. To better resist barrier rotation under vehicle impact, the drop-pin angle relative to the ground was reduced to 40 degrees. Rebar details of the Oregon/Louisiana barrier were slightly modified to ensure that at least one longitudinal rebar passes below the drop-pins. This provides an opportunity for the drop-pin cap to catch onto the rebar in case of significant concrete failure around the pin. The thickness of the drop-pin cap was also increased to 1/2 inch as the thinner 1/4-inch cap was easily peeled off one of the pins in the WSDOT barrier test. Figure 2.18 shows the drop-pin orientation and a comparison of the changes made to the reinforcement. It should be noted that while the simulation analysis was performed using the reinforcement layout shown in figure 2.18, some modifications were made prior to crash testing as shown in figure 2.19. These included a slightly changed shape of the stirrups to provide adequate concrete cover for the longitudinal inset at the bottom of the barrier. A diagonal U-bar, which passed underneath the hole for the drop-pins, was also incorporated to act as a backup for engaging the drop-pins in case of catastrophic concrete failure around the pins.

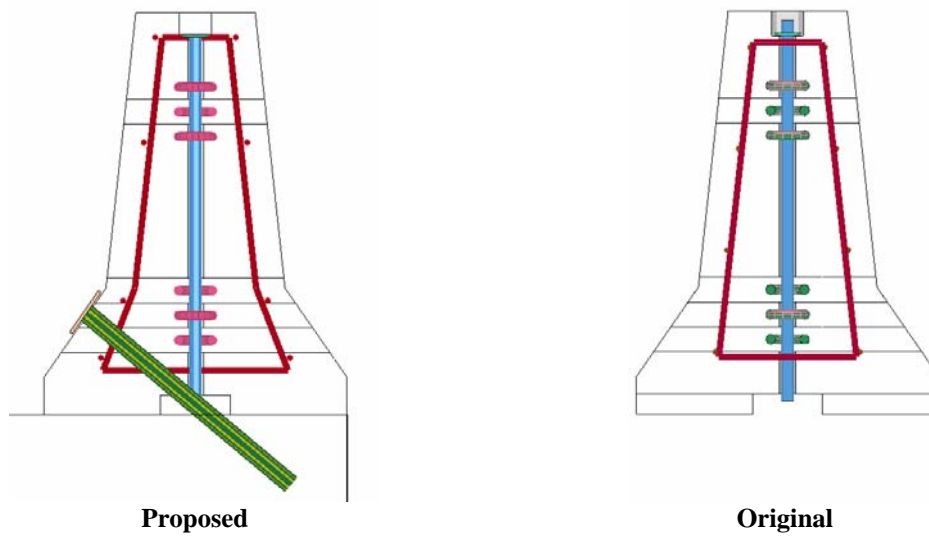


Figure 2.18. Changes in barrier reinforcement.

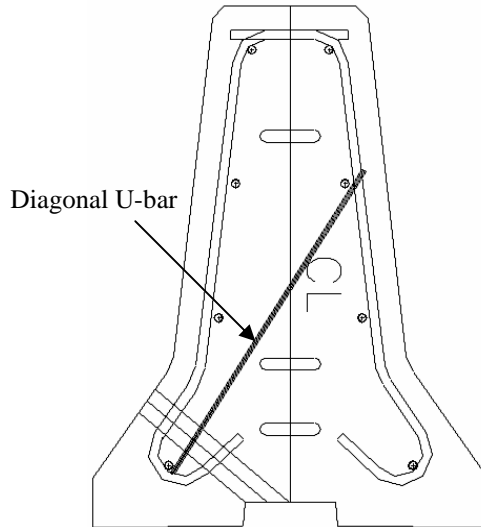


Figure 2.19. Modified barrier reinforcement for crash testing.

The finite element model of the new drop-pin design incorporated similar modeling techniques used in the modified WSDOT pinned barrier simulations. Figures 2.20 and 2.21 show the individual barrier segment model and the full system model, respectively. Simulations were performed with the pinned-down barrier placed at the edge of the deck and at a six-inch offset from the edge.

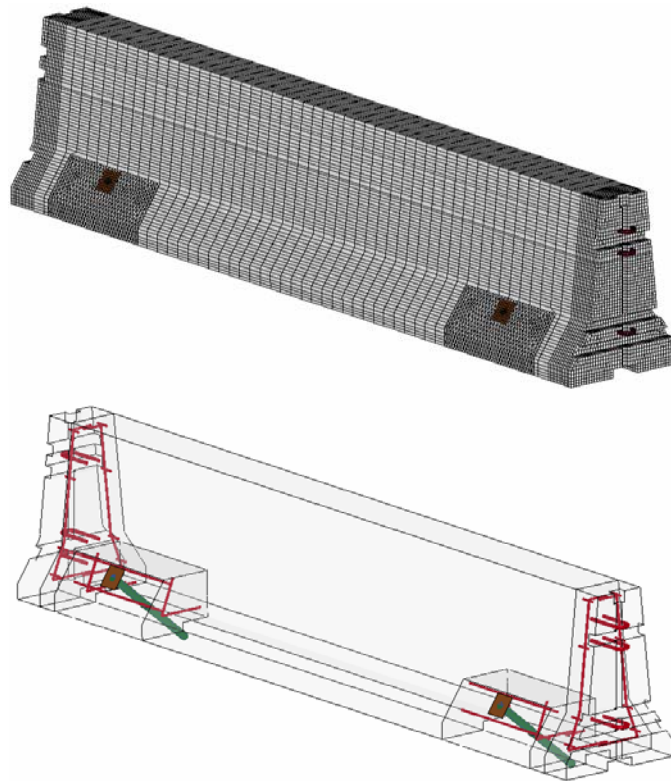


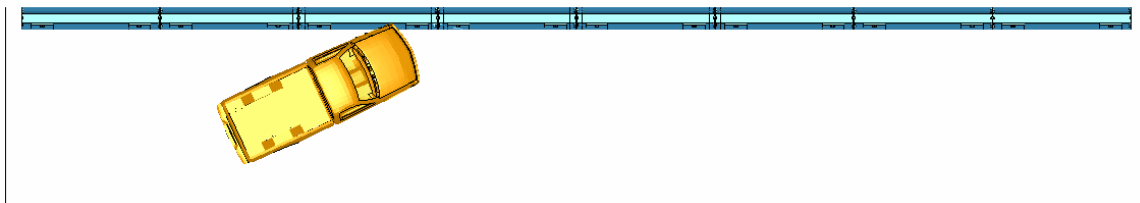
Figure 2.20. Barrier model for the new pinned-down F-shaped barrier.



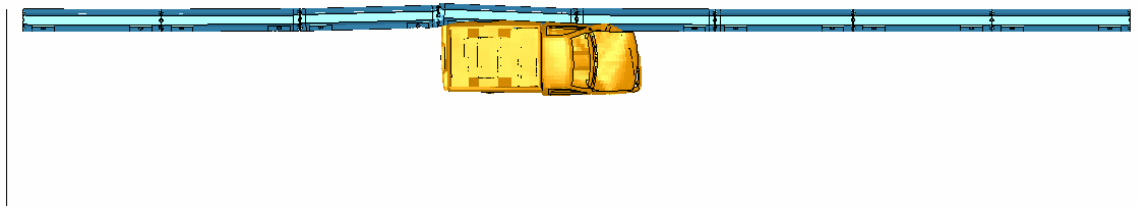
Figure 2.21. System model for the new pinned-down F-shaped barrier.

Simulation Results

The initial vehicle impact simulation was performed with the barrier placed at the edge of the deck drop-off. The results of the simulation are shown in figure 2.22, which indicate that the vehicle was successfully redirected. The maximum deflection of the barrier system was 6.5 inches.



Initial state



Deformed state

Figure 2.22. Simulation results of the new pinned-down F-shaped barrier when placed at the edge of the deck.

Due to the change in the profile of the barrier (i.e. from NJ profile to F-shaped profile), and other design changes such as the decrease in the drop-pin angle and stiffer solid steel loops in the pin-and-loop connection, the climb of the vehicle was reduced in the new pinned-down barrier simulation. Figure 2.23 shows the comparison between vehicle climb in the modified WSDOT pinned barrier simulation and the new F-shaped barrier simulation.

The roll angle of the barriers during impact was also significantly reduced between the new F-shaped barrier simulation and the modified WSDOT pinned barrier model. Figure 2.24 shows this difference for the barrier segment exhibiting maximum roll in both designs. The reduction in the angle of the drop-pins helped restrain barrier-roll and prevented the lifting of the barriers that was observed in the WSDOT test and simulation. Figure 2.25 shows the reduction in the barrier lift between the two designs.

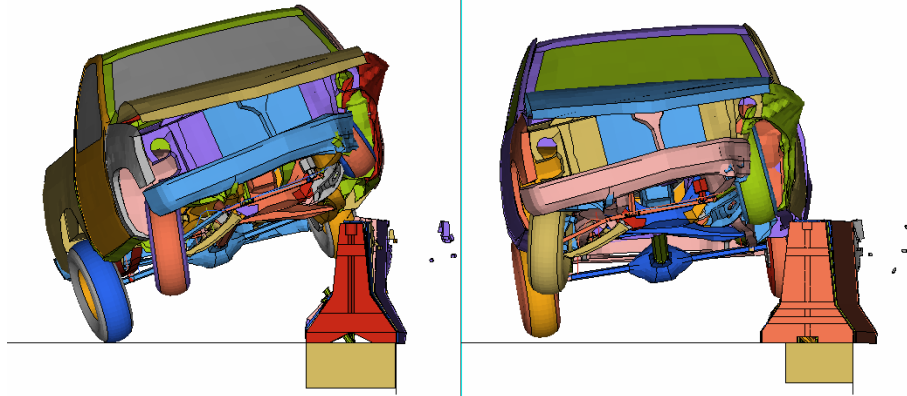


Figure 2.23. Vehicle climb observed in WSDOT barrier (left) and the new pinned-down barrier (right).

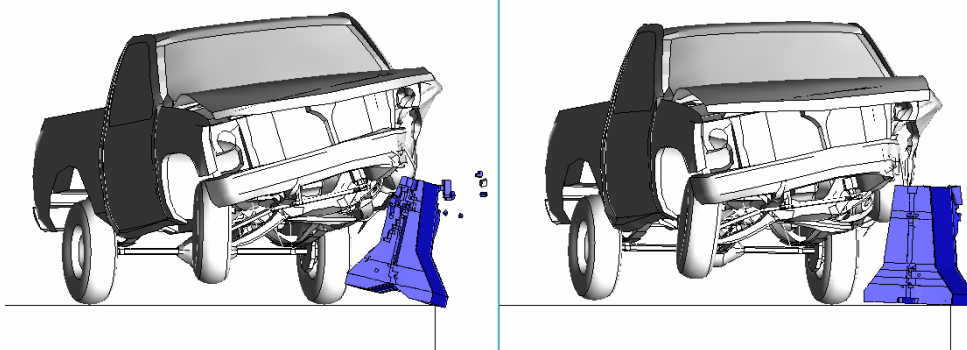


Figure 2.24. Maximum barrier roll in WSDOT barrier (left) and the new pinned-down barrier (right).

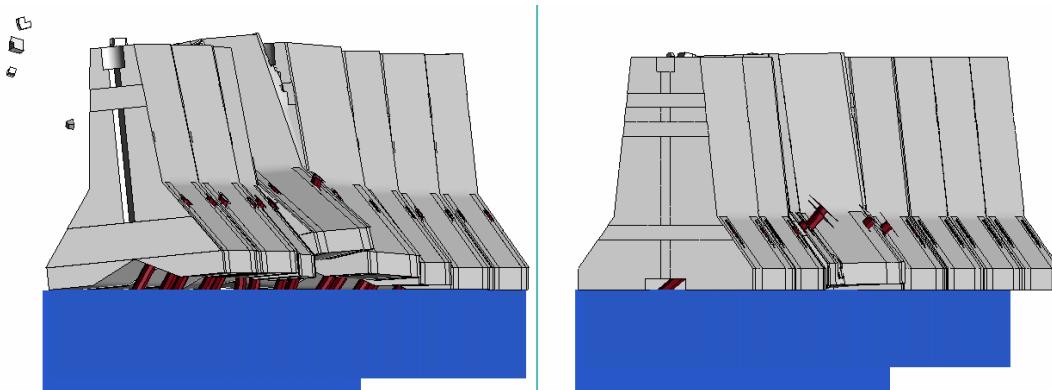


Figure 2.25. Barrier lift observed in the WSDOT simulation (left) is improved in new design (right). (Vehicle not shown).

A simulation with the barrier placed at a 6-inch lateral offset from the edge of the deck drop-off was also performed. The objective of this simulation was to investigate if allowing lateral off-set behind the barrier would positively affect barrier performance by reducing barrier roll. Simulation results did not indicate any significant difference in the barrier roll as shown in figure 2.26.

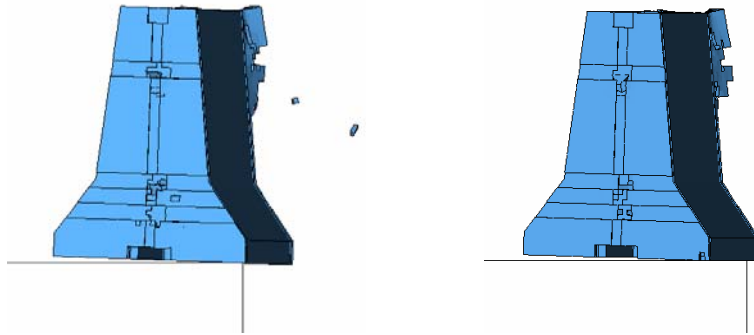


Figure 2.26. Barrier rotation comparison with the barrier placed on edge (left) and barrier placed at a 6-inch offset (right).

While the simulation results indicated an improvement in vehicle climb with the new F-shaped pinned-down barrier compared to the WSDOT pinned barrier design, the vehicle still exhibited a relatively high amount of climb. This high climb is inherent in impacts with safety shaped barriers and is aggravated by the barrier roll angle. Other aspects of the barrier performance, such as barrier roll and barrier lift were significantly improved in the new F-shaped pinned-down barrier. It was therefore concluded that even though the barrier may cause relatively high vehicle climb, the new pinned-down design is expected to result in significant improvement in barrier performance and has a reasonable chance of passing the NCHRP Report 350 Test Level 3 criteria. Subsequently, a crash test was successfully performed with the new F-shaped pinned-down barrier, the details of which are presented in Chapter 5.

CHAPTER 3. TESTING PARAMETERS

TEST FACILITY

The test facilities at the Texas Transportation Institute's Proving Ground consist of a 2000 acre complex of research and training facilities situated 10 mi northwest of the main campus of Texas A&M University. The site, formerly an Air Force Base, has large expanses of concrete runways and parking aprons well suited for experimental research and testing in the areas of vehicle performance and handling, vehicle-roadway interaction, durability and efficacy of highway pavements, and safety evaluation of roadside safety hardware. The site selected for the installation of the pinned temporary barrier system is along the edge a wide out-of-service apron. The apron consists of an unreinforced jointed concrete pavement in 12.5 ft by 15 ft blocks nominally 8-12 inches deep. The apron is over 50 years old and the joints have some displacement, but are otherwise flat and level.

TEST CONDITIONS

According to *NCHRP Report 350*, two tests are recommended to evaluate longitudinal barriers to test level three (TL-3) as described below.

NCHRP Report 350 Test Designation 3-10: 1808 lb vehicle impacting the length of need section at a speed of 62 mi/h and an angle of 20 degrees.

NCHRP Report 350 Test Designation 3-11: 4409 lb pickup truck impacting the length of need section at a speed of 62 mi/h and an angle of 25 degrees.

Due to higher impact energy, test 3-11 results in greater lateral deflection and helps evaluate connection strength and the tendency of the barriers to rotate. An impact following the conditions of *NCHRP Report 350* test 3-10 will not result in any significant lateral deflection of the pinned barrier nor will it impart enough force on the barrier to evaluate connection strength and barrier rotation. Given the pinned barrier will not deflect appreciably when subjected to test 3-10, and test 3-10 has been successfully performed on permanent barriers of the same profile, this test is not considered necessary for evaluation of the pinned barrier connection. Target impact point for test 3-11 was determined to be 4 ft upstream of the joint near one-third point.

The crash test and data analysis procedures were in accordance with guidelines presented in *NCHRP Report 350*. Appendix A presents brief descriptions of these procedures.

EVALUATION CRITERIA

The crash test was evaluated in accordance with the criteria presented in *NCHRP Report 350*. As stated in *NCHRP Report 350*, "Safety performance of a highway appurtenance cannot be measured directly but can be judged on the basis of three factors: structural adequacy,

occupant risk, and vehicle trajectory after collision.” Safety evaluation criteria from table 5.1 of *NCHRP Report 350* were used to evaluate the crash test reported herein.

CHAPTER 4. CRASH TEST 405160-3-1 (NCHRP REPORT 350 TEST NO. 3-11)

TEST ARTICLE – DESIGN AND CONSTRUCTION

The precast concrete segments used in this crash test were 12.5 ft long and had the standard New Jersey profile. The barriers were 32 inches tall, 24 inches wide at the base, and 6 inches wide at the top. The longitudinal reinforcement of the barrier segments consisted of three #5 bars. One of the longitudinal bars was placed near the top of the barrier while the other two were placed in the toe region on each side of the barrier. The vertical reinforcement consisted of three #5 bars that formed an inverted “Y” on each end of the segment.

Adjacent barrier segments were connected using a pin-and-loop type connection. The loops were made of 5/8-inch diameter wire-rope. The inner diameter of the loop was 1.75 inches and it extended 1.5 inches outside the face of the barrier segment. Inside the barrier segment, the wire-rope extended 42.5 inches horizontally towards the center of the barrier. The barrier connection was comprised of two sets of two loops. When installed, the distance between adjacent barrier segments was 0.25 inches. A 1-inch diameter x 26-inch long connecting pin was inserted between the loops to establish the connection. A 2.5-inch diameter x 1/8-inch thick washer was welded to the top of the connecting pin. The pin was held in place by resting the washer on insets built into the ends of adjacent barriers.

Two 1.75-inch diameter holes were drilled into each barrier segment at an angle of 55 degrees from the ground. The holes passed through the barrier and extended into the un-reinforced concrete pavement that had an average thickness of eight inches. The depth of the holes inside the pavement was six inches when measured vertically. The holes were located 22-inches horizontally away from the ends of the barrier segments. A 1.5-inch diameter x 18.375-inch long ASTM A36 steel drop-pin was placed into each hole. A 1/4-inch thick x 2.25-inch diameter washer was welded to the top of each drop-pin. The washers were welded at an 11-degree angle from the vertical so that they matched the profile of the barrier toe.

The completed test installation consisted of eight barrier segments connected together for a total length of approximately 100 ft (30.5 m). Details of the barrier and the pin-down restraint are shown in figures 4.1 through 4.4. Figure 4.5 shows photographs of the completed test installation.

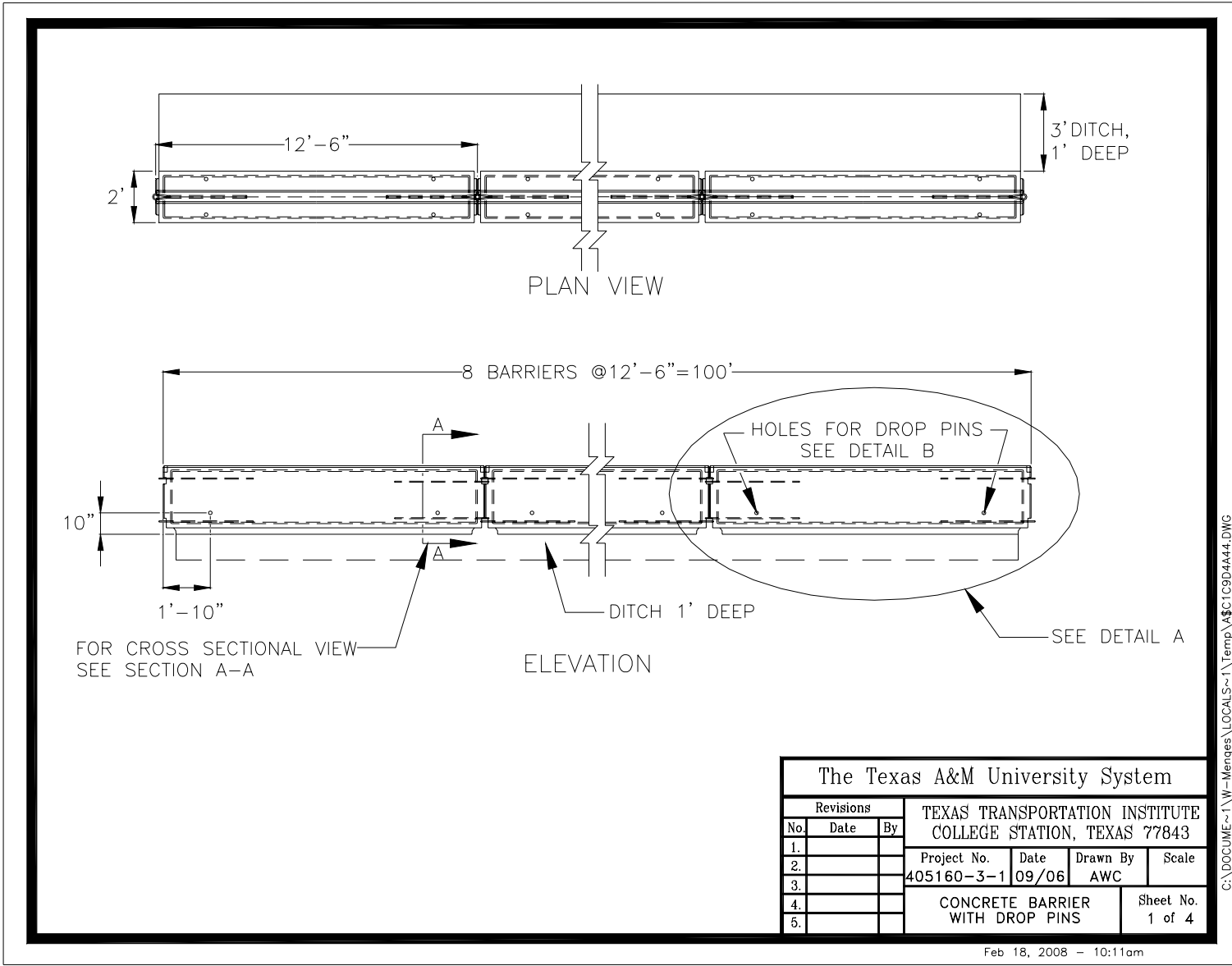


Figure 4.1. Details of the pinned F-shape barrier – layout.

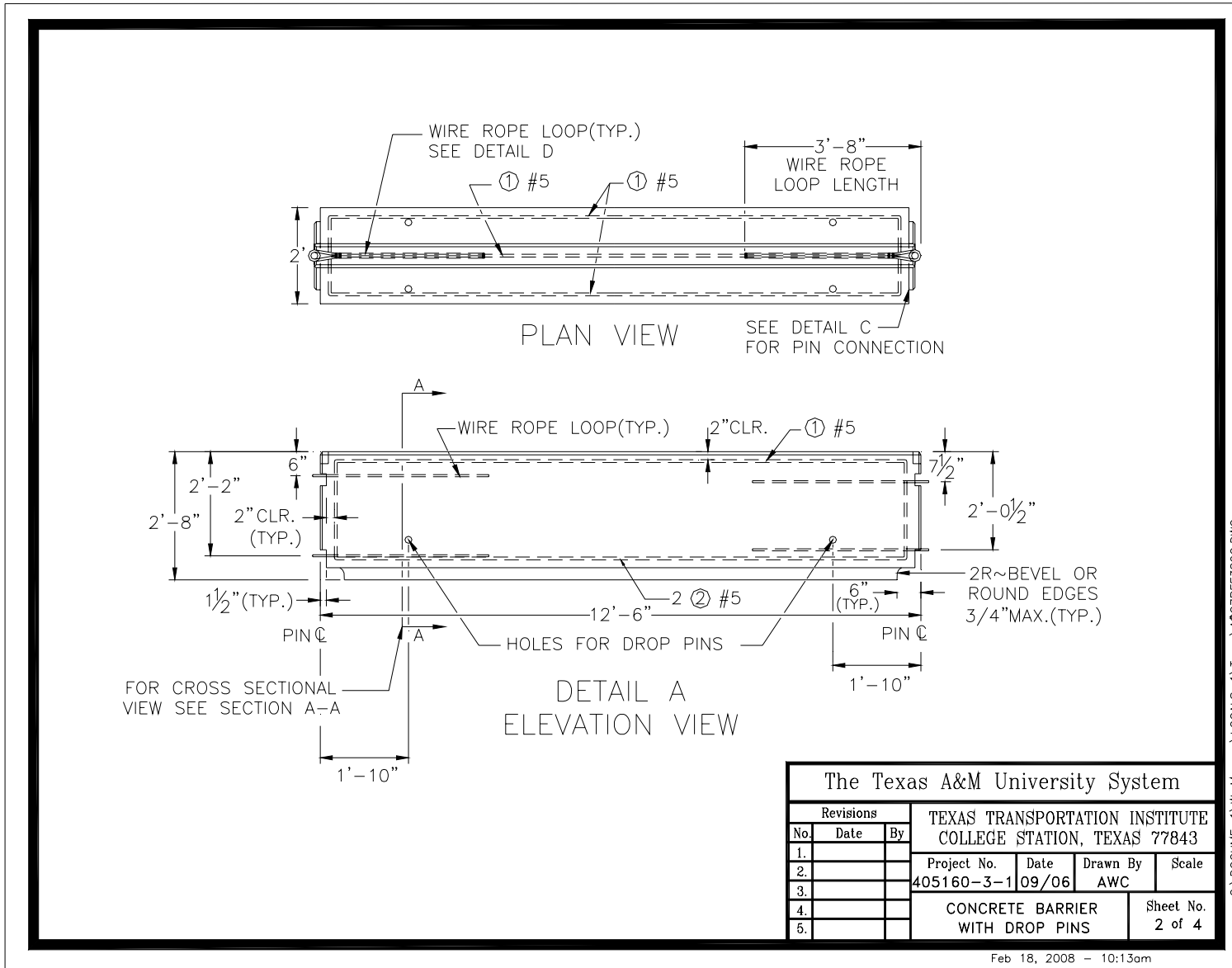


Figure 4.2. Details of the pinned F-shape barrier – detail A.

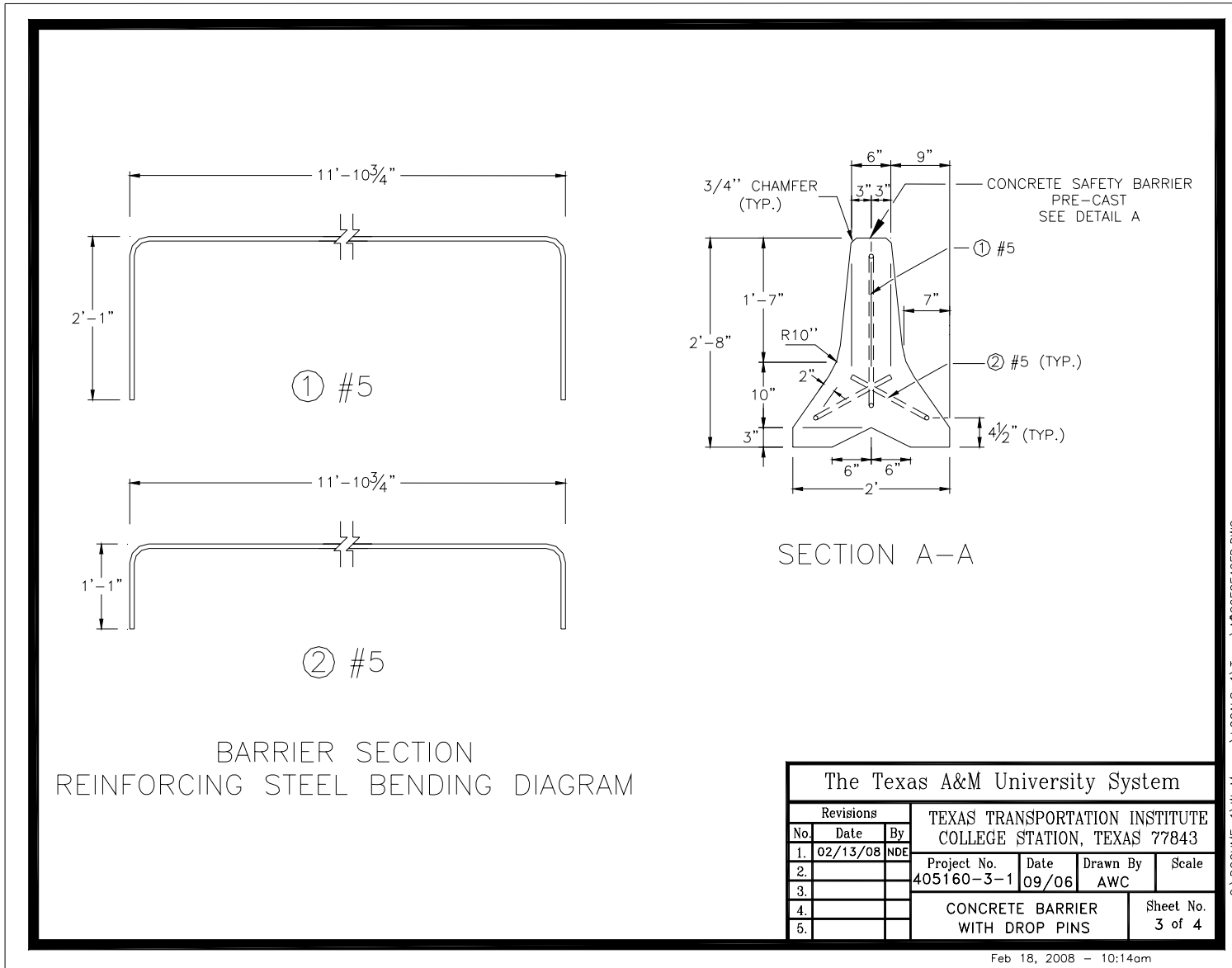


Figure 4.3. Details of the pinned F-shape barrier – cross section.

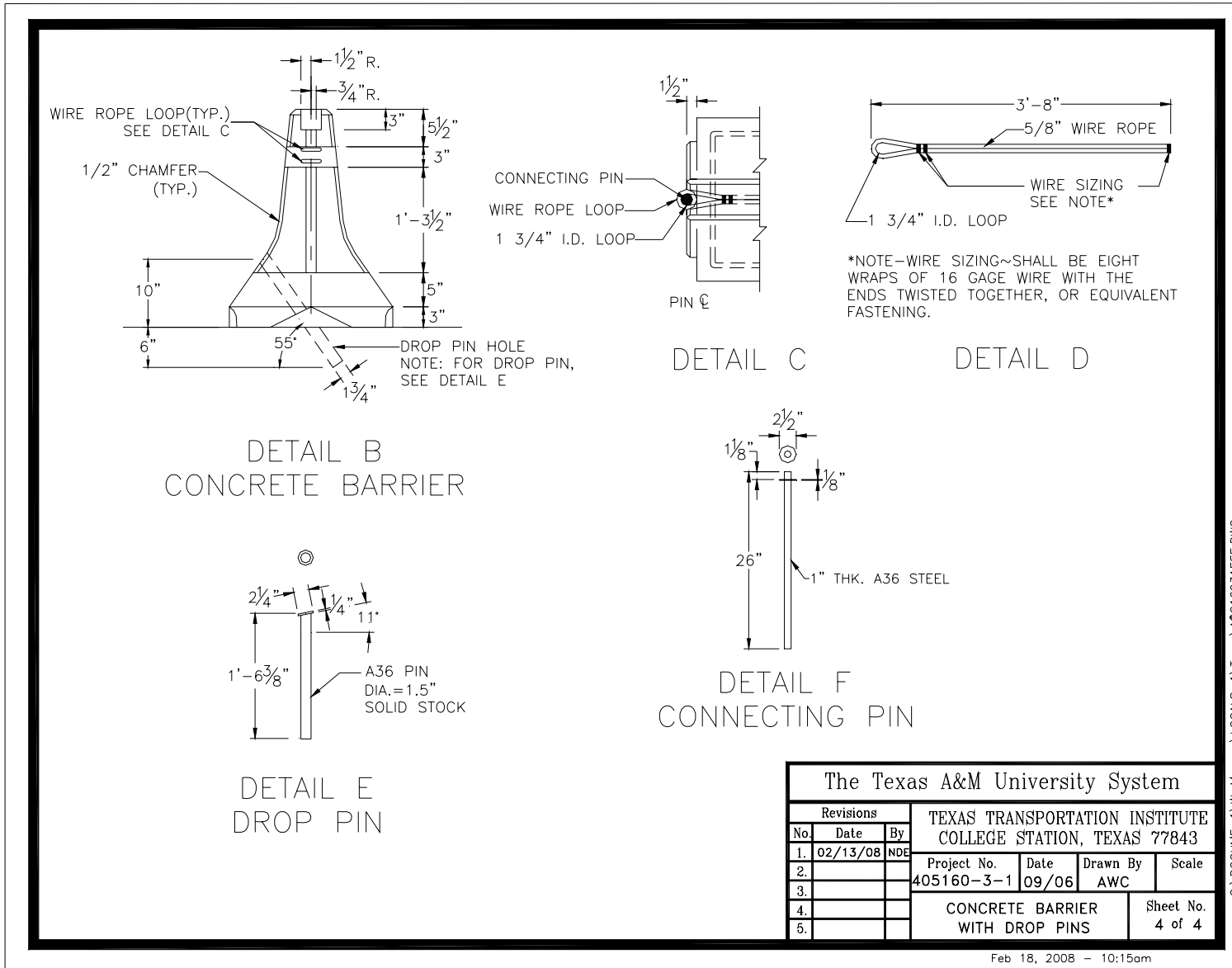


Figure 4.4. Details of the pinned F-shape barrier – rebar.



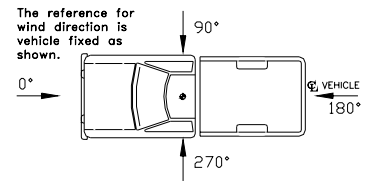
Figure 4.5. Pinned F-shape barrier prior to testing.

TEST VEHICLE

A 2000 Chevrolet C2500 pickup truck, shown in figures 4.6 and 4.7, was used for the crash test. Test inertia weight of the vehicle was 4575 lb, and its gross static weight was 4575 lb. The height to the lower edge of the vehicle front bumper was 16.25 inches, and the height to the upper edge of the front bumper was 25.0 inches. Additional dimensions and information on the vehicle are given in appendix B, figure B1. The vehicle was directed into the installation using the cable reverse tow and guidance system, and was released to be free-wheeling and unrestrained just prior to impact.

WEATHER CONDITIONS

The crash test was performed the morning of September 19, 2006. Weather conditions at the time of testing were: Wind speed: 4 mi/h; wind direction: 170 degrees with respect to the vehicle (vehicle was traveling in a southeasterly direction); temperature: 76 °F; relative humidity: 50 percent.



IMPACT DESCRIPTION

The 2000 Chevrolet C2500 pickup truck, traveling at an impact speed of 61.6 mi/h, impacted the installation 4.4 ft upstream of joint 3-4 at an impact angle of 26.5 degrees. At 0.036 s, the vehicle began to redirect, and at 0.044 s, the fourth segment began to move toward the field side. The third segment began to move toward the field side at 0.049 s, and the vehicle began to climb the face of the barrier at 0.078 s. At 0.152 s, the fifth segment began to move toward the field side, and at 0.300 s, the vehicle was traveling parallel with the installation at a speed of 51.8 mi/h. The second segment began to move toward the field side at 0.303 s. As the vehicle exited the view of the overhead camera, the vehicle was traveling along the top of the segments at a speed of 51.4 mi/h. The first three segments fell into the ditch to the field side of the barrier, and part of the fourth segment fell in the ditch with part remaining on the concrete. Sequential photographs of the test period are shown in appendix C, figures C1 and C2.

DAMAGE TO TEST ARTICLE

As shown in figures 4.8 and 4.9, the first three segments fell into the ditch to the field side of the barrier. Part of the fourth segment fell in the ditch with part remaining on the concrete surface. The remaining segments remained completely on the concrete surface. The vehicle contacted the installation 4.4 ft upstream of the joint between segments 3 and 4, and remained in contact to the end of the installation, for a total length of contact of 64.3 ft. Concrete around one of the drop-pins failed catastrophically, exposing the longitudinal rebar as shown in figure 4.10. This was the upstream pin of the fourth barrier. There was no concrete failure observed at other drop-pin locations. No significant failure was observed in the concrete pavement around the drop-pin holes.



Figure 4.6. Vehicle/installation geometrics for test 405160-3-1.



Figure 4.7. Vehicle before test 405160-3-1.



Figure 4.8. Vehicle trajectory path after test 405160-3-1.



Figure 4.9. Installation after test 405160-3-1.



Figure 4.10. Concrete failure around the upstream drop-pin of the forth barrier segment after test 405160-3-1.

VEHICLE DAMAGE

Damage to the vehicle is shown in figure 4.11. Structural damage included deformed right front frame rail, sway bar, right upper and lower A-arm, and right tie rod end; the right side rear U-bolts broke and the rear axle was pushed back. Also damaged were the front bumper, hood, grill, right and left front quarter panels, right front tire and wheel rim, right door, right rear exterior bed, and right rear tire and wheel rim. The windshield was cracked in the right lower corner. The left door, door glass, and left exterior bed were damaged due to the impact. Maximum exterior crush to the vehicle was 19.7 inches in the side plane at the right front corner at bumper height. Maximum occupant compartment deformation was 1.0 inch in the right side firewall area near the toe pan. Exterior vehicle crush and occupant compartment measurements are shown in appendix B, tables B1 and B2.

OCCUPANT RISK FACTORS

Data from the triaxial accelerometer, located at the vehicle center of gravity, were digitized to compute occupant impact velocity and ridedown accelerations. Only the occupant impact velocity and ridedown accelerations in the longitudinal axis are required from these data for evaluation of criterion L of *NCHRP Report 350*. In the longitudinal direction, occupant impact velocity was 15.4 ft/s at 0.117 s, maximum 0.010-s ridedown acceleration was -4.1 g's from 0.212 to 0.222 s, and the maximum 0.050-s average was -6.8 g's between 0.020 and 0.070 s. In the lateral direction, the occupant impact velocity was 15.7 ft/s at 0.117 s, the highest 0.010-s occupant ridedown acceleration was -4.8 g's from 0.118 to 0.128 s, and the maximum 0.050-s average was -7.5 g's between 0.034 and 0.084 s. These data and other information pertinent to the test are presented in figure 4.12. Vehicle angular displacements and accelerations versus time traces are shown in appendix D, figures D1 through D7.

ASSESSMENT OF TEST RESULTS

Following is an assessment of the test based on the applicable *NCHRP Report 350* safety evaluation criteria.

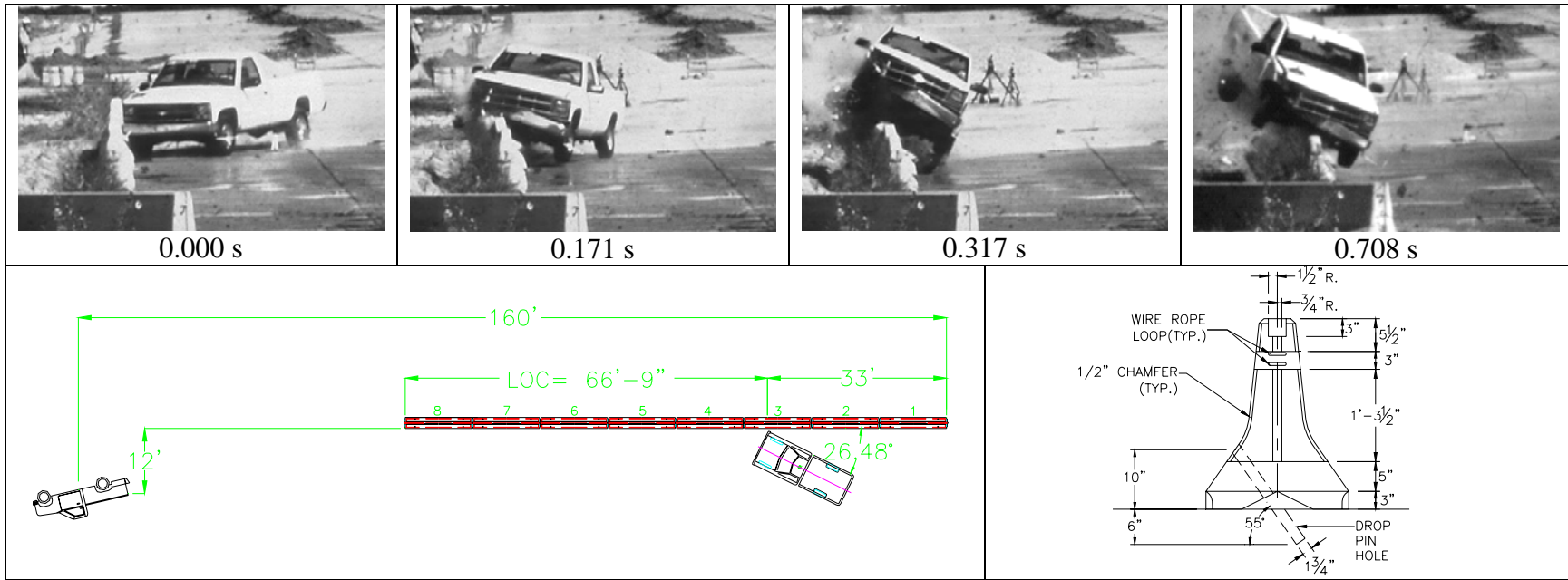
Structural Adequacy

- A. *Test article should contain and redirect the vehicle; the vehicle should not penetrate, underride, or override the installation although controlled lateral deflection of the test article is acceptable.*

Results: The barrier segments at impact began to rotate toward the field side and the 2000P vehicle rode up the traffic face of the barrier. As the vehicle reached the top of the barriers, the first three segments and part of the fourth segment rotated into the ditch on the field side of the installation.
(FAIL)



Figure 4.11. Vehicle after test 405160-3-1.



General Information

Test Agency..... Texas Transportation Institute
 Test No. 405160-3-1
 Date 09-19-2006

Test Article

Type..... Pinned Temporary Barrier
 Name Pinned F-Shape CMB
 Installation Length (ft) 100
 Material or Key Elements 12.5 ft long NJ profile precast concrete segments with pin-and-loop connection with two 1.75-inch diameter holes drilled into each barrier segment at 55 degrees with 1.5-inch diameter 18.375-inch long ASTM A36 steel drop-pin anchors
 Soil Type and Condition..... Concrete Pavement, Dry

Test Vehicle

Designation..... 2000P
 Model..... 2000 Chevrolet C2500 Pickup Truck
 Mass (lb)
 Curb..... 4760
 Test Inertial..... 4575
 Dummy No Dummy
 Gross Static..... 4575

Impact Conditions

Speed (mi/h) 61.6
 Angle (deg) 26.5

Exit Conditions

Speed (km/h) N.A.
 Angle (deg) Parallel

Occupant Risk Values

Impact Velocity (ft/s)
 Longitudinal 15.4
 Lateral 15.7
 THIV (km/h) 23.3
 Ridedown Accelerations (g's)
 Longitudinal -4.1
 Lateral -4.8
 PHD (g's) 5.3
 ASI 0.96
 Max. 0.050-s Average (g's)
 Longitudinal -6.8
 Lateral -7.5
 Vertical -4.1

Test Article Deflections (ft)

Dynamic N.A.
 Permanent..... N.A.
 Working Width..... N.A.

Vehicle Damage

Exterior
 VDS..... 01RFQ5
 CDC 01FREW5
 Max. Exterior
 Vehicle Crush (inch)..... 19.7
 Interior
 OCDI RF0001000
 Max. Occupant Compartment
 Deformation (inch) 1.0

Post-Impact Behavior

(during 1.0 sec after impact)
 Max. Yaw Angle (deg)..... -35
 Max. Pitch Angle (deg)..... 10
 Max. Roll Angle (deg) -36

Figure 4.12. Summary of results for NCHRP Report 350 test 3-11 on the pinned F-shape barrier.

Occupant Risk

D. Detached elements, fragments, or other debris from the test article should not penetrate or show potential for penetrating the occupant compartment, or present an undue hazard to other traffic, pedestrians, or personnel in a work zone. Deformation of, or intrusions into, the occupant compartment that could cause serious injuries should not be permitted.

Results: No detached elements, fragments, or other debris was present to penetrate or show potential to penetrate the occupant compartment. Maximum occupant compartment deformation was 1 inch. However, the barriers rotated toward the field side and fell over into the ditch, which would be hazardous and unacceptable when used on a bridge deck. (FAIL)

F. The vehicle should remain upright during and after collision although moderate roll, pitching, and yawing are acceptable.

Results: The vehicle remained upright during the impact event, however it rolled over onto its side after exiting the installation and impacting a concrete barrier segment placed further downstream to guard photography equipment. (FAIL)

Vehicle Trajectory

K. After collision, it is preferable that the vehicle's trajectory not intrude into adjacent traffic lanes.

Result: The vehicle came to rest on its side 160 ft downstream of impact and 12 ft forward of the traffic face of the installation. (FAIL)

L. The occupant impact velocity in the longitudinal direction should not exceed 12 m/s and the occupant ridedown acceleration in the longitudinal direction should not exceed 20 g's.

Result: Longitudinal occupant impact velocity was 15.4 ft/s, and longitudinal ridedown acceleration was -4.1 g's. (PASS)

M. The exit angle from the test article preferably should be less than 60 percent of the test impact angle, measured at time of vehicle loss of contact with the test device.

Result: The vehicle was traveling parallel with the installation as it lost contact. (PASS)

The following supplemental evaluation factors and terminology, as presented in the FHWA memo entitled "Action: Identifying Acceptable Highway Safety Features," were used for visual assessment of test results: ⁽⁷⁾

Passenger Compartment Intrusion

- 1. Windshield Intrusion
 - a. No windshield contact
 - b. Windshield contact, no damage
 - c. Windshield contact, no intrusion
 - d. Device embedded in windshield, no significant intrusion
 - e. Complete intrusion into passenger compartment
 - f. Partial intrusion into passenger compartment
- 2. Body Panel Intrusion yes or no

Loss of Vehicle Control

- 1. Physical loss of control
- 2. Loss of windshield visibility
- 3. Perceived threat to other vehicles
- 4. Debris on pavement

Physical Threat to Workers or Other Vehicles

- 1. Harmful debris that could injure workers or others in the area
 - 2. Harmful debris that could injure occupants in other vehicles
- The barriers rotated toward the field side and fell over into the ditch, which would be hazardous and unacceptable when used on a bridge deck.

Vehicle and Device Condition

- 1. Vehicle Damage
 - a. None
 - b. Minor scrapes, scratches or dents
 - c. Significant cosmetic dents
 - d. Major dents to grill and body panels
- 2. Windshield Damage
 - a. None
 - b. Minor chip or crack
 - c. Broken, no interference with visibility
 - d. Broken or shattered, visibility restricted but remained intact
 - e. Major structural damage
 - f. Shattered, remained intact but partially dislodged
 - g. Large portion removed
 - h. Completely removed
- 3. Device Damage
 - a. None
 - b. Superficial
 - c. Substantial, but can be straightened
 - d. Substantial, replacement parts needed for repair
 - e. Cannot be repaired

CHAPTER 5. CRASH TEST 405160-3-2a (NCHRP REPORT 350 TEST NO. 3-11)

TEST ARTICLE – DESIGN AND CONSTRUCTION

The precast concrete segments used in this crash test were 12.5 ft long and had the standard “F” profile. The barriers were 32 inches tall, 24 inches wide at the base, and 9.5 inches wide at the top. Horizontal barrier reinforcement consisted of eight #4 bars spaced at heights of 3-3/4 inches, 12-7/8 inches, 21-1/8 inches, and 29-3/8 inches from the bottom of the barrier within the vertical reinforcement. Vertical barrier reinforcement consisted of pairs of #4 bars spaced 18 inches on centers. These vertical bars were bent in a “hook” fashion to conform to the F-shape barrier profile and to provide sufficient concrete cover for the drainage scupper and the horizontal inset at the base of the barrier. For the two vertical bar pairs adjacent to the ends of the barrier segments, the spacing was reduced to 16.75 inches and 9 inches, respectively.

Adjacent barrier segments were connected using a pin-and-loop type connection. The loops were made of 3/4-inch diameter round stock steel. The outer diameter of the loops was 3.5 inches and they extended 2 inches outside the end of the barrier segment. The barrier connection was comprised of two sets of three loops. When installed, the distance between adjacent barrier segments was 0.25 inches. A 1-inch diameter × 30-inch long ASTM A449 connecting pin was inserted between the loops to establish the connection. A 2-inch diameter × 1/4-inch thick washer was welded 3/4 inches from the top of the connecting pin. The pin was held in place by resting the washer on insets built into the faces of adjacent barriers.

Two 1.875-inch diameter holes inclined 40 degrees from the ground, were cast into the toe of each barrier segment. The holes started from the traffic face of the barrier and exited the near its bottom centerline. The holes in the barrier were used as a guide to drill 1.75 inch diameter holes into the un-reinforced concrete pavement. The depth of the holes inside the pavement was 6.25 inches when measured vertically. The average thickness of concrete pavement was 8 inches. The holes for the drop-pins were located 16-inches horizontally away from the ends of the barrier segments. A 1.5-inch diameter × 21.25-inch long ASTM A36 steel drop-pin was placed into each hole. A 1/2-inch thick, 4-inch×4-inch A36 plate cover was welded to the top of each drop-pin. The plate covers were welded at a 5-degree angle from the vertical so that they matched the profile of the barrier toe.

Inside the barrier segments, a 22-inch long U-shaped #4 bar was diagonally placed at the location of each drop-pin hole. The U-shaped bar was placed around the drop-pin hole to provide resistance to drop-pin pullout in the event of concrete failure in the vicinity of the hole.

The completed test installation consisted of eight barrier segments connected together for a total length of approximately 100 ft. Details of the barrier and the pin-down restraint are shown in figures 5.1 through 5.9. Figure 5.10 shows photographs of the completed test installation.

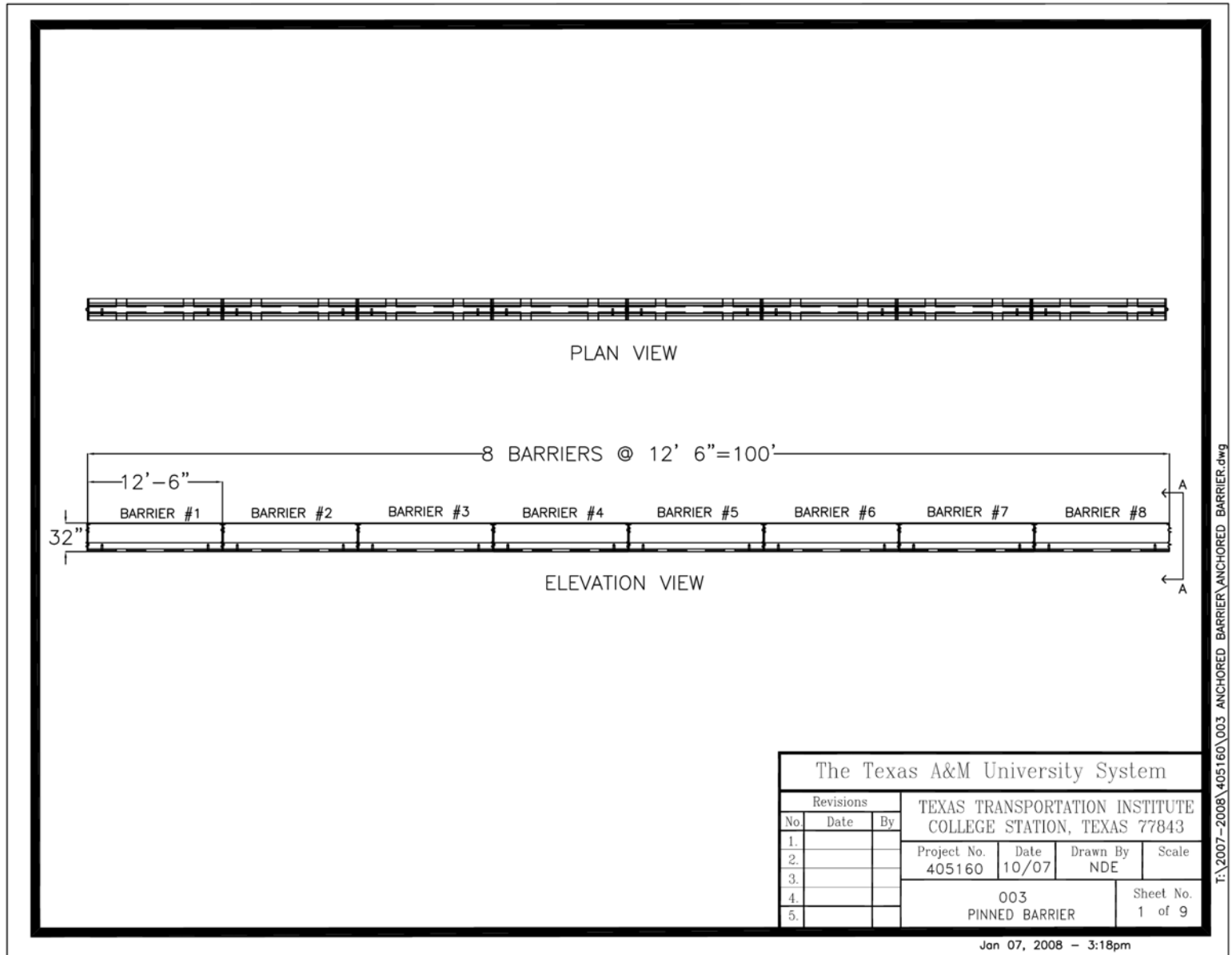


Figure 5.1. Details of the pinned F-shape barrier – installation layout.

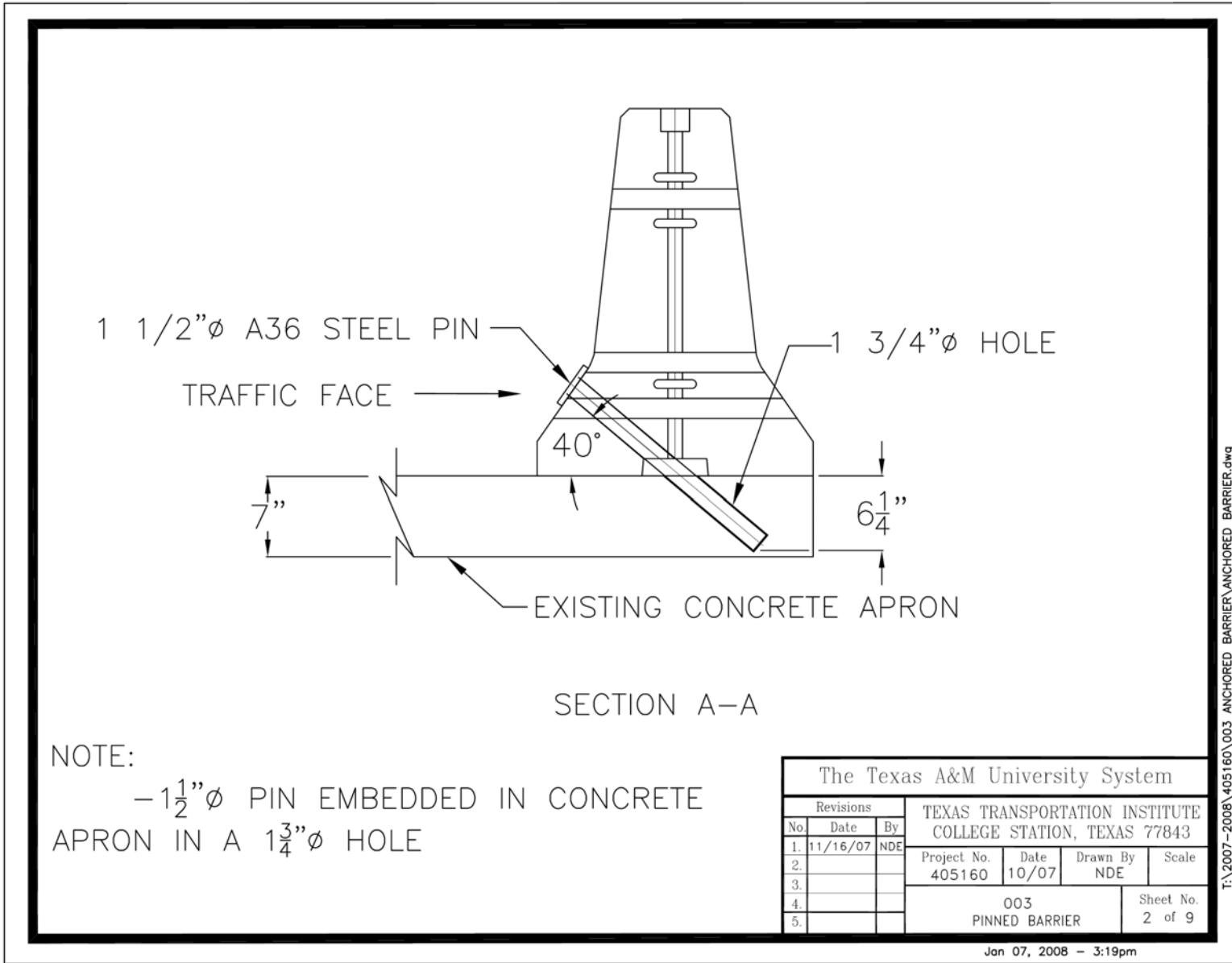
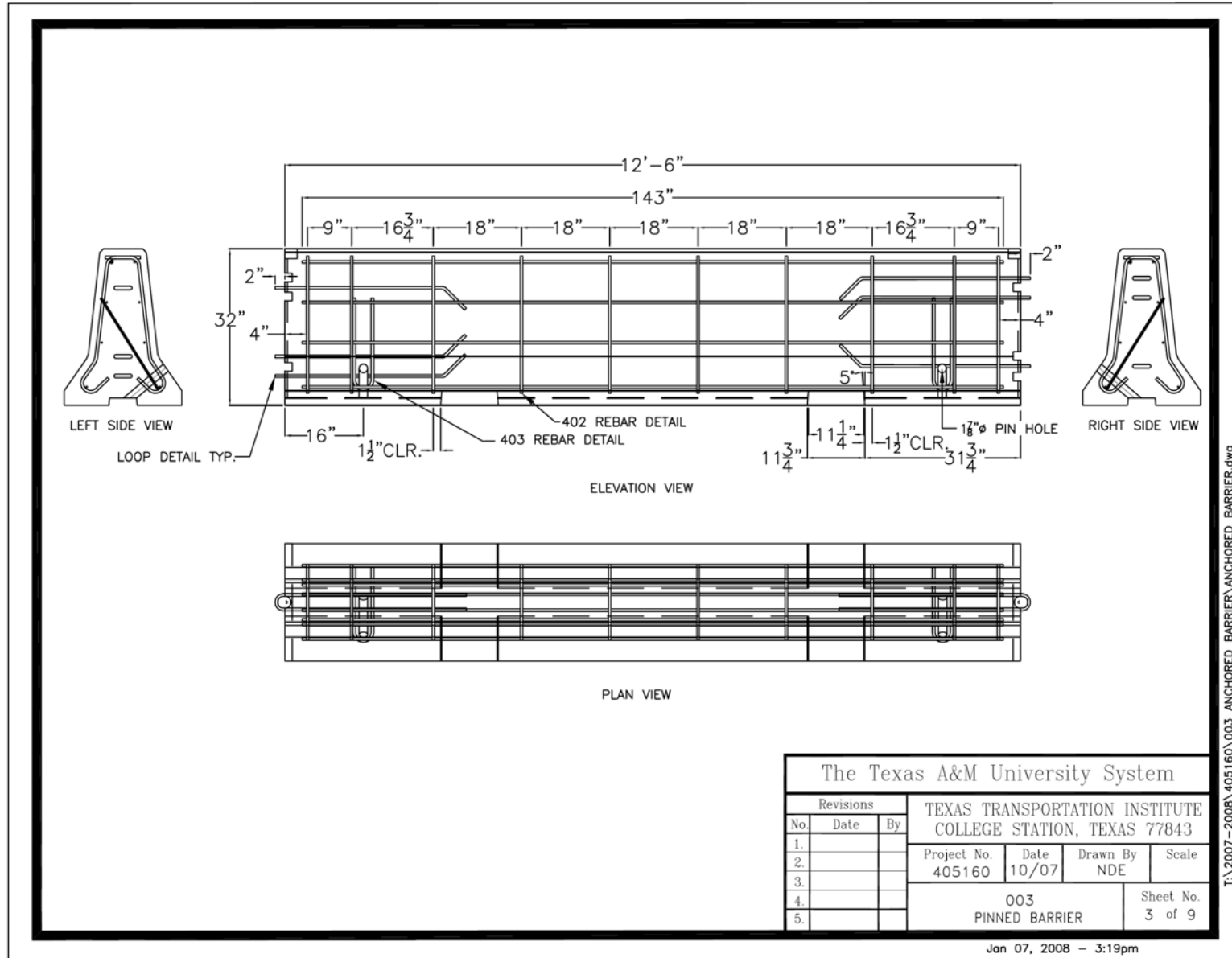


Figure 5.2. Details of the pinned F-shape barrier – Section A-A.



The Texas A&M University System			
TEXAS TRANSPORTATION INSTITUTE COLLEGE STATION, TEXAS 77843			
Project No.		Date	Drawn By
405160		10/07	NDE
003 PINNED BARRIER			Sheet No. 3 of 9

Jan 07, 2008 - 3:19pm

T:\2007-2008\405160\003 ANCHORED BARRIER\ANCHORED BARRIER.dwg

Figure 5.3. Details of the pinned F-shape barrier –segment detail.

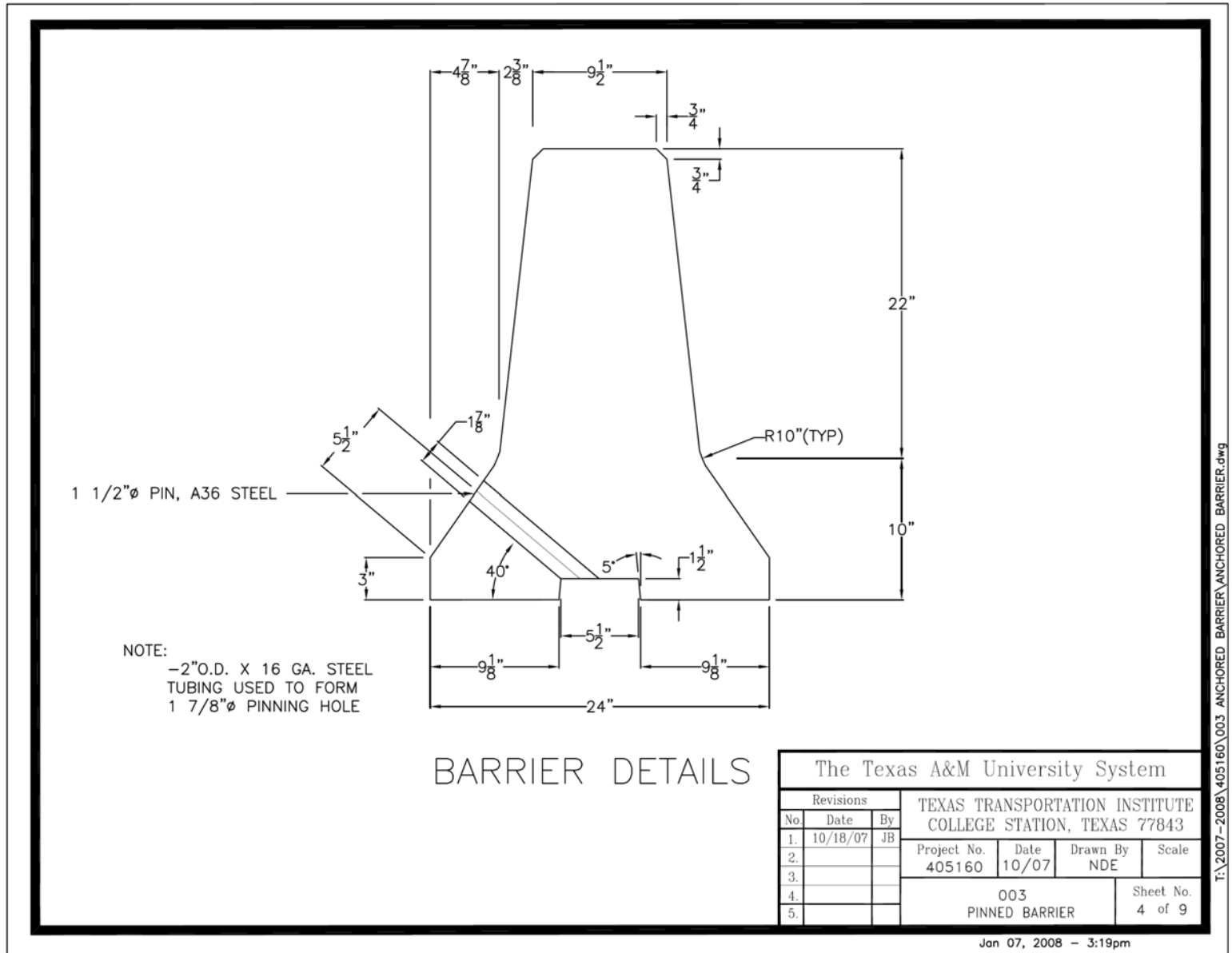
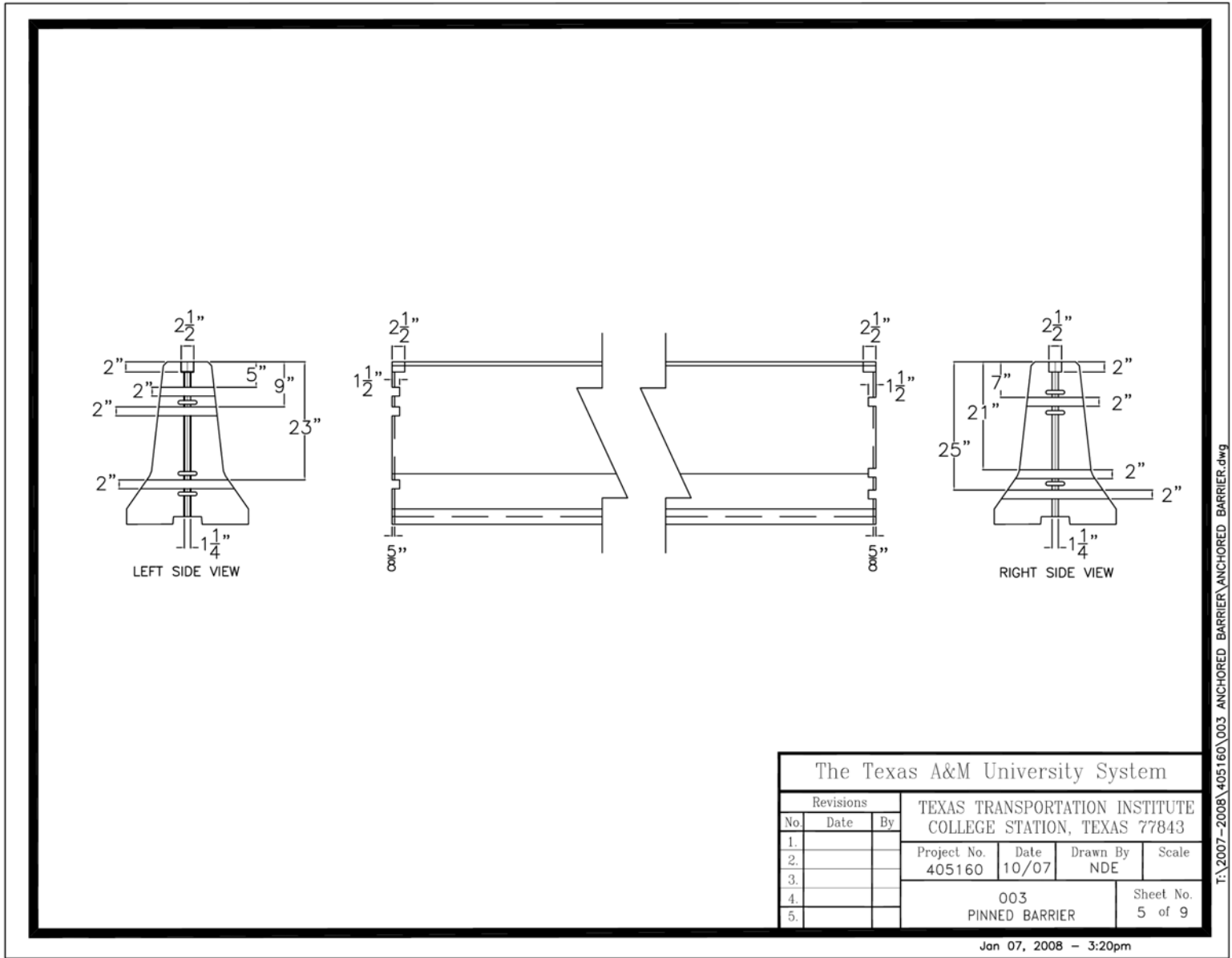


Figure 5.4. Details of the pinned F-shape barrier – cross section.

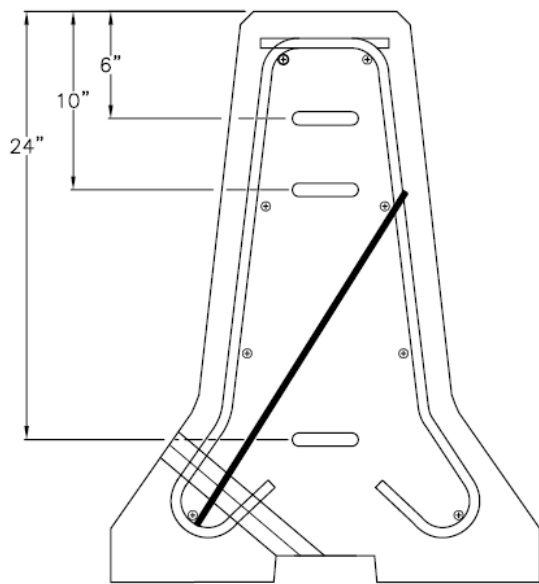


The Texas A&M University System			
TEXAS TRANSPORTATION INSTITUTE COLLEGE STATION, TEXAS 77843			
Revisions		Project No.	Date
No.	Date	By	Drawn By
1.			NDE
2.			
3.			
4.			
5.			
003 PINNED BARRIER			Scale
			Sheet No. 5 of 9

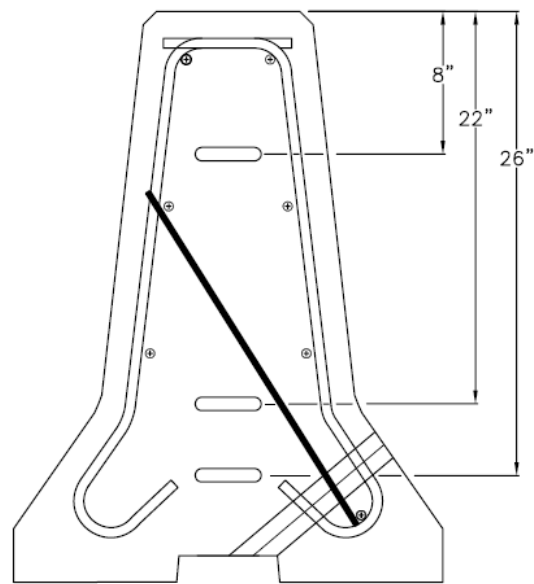
T:\2007-2008\405160\003 ANCHORED BARRIER\ANCHORED BARRIER.dwg

Jan 07, 2008 - 3:20pm

Figure 5.5. Details of the pinned F-shape barrier – barrier details.



RIGHT SIDE VIEW



LEFT SIDE VIEW

Revisions				The Texas A&M University System			
No.	Date	By	TEXAS TRANSPORTATION INSTITUTE COLLEGE STATION, TEXAS 77843				
1.	10/18/07	JB	Project No.	Date	Drawn By	Scale	
2.	10/22/07	NDE	405160	10/07	NDE		
3.			003			Sheet No.	
4.			PINNED BARRIER			6 of 9	
5.							

Jan 07, 2008 - 3:20pm

T:\2007-2008\405160\003 ANCHORED BARRIER\ANCHORED BARRIER.dwg

Figure 5.6. Details of the pinned F-shape barrier – pin placement.

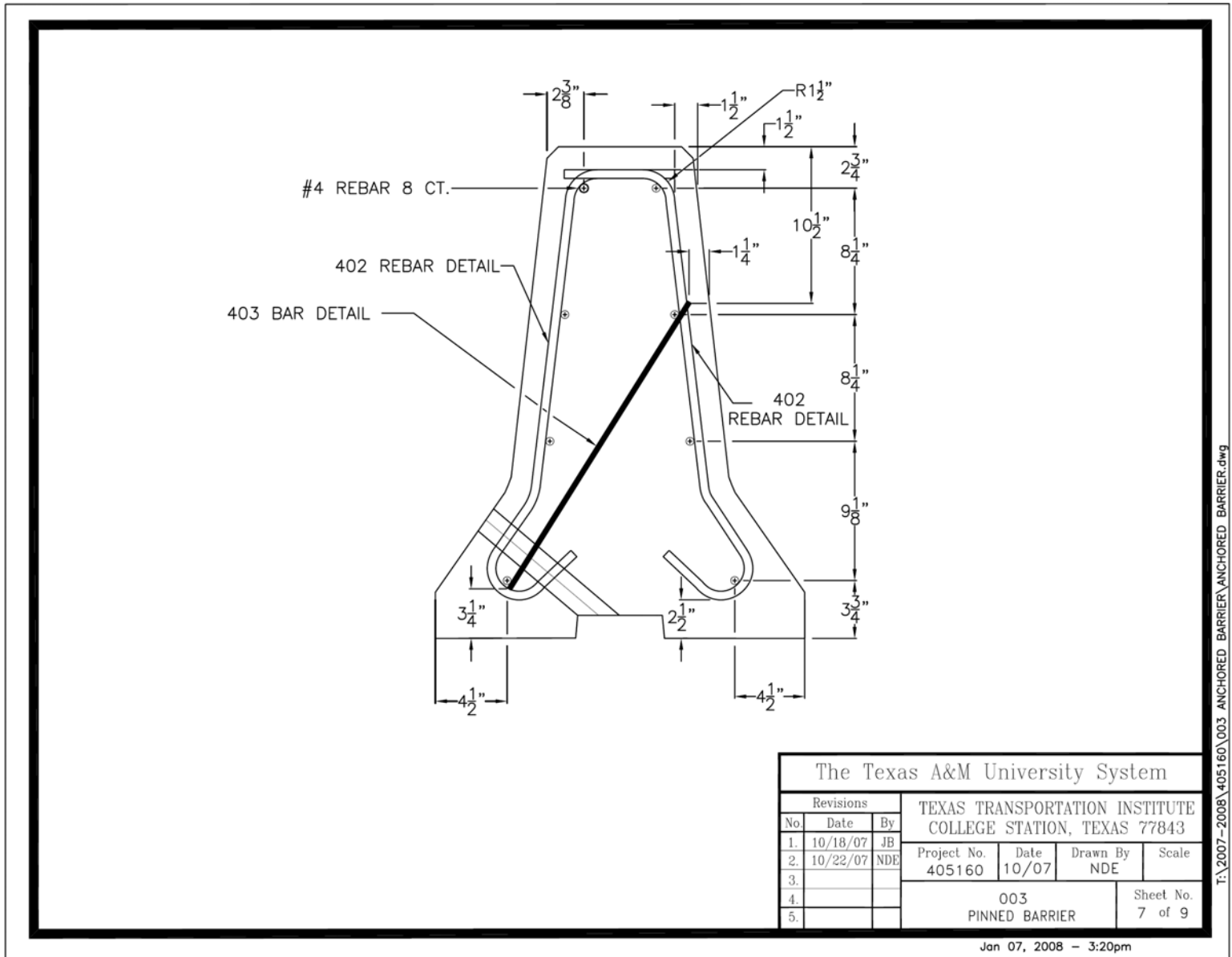
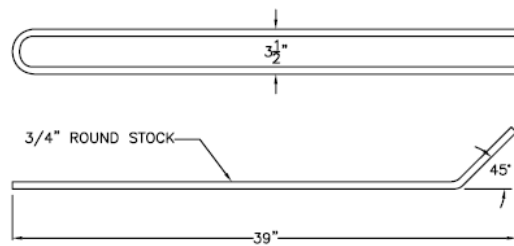
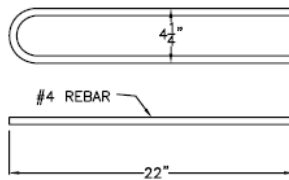


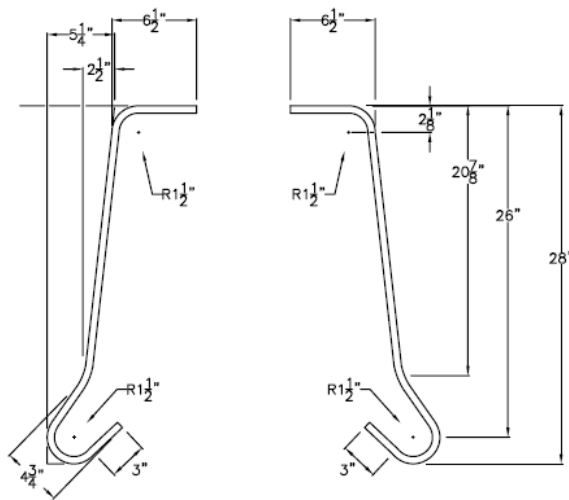
Figure 5.7. Details of the pinned F-shape barrier – rebar placement.



LOOP DETAIL
6 CT. PER BARRIER



403 REBAR DETAIL
2 CT. PER BARRIER



402 REBAR DETAIL
18 CT. PER BARRIER

The Texas A&M University System				
Revisions			TEXAS TRANSPORTATION INSTITUTE COLLEGE STATION, TEXAS 77843	
No.	Date	By	Project No.	Date
1.	10/18/07	JB	405160	10/07
2.	10/22/07	NDE	Drawn By	Scale
3.			NDE	
4.			003 PINNED BARRIER	
5.			Sheet No. 8 of 9	

Jan 07, 2008 - 3:21pm

I:\2007-2008\405160\003 ANCHORED BARRIER\ANCHORED BARRIER.dwg

Figure 5.8. Details of the pinned F-shape barrier – rebar details.

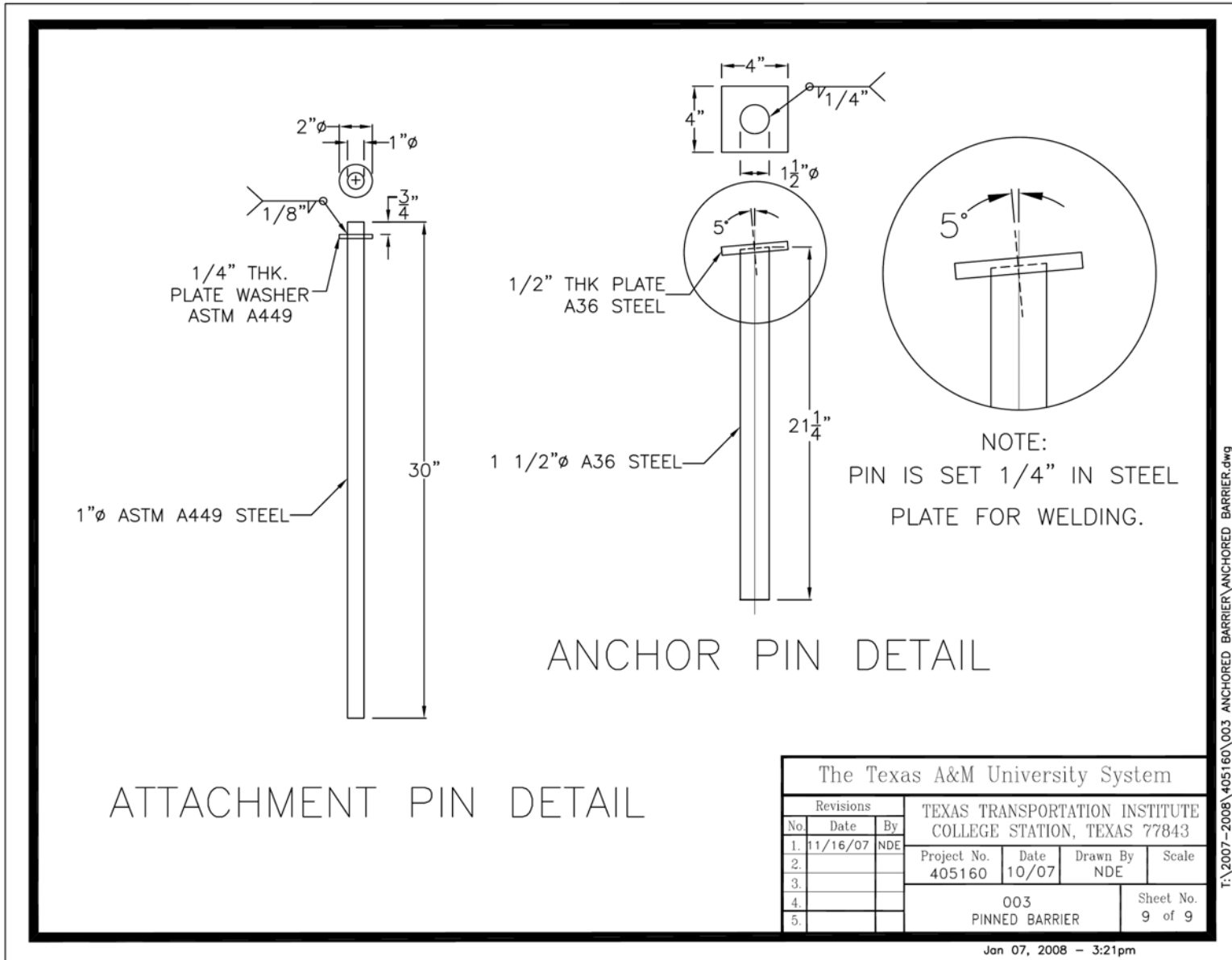


Figure 5.9. Details of the pinned F-shape barrier – pin details.



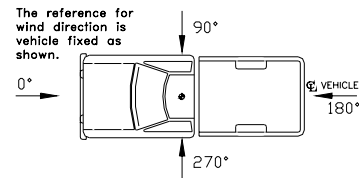
Figure 5.10. Pinned F-shape barrier prior to testing.

TEST VEHICLE

A 2000 Chevrolet C2500 pickup truck, shown in figures 5.11 and 5.12, was used for the crash test. Test inertia weight of the vehicle was 4674 lb, and its gross static weight was 4674 lb. The height to the lower edge of the vehicle front bumper was 16.25 inches, and the height to the upper edge of the front bumper was 25.0 inches. Additional dimensions and information on the vehicle are given in appendix B, figure B2. The vehicle was directed into the installation using the cable reverse tow and guidance system, and was released to be free-wheeling and unrestrained just prior to impact.

WEATHER CONDITIONS

The crash test was performed the morning of November 15, 2007. Weather conditions at the time of testing were: Wind speed: 10-15 mi/h; wind direction: 25 degrees with respect to the vehicle (vehicle was traveling in a southeasterly direction); temperature: 63 °F; relative humidity: 23 percent.



IMPACT DESCRIPTION

The 2000 Chevrolet C2500 pickup truck, traveling at an impact speed of 62.7 mi/h, impacted the installation 4.0 ft upstream of joint 3-4 at an impact angle of 25.4 degrees. Shortly after impact, segment 3 began to deflect toward the field side, and at 0.012 s, segment 3 began to rise and lose contact with the surface of the ground. At 0.015 s, the joint between segment 2 and 3 began to open up, and at 0.018 s, segment 4 began to deflect toward the field side. The vehicle began to redirect at 0.032 s, and the vehicle contacted the end of segment 4 at 0.034 s. The front edge of segments 2, 5, 1, 6, and 7 began to rise at 0.057 s, 0.066 s, 0.086 s, 0.095 s, and 0.111 s, respectively. By 0.121 s, the front bumper reached the top of the barrier, and at 0.170 s, the left rear tire contacted the toe of the barrier. At 0.181 s, the vehicle contacted the end of segment 5, and at 0.205 s, the left rear tire on the vehicle ruptured. At 0.283 s, the vehicle began to travel parallel with the barrier at a speed of 46.8 mi/h. The right rear tire contacted the barrier face at 0.387 s. Segment 1 and 2 re-contacted the ground at 0.479 s and 0.551 s, respectively. At 0.695 s, the left rear tire contacted the face of the rear of the barrier, and at 0.847 s, the vehicle lost contact with the end of the barrier. Exit speed and angle were not obtainable due to excessive dust. Brakes on the vehicle were applied, and the vehicle subsequently came to rest facing the installation 190 feet downstream of the impact point and aligned with the traffic face. Sequential photographs of the test period are shown in appendix C, figures C3 and C4.



Figure 5.11. Vehicle/installation geometrics for test 405160-3-1.



Figure 5.12. Vehicle before test 405160-3-1.

DAMAGE TO TEST ARTICLE

Damage to the installation is shown in figures 5.13 and 5.14. Tire marks and scrapes marred the face of the CMBs. The corner of segment 4 at the connection to segment 5 on the rear at ground level was broken. The drop-pins were pulled up as follows: Pin 2A 0.5 inches; pin 2B 0.4 inches; pin 3A 2.6 inches; pin 3B 1.3 inches; pin 4A 1.9 inches; and pin 5A 0.4 inches. The drop-pins adjacent to the impact joint were deformed, but none of the pins pulled out of the concrete pavement. Figure 5.15 shows the deformed pins. Segment 3 was pulled up on the end near segment 2 by 0.7 inches and on the end near segment 4 by 1.6 inches. Segment 4 was pulled up 1.4 inches near the end of segment 3 and by 1.0 inch at the end near segment 5. The vehicle contacted the installation 4.0 ft upstream of the joint between segments 3 and 4, and remained in contact for a total length of contact of 22 ft. Working width was 2.83 ft. Maximum permanent deformation of the barrier was 0.48 ft, and maximum dynamic deflection during the test was 0.96 ft.

VEHICLE DAMAGE

Damage to the vehicle is shown in figure 5.16. Structural damage included deformed left front frame rail, and left upper and lower A-arm. Also damaged were the front bumper, hood, grill, left front fender, left door and glass, and left rear exterior bed. The left front and rear tires were flat, left front wheel rim was separated, and left rear wheel rim deformed. Maximum exterior crush to the vehicle was 21.7 inches in the left front corner side plane at bumper height. Maximum occupant compartment deformation was 1.1 inches in the left side firewall area near the toe pan with some separation in the seam. Photographs of the interior of the vehicle are shown in figure 5.17. Exterior vehicle crush and occupant compartment measurements are shown in appendix B, tables 4 and 5.

OCCUPANT RISK FACTORS

Data from the triaxial accelerometer, located at the vehicle center of gravity, were digitized to compute occupant impact velocity and ridedown accelerations. Only the occupant impact velocity and ridedown accelerations in the longitudinal axis are required from these data for evaluation of criterion L of *NCHRP Report 350*. In the longitudinal direction, occupant impact velocity was 20.3 ft/s at 0.105 s, maximum 0.010-s ridedown acceleration was -6.4 g's from 0.109 to 0.119 s, and the maximum 0.050-s average was -8.7 g's between 0.032 and 0.082 s. In the lateral direction, the occupant impact velocity was 19.0 ft/s at 0.105 s, the highest 0.010-s occupant ridedown acceleration was 4.7 g's from 0.147 to 0.157 s, and the maximum 0.050-s average was 9.7 g's between 0.026 and 0.076 s. These data and other information pertinent to the test are presented in figure 5.18. Vehicle angular displacements and accelerations versus time traces are shown in appendix D, figures D8 through D14.



Figure 5.13. Vehicle trajectory path after test 405160-3-1.



Figure 5.14. Installation after test 405160-3-1.



Figure 5.15. Deformed drop-pins after test 405160-3-1.



Figure 5.16. Vehicle after test 405160-3-1.

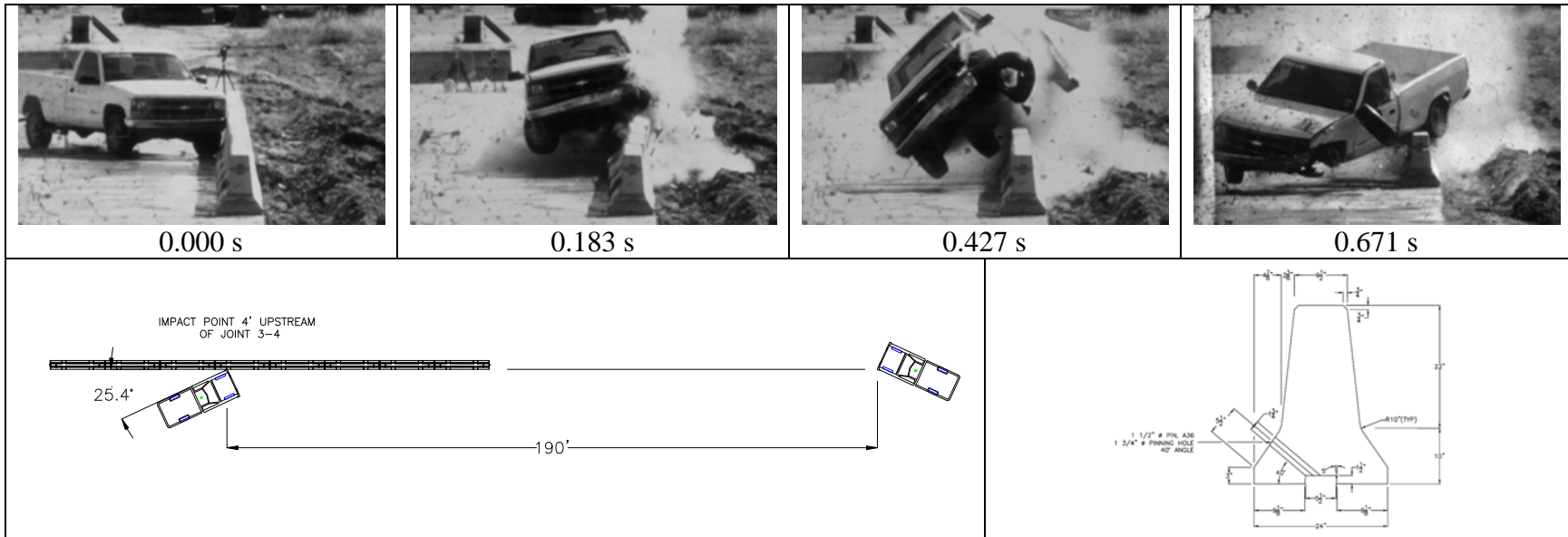


Before Test



After Test

Figure 5.17. Interior of vehicle for test 405160-3-1.



67

General Information

Test Agency..... Texas Transportation Institute
 Test No. 405160-3-2a
 Date 11-15-2007

Test Article

Type..... Pinned Temporary Barrier
 Name Pinned F-Shape CMB
 Installation Length (ft) 100
 Material or Key Elements 12.5 ft long F-shape precast concrete segments with pin-and-loop connection with two 1.875-inch diameter holes drilled into each barrier segment at 40 degrees with 1.5-inch diameter 21.25-inch long ASTM A36 steel drop-pin anchors
 Soil Type and Condition Concrete Pavement, Dry

Test Vehicle

Designation..... 2000P
 Model..... 2000 Chevrolet C2500 Pickup Truck
 Mass (lb)
 Curb..... 4993
 Test Inertial..... 4674
 Dummy No Dummy
 Gross Static..... 4674

Impact Conditions

Speed (mi/h) 62.7
 Angle (deg) 25.4

Exit Conditions

Speed (mi/h) Not Obtainable
 Angle (deg) Obtainable

Occupant Risk Values

Impact Velocity (ft/s)
 Longitudinal 20.3
 Lateral..... 19.0
 THIV (km/h)..... 28.9
 Ridedown Accelerations (g's)
 Longitudinal -6.4
 Lateral..... 4.7
 PHD (g's) 6.4
 ASI 1.32
 Max. 0.050-s Average (g's)
 Longitudinal -8.7
 Lateral..... 9.7
 Vertical..... -5.6

Test Article Deflections (ft)

Dynamic 0.96
 Permanent..... 0.48
 Working Width 2.83

Vehicle Damage

Exterior
 VDS..... 01LFQ5
 CDC 01FLEW5
 Max. Exterior
 Vehicle Crush (inches) 21.7
 Interior
 OCDI RF0002000
 Max. Occupant Compartment
 Deformation (inches) 1.1

Post-Impact Behavior

(during 1.0 sec after impact)
 Max. Yaw Angle (deg) 45
 Max. Pitch Angle (deg) -13
 Max. Roll Angle (deg) 41

Figure 5.18. Summary of results for NCHRP Report 350 test 3-11 on the modified pinned F-shape barrier.

* Corrected 2012-09-04

ASSESSMENT OF TEST RESULTS

Following is an assessment of the test based on the applicable *NCHRP Report 350* safety evaluation criteria.

Structural Adequacy

- B. *Test article should contain and redirect the vehicle; the vehicle should not penetrate, underide, or override the installation although controlled lateral deflection of the test article is acceptable.*

Results: The pinned barriers contained and redirected the 2000P vehicle. The vehicle did not penetrate, underide, or override the installation. Maximum permanent deformation of the barrier was 5.7 inches. (PASS)

Occupant Risk

- D. *Detached elements, fragments, or other debris from the test article should not penetrate or show potential for penetrating the occupant compartment, or present an undue hazard to other traffic, pedestrians, or personnel in a work zone. Deformation of, or intrusions into, the occupant compartment that could cause serious injuries should not be permitted.*

Results: No detached elements, fragments, or other debris were present to penetrate or show potential to penetrate the occupant compartment, or to present hazard to others in the area. Maximum occupant compartment deformation was 1.1 inch. (PASS)

- F. *The vehicle should remain upright during and after collision although moderate roll, pitching, and yawing are acceptable.*

Results: The vehicle remained upright during and after the impact event. (PASS)

Vehicle Trajectory

- K. *After collision, it is preferable that the vehicle's trajectory not intrude into adjacent traffic lanes.*

Result: The vehicle came to rest upright facing the installation 190 ft downstream of impact and aligned with the traffic face of the installation. (PASS)

- L. *The occupant impact velocity in the longitudinal direction should not exceed 12 m/s and the occupant ridedown acceleration in the longitudinal direction should not exceed 20 g's.*

Result: Longitudinal occupant impact velocity was 20.3 ft/s (6.19 m/s), and longitudinal ridedown acceleration was -6.4 g's. (PASS)

- M. *The exit angle from the test article preferably should be less than 60 percent of the test impact angle, measured at time of vehicle loss of contact with the test device.*

Result: Exit angle was not obtainable due to excessive dust. (N/A)

The following supplemental evaluation factors and terminology, as presented in the FHWA memo entitled “Action: Identifying Acceptable Highway Safety Features,” were used for visual assessment of test results: ⁽⁷⁾

Passenger Compartment Intrusion

- | | |
|---|---|
| 1. <i>Windshield Intrusion</i> | |
| a. <i>No windshield contact</i> | e. <i>Complete intrusion into passenger compartment</i> |
| b. <i>Windshield contact, no damage</i> | f. <i>Partial intrusion into passenger compartment</i> |
| c. <i>Windshield contact, no intrusion</i> | |
| d. <i>Device embedded in windshield, no significant intrusion</i> | |
| 2. <i>Body Panel Intrusion</i> | <u>yes</u> or no |

Loss of Vehicle Control

- | | |
|---|--|
| 1. <i>Physical loss of control</i> | 3. <i>Perceived threat to other vehicles</i> |
| 2. <i>Loss of windshield visibility</i> | 4. <i>Debris on pavement</i> |

Physical Threat to Workers or Other Vehicles

1. *Harmful debris that could injure workers or others in the area*
 2. *Harmful debris that could injure occupants in other vehicles*
- No debris was present.

Vehicle and Device Condition

- | | |
|--|--|
| 1. <i>Vehicle Damage</i> | |
| a. <i>None</i> | d. <i>Major dents to grill and body panels</i> |
| b. <i>Minor scrapes, scratches or dents</i> | e. <u>Major structural damage</u> |
| c. <i>Significant cosmetic dents</i> | |
| 2. <i>Windshield Damage</i> | |
| a. <u>None</u> | e. <i>Shattered, remained intact but partially dislodged</i> |
| b. <i>Minor chip or crack</i> | f. <i>Large portion removed</i> |
| c. <i>Broken, no interference with visibility</i> | g. <i>Completely removed</i> |
| d. <i>Broken or shattered, visibility restricted but remained intact</i> | |
| 3. <i>Device Damage</i> | |
| a. <i>None</i> | d. <u>Substantial, replacement parts needed for repair</u> |
| b. <i>Superficial</i> | e. <i>Cannot be repaired</i> |
| c. <i>Substantial, but can be straightened</i> | |

CHAPTER 6. SUMMARY AND CONCLUSIONS

Bridge replacement and repair projects often require the use of phased bridge construction techniques to maintain traffic operation during construction. Restrained temporary concrete barriers are used during these operations to protect motorists from extreme drop-offs at the edge of existing bridge decks. There are few restrained temporary concrete barrier designs that have been crash tested to provide limited deflection requirements. Among the existing designs, most require through the deck bolting or use anchor bolts, or other constraining straps. Such designs are difficult to install, inspect, and remove in the field. Furthermore, through the deck bolting often results in significant damage to thin bridge decks.

In this project, the researchers have developed a restraining mechanism that limits lateral deflections of concrete barriers, is easy to install, inspect, and remove, and minimizes damage to the bridge deck or concrete pavements. This mechanism uses the pinned-down approach to restrain the barriers. Pins are simply dropped into inclined holes that start from the toe of the barrier and continue into the bridge deck or concrete pavement underneath.

The sponsoring states of this pooled fund research program initially desired to have a design that works in conjunction with concrete barrier designs being used by most of the states. A preliminary evaluation of all barrier designs was conducted and Washington State DOT's pin-and-loop New Jersey profile barrier was identified as the most critical design. It was argued that a restraint mechanism which performs adequately for this design, will work acceptably for the designs being used by the other participating states.

A finite element model of the WSDOT barrier was developed and impact simulations were performed to assist in the development of an appropriate pinned-down design for this barrier. Simulation results prior to crash testing showed that due to the NJ profile of the barrier and rotation induced during impact, high vehicle climb was expected and the test results would be marginal. However, since this design offered the most flexibility in applying the pinned-down design to barriers used by the participating states, the states decided to proceed with a full-scale crash test. The WSDOT pinned-down barrier was subsequently crash tested, but failed to meet the design requirements due to excessive rotation of the barriers and excessive vehicle climb.

A second phase of the analysis was performed to develop a new pinned-down temporary concrete barrier design, which did not necessarily incorporate all of the existing barrier designs of the participating states. The researchers performed a detailed evaluation of crash test results to make necessary modifications to the barrier design. The profile of the new pinned-down barrier was changed from NJ to F-shaped. The angle of the drop-pins and the barrier connection design were modified among other changes, to provide better resistance to barrier roll.

A finite element analysis of the new pinned barrier design was performed. To improve simulation results, concrete failure was incorporated in further analysis of the new barrier. The results of the analysis showed significant improvement in barrier performance compared to the WSDOT pinned-down design. A crash test was subsequently performed with the new F-shaped pinned-down concrete barrier design.

The new F-shaped pinned-down barrier successfully passed the *NCHRP Report 350* Test Level 3 requirements, as shown in tables 6.1 and 6.2. The occupant risk factors were within the preferred limits specified in *NCHRP Report 350*. Although the barrier sustained some damage that would require repair, there were no detached elements, fragments, or other debris that showed potential for penetrating the occupant compartment, or presented a hazard to workers or others in the area. The maximum permanent and dynamic barrier deflections were 5.76 inches (483 mm) and 11.52 inches (293 mm), respectively. There was no significant damage to the underlying bridge deck.

In the crash tested barrier, a 1.5-inch tall and 5-inch wide channel was cast into the bottom of the barrier, running longitudinally along its centerline as shown in figures 5.4 and 5.10. Some barrier designs use such a detail to assist with barrier placement on unlevel ground. However, since the pinning holes cast into the barrier did not run through to ground level, it was observed that the drill bit had more play as the holes were being drilled into the deck. This created the potential for a slight misalignment of the pinning holes cast in the barriers with respect to the holes drilled into the deck. Due to the misalignment, the placement of the drop-pins was complicated at some of the locations during installation of the test barrier.

In order to simplify the drilling of the pinning holes into the concrete deck or pavement and placement of the pins, it is recommended that the longitudinal channel at the bottom-centerline of the barrier be eliminated from the barrier design. Analysis of the test results and the deformed drop pins indicates that eliminating the longitudinal channel will not affect impact performance of the barrier nor damage to the deck structure to which the barrier is pinned. This option without the channel is preferred because it will eliminate any potential complications associated with drop-pin placement and make casting of the barrier simpler. Since the barrier will be pinned to either concrete pavement or a bridge deck, unlevel terrain is not likely to be a problem. However, if desired, a shallow channel (e.g., ¼-inch deep) could be used without affecting drilling and drop-pin placement.

Table 6.1. Performance evaluation summary for *NCHRP Report 350* test 3-11 on the pinned F-shape temporary barrier.

Test Agency: Texas Transportation Institute

Test No.: 405160-3-1

Test Date: 09-19-2006

<i>NCHRP Report 350</i> Test 3-11 Evaluation Criteria	Test Results	Assessment
<p><u>Structural Adequacy</u></p> <p>A. <i>Test article should contain and redirect the vehicle; the vehicle should not penetrate, underride, or override the installation although controlled lateral deflection of the test article is acceptable</i></p>	<p>The barrier segments at impact began to rotate toward the field side and the 2000P vehicle rode up the traffic face of the barrier. As the vehicle reached the top of the barriers, the first three segments and part of the fourth rotated into the ditch on the field side of the installation.</p>	<p>Fail</p>
<p><u>Occupant Risk</u></p> <p>D. <i>Detached elements, fragments, or other debris from the test article should not penetrate or show potential for penetrating the occupant compartment, or present an undue hazard to other traffic, pedestrians, or personnel in a work zone. Deformations of, or intrusions into, the occupant compartment that could cause serious injuries should not be permitted.</i></p>	<p>No detached elements, fragments, or other debris was present to penetrate or show potential to penetrate the occupant compartment. Maximum occupant compartment deformation was 26 mm (1 inch). However, the barriers rotated toward the field side and fell over into the ditch, which would be hazardous and unacceptable when used on a bridge deck.</p>	<p>Fail</p>
<p>F. <i>The vehicle should remain upright during and after collision although moderate roll, pitching, and yawing are acceptable.</i></p>	<p>The vehicle remained upright during the impact event, however, it rolled over onto its side after exiting the installation and impacting a concrete barrier segment placed further downstream to guard photography equipment.</p>	<p>Fail</p>
<p><u>Vehicle Trajectory</u></p> <p>K. <i>After collision, it is preferable that the vehicle's trajectory not intrude into adjacent traffic lanes.</i></p>	<p>The vehicle came to rest on its side 48.8 m (160 ft) downstream of impact and 3.7 m (12 ft) forward of the traffic face of the installation.</p>	<p>Fail*</p>
<p>L. <i>The occupant impact velocity in the longitudinal direction should not exceed 12 m/s and the occupant ridedown acceleration in the longitudinal direction should not exceed 20 g's.</i></p>	<p>Longitudinal occupant impact velocity was 4.7 m/s (15.4 ft/s), and longitudinal ridedown acceleration was -4.1 g's.</p>	<p>Pass</p>
<p>M. <i>The exit angle from the test article preferably should be less than 60 percent of test impact angle, measured at time of vehicle loss of contact with test device.</i></p>	<p>The vehicle was traveling parallel with the installation as it lost contact.</p>	<p>Pass*</p>

*Criterion K and M are preferable, not required.

Table 6.2. Performance evaluation summary for *NCHRP Report 350* test 3-11 on the modified pinned F-shape temporary barrier.

Test Agency: Texas Transportation Institute

Test No.: 405160-3-2a

Test Date: 11-15-2007

<i>NCHRP Report 350</i> Test 3-11 Evaluation Criteria	Test Results	Assessment
<u>Structural Adequacy</u> A. <i>Test article should contain and redirect the vehicle; the vehicle should not penetrate, underride, or override the installation although controlled lateral deflection of the test article is acceptable</i>	The pinned barriers contained and redirected the 2000P vehicle. The vehicle did not penetrate, underride, or override the installation. Maximum permanent deformation of the barrier was 5.7 inches.	Pass
<u>Occupant Risk</u> D. <i>Detached elements, fragments, or other debris from the test article should not penetrate or show potential for penetrating the occupant compartment, or present an undue hazard to other traffic, pedestrians, or personnel in a work zone. Deformations of, or intrusions into, the occupant compartment that could cause serious injuries should not be permitted.</i>	No detached elements, fragments, or other debris was present to penetrate or show potential to penetrate the occupant compartment, or to present hazard to others in the area. Maximum occupant compartment deformation was 1.1 inch.	Pass
F. <i>The vehicle should remain upright during and after collision although moderate roll, pitching, and yawing are acceptable.</i>	The vehicle remained upright during and after the impact event.	Pass
<u>Vehicle Trajectory</u> K. <i>After collision, it is preferable that the vehicle's trajectory not intrude into adjacent traffic lanes.</i>	The vehicle came to rest 190 ft downstream of impact and aligned with the traffic face of the installation.	Pass*
L. <i>The occupant impact velocity in the longitudinal direction should not exceed 12 m/s and the occupant ridedown acceleration in the longitudinal direction should not exceed 20 g's.</i>	Longitudinal occupant impact velocity was 20.3 ft/s, and longitudinal ridedown acceleration was -6.4 g's.	Pass
M. <i>The exit angle from the test article preferably should be less than 60 percent of test impact angle, measured at time of vehicle loss of contact with test device.</i>	Exit angle were not obtainable due to excessive dust.	N/A*

*Criterion K and M are preferable, not required.

REFERENCES

1. W. L. Beason and D.L. Bullard, Jr., *Development of a Limited-Slip Portable Concrete Barrier Connection*. Research Report 1959, Texas Transportation Institute, College Station, TX, 1993.
2. H.E. Ross, Jr., D.L. Sicking, R.A. Zimmer and J.D. Michie, *Recommended Procedures for the Safety Performance Evaluation of Highway Features*, National Cooperative Highway Research Program Report 350, Transportation Research Board, National Research Council, Washington, D.C., 1993.
3. B.W. Bielenberg, R.K. Faller, D.L. Sicking, J.R. Rohde, J.D. Reid, and J.C. Holloway, *Development of a Tie-Down Systems for Temporary Concrete Barriers*, Midwest Roadside Safety Facility, Lincoln, Nebraska, 2002.
4. K.A. Polivka, B.W. Bielenberg, R.K. Faller, D.L. Sicking, J.R. Rohde, J.D. Reid and J.C. Holloway, *Development of a Steel H-Section Temporary Barrier for Use in Limited Deflection Applications*. Midwest Roadside Safety Facility, Lincoln, Nebraska, 2003.
5. K.A. Polivka, R.K. Faller, J.R. Rohde, J.C. Holloway, B.W. Bielenberg, and D.L. Sicking, *Development and Evaluation of a Tie-Down Systems for Redesigned F-Shape Concrete Temporary Barrier*, Midwest Roadside Safety Facility, Lincoln, Nebraska, 2003.
6. FHWA contract DTFH61-71-C-00064. "Work Zone Appurtenances Tested to *NCHRP Report 350*."
7. Federal Highway Administration Memorandum, from the Director, Office of Engineering, entitled: "ACTION: Identifying Acceptable Highway Safety Features," dated July 25, 1997.

APPENDIX A. CRASH TEST PROCEDURES AND DATA ANALYSIS

The crash test and data analysis procedures were in accordance with guidelines presented in *NCHRP Report 350*. Brief descriptions of these procedures are presented as follows.

ELECTRONIC INSTRUMENTATION AND DATA PROCESSING

The test vehicle was instrumented with three solid-state angular rate transducers to measure roll, pitch, and yaw rates; a triaxial accelerometer near the vehicle center of gravity (c.g.) to measure longitudinal, lateral, and vertical acceleration levels; and a backup biaxial accelerometer in the rear of the vehicle to measure longitudinal and lateral acceleration levels. These accelerometers were ENDEVCO[®] Model 2262CA, piezoresistive accelerometers with a ± 100 g range.

The accelerometers are strain gage type with a linear millivolt output proportional to acceleration. Angular rate transducers are solid state, gas flow units designed for high-“g” service. Signal conditioners and amplifiers in the test vehicle increase the low-level signals to a ± 2.5 volt maximum level. The signal conditioners also provide the capability of an R-cal (resistive calibration) or shunt calibration for the accelerometers and a precision voltage calibration for the rate transducers. The electronic signals from the accelerometers and rate transducers are transmitted to a base station by means of a 15-channel, constant-bandwidth, Inter-Range Instrumentation Group (IRIG), FM/FM telemetry link for recording and for display. Calibration signals from the test vehicle are recorded before the test and immediately afterwards. A crystal-controlled time reference signal is simultaneously recorded with the data. Wooden dowels actuate pressure-sensitive switches on the bumper of the impacting vehicle prior to impact by wooden dowels to indicate the elapsed time over a known distance to provide a measurement of impact velocity. The initial contact also produces an “event” mark on the data record to establish the instant of contact with the installation.

The multiplex of data channels, transmitted on one radio frequency, is received and demultiplexed onto TEAC[®] instrumentation data recorder. After the test, the data are played back from the TEAC[®] recorder and digitized. A proprietary software program (WinDigit) converts the analog data from each transducer into engineering units using the R-cal and pre-zero values at 10,000 samples per second, per channel. WinDigit also provides Society of Automotive Engineers (SAE) J211 class 180 phaseless digital filtering and vehicle impact velocity.

All accelerometers are calibrated annually according to the (SAE) J211 4.6.1 by means of an ENDEVCO[®] 2901, precision primary vibration standard. This device and its support instruments are returned to the factory annually for a National Institute of Standards Technology (NIST) traceable calibration. The subsystems of each data channel are also evaluated annually, using instruments with current NIST traceability, and the results are factored into the accuracy of the total data channel, per SAE J211. Calibrations and evaluations are made any time data are suspect.

The Test Risk Assessment Program (TRAP) uses the data from WinDigit to compute occupant/compartiment impact velocities, time of occupant/compartiment impact after vehicle impact, and the highest 10-milliseconds (ms) average ridedown acceleration. WinDigit calculates change in vehicle velocity at the end of a given impulse period. In addition, maximum average accelerations over 50-ms intervals in each of the three directions are computed. For reporting purposes, the data from the vehicle-mounted accelerometers are filtered with a 60-Hz digital filter, and acceleration versus time curves for the longitudinal, lateral, and vertical directions are plotted using TRAP.

TRAP uses the data from the yaw, pitch, and roll rate transducers to compute angular displacement in degrees at 0.0001-s intervals and then plots yaw, pitch, and roll versus time. These displacements are in reference to the vehicle-fixed coordinate system with the initial position and orientation of the vehicle-fixed coordinate systems being initial impact.

ANTHROPOMORPHIC DUMMY INSTRUMENTATION

Use of a dummy in the 2000P vehicle is optional according to *NCHRP Report 350*, and there was no dummy used in the tests with the 2000P vehicle.

PHOTOGRAPHIC INSTRUMENTATION AND DATA PROCESSING

Photographic coverage of the test included three high-speed cameras: one overhead with a field of view perpendicular to the ground and directly over the impact point; one placed behind the installation at an angle; and a third placed to have a field of view parallel to and aligned with the installation at the downstream end. A flashbulb activated by pressure-sensitive tape switches was positioned on the impacting vehicle to indicate the instant of contact with the installation and was visible from each camera. The films from these high-speed cameras were analyzed on a computer-linked motion analyzer to observe phenomena occurring during the collision and to obtain time-event, displacement, and angular data. A mini-DV camera and still cameras recorded and documented conditions of the test vehicle and installation before and after the test.

TEST VEHICLE PROPULSION AND GUIDANCE

The test vehicle was towed into the test installation using a steel cable guidance and reverse tow system. A steel cable for guiding the test vehicle was tensioned along the path, anchored at each end, and threaded through an attachment to the front wheel of the test vehicle. An additional steel cable was connected to the test vehicle, passed around a pulley near the impact point, through a pulley on the tow vehicle, and then anchored to the ground such that the tow vehicle moved away from the test site. A two-to-one speed ratio between the test and tow vehicle existed with this system. Just prior to impact with the installation, the test vehicle was released to be free-wheeling and unrestrained. The vehicle remained free-wheeling, i.e., no steering or braking inputs, until the vehicle cleared the immediate area of the test site, at which time brakes on the vehicle were activated to bring it to a safe and controlled stop.

APPENDIX B. TEST VEHICLE PROPERTIES AND INFORMATION

Date: 09-19-2006 Test No.: 405160-3-1 VIN No.: 1GCGC24R6YR192364

Year: 2000 Make: Chevrolet Model: C2500 Pickup Truck

Tire Inflation Pressure: 50/80 psi Odometer: 134308 Tire Size: 245/75R16

Describe any damage to the vehicle prior to test: _____

● Denotes accelerometer location.

NOTES: _____

Engine Type: V8

Engine CID: 5.7 liter

Transmission Type:

 Auto

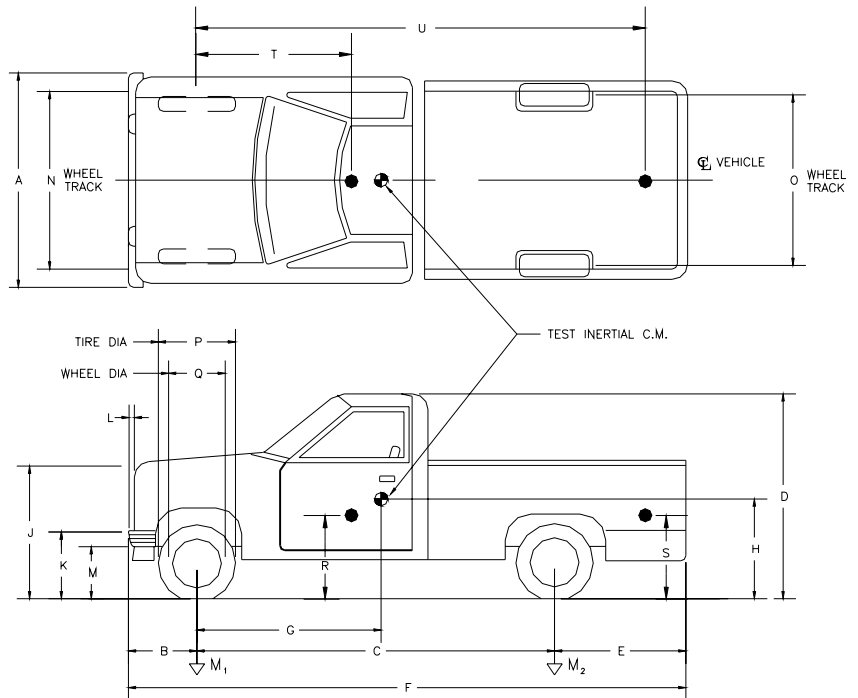
 X Manual

Optional Equipment: _____

Dummy Data: Type: No Dummy

Mass: _____

Seat Position: _____



Geometry (inches)

A	<u>74</u>	E	<u>51.5</u>	J	<u>41</u>	N	<u>62.5</u>	R	<u>29.5</u>
B	<u>32</u>	F	<u>215.5</u>	K	<u>25</u>	O	<u>63.25</u>	S	<u>35.5</u>
C	<u>132</u>	G	<u>57.7</u>	L	<u>2.75</u>	P	<u>28.5</u>	T	<u>57.5</u>
D	<u>71.75</u>	H	_____	M	<u>16.25</u>	Q	<u>17.25</u>	U	<u>132.25</u>

<u>Mass (lb)</u>	<u>Curb</u>	<u>Test Inertial</u>	<u>Gross Static</u>
M ₁	<u>2644</u>	<u>2573</u>	_____
M ₂	<u>2116</u>	<u>2002</u>	_____
M _{Total}	<u>4760</u>	<u>4575</u>	_____

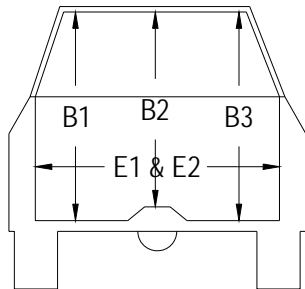
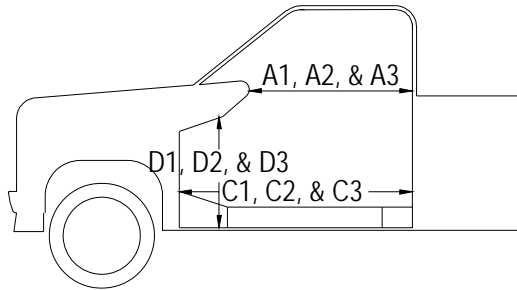
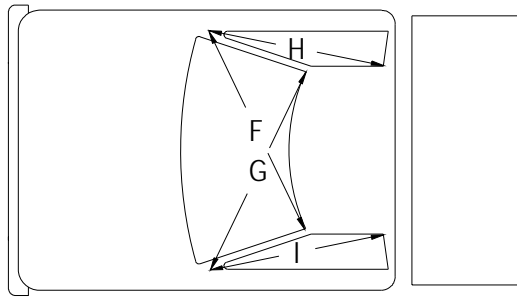
Mass Distribution (lb): LF: 1274 RF: 1299 LR: 1021 RR: 981

Figure B1. Vehicle properties for test 405160-3-1.

Table B2. Occupant compartment measurements for test 405160-3-1.

Truck

Occupant Compartment Deformation



	BEFORE (inches)	AFTER (inches)
A1	34.3	34.3
A2	37.3	37.3
A3	36.7	36.7
B1	42.4	42.4
B2	37.3	37.3
B3	41.8	42.3
C1	54.1	54.1
C2	----	----
C3	53.8	53.1
D1	12.9	12.9
D2	6.3	6.3
D3	12.2	11.2
E1	62.2	62.2
E2	62.6	62.6
F	57.7	57.7
G	57.7	57.7
H	41.7	41.7
I	41.7	41.7
J*	59.8	59.4

*Lateral area across the cab from driver's side kickpanel to passenger's side kickpanel.

Date: 11-15-2007 Test No.: 405160-3-2a VIN No.: 1GCGC24F2YR171334

Year: 2000 Make: Chevrolet Model: C2500

Tire Inflation Pressure: 60 psi Odometer: 234029 Tire Size: 245 75R16

Describe any damage to the vehicle prior to test: _____

● Denotes accelerometer location.

NOTES: _____

Engine Type: V8

Engine CID: 5.7 liter

Transmission Type:

 Auto
 X Manual

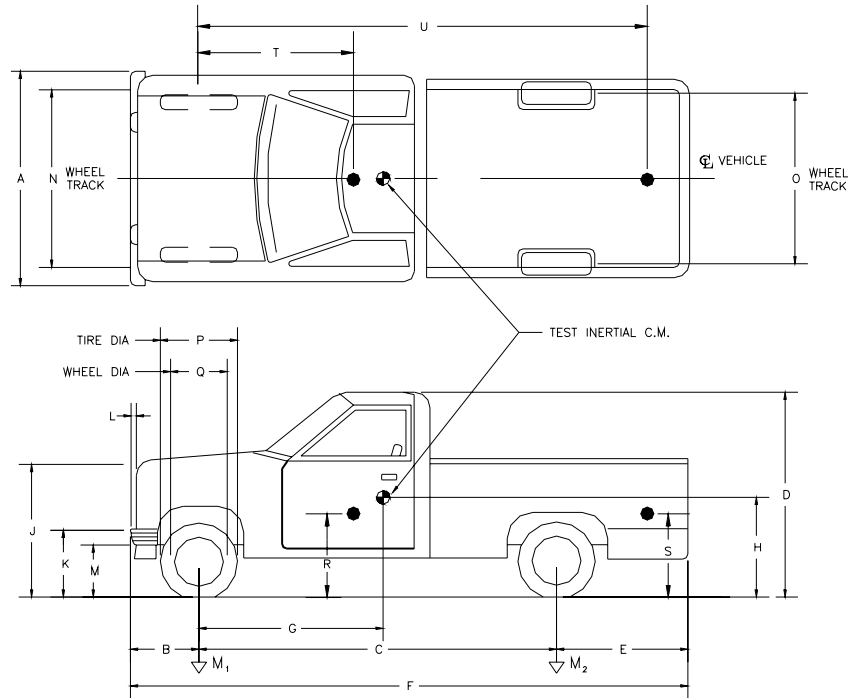
Optional Equipment:

Dummy Data:

Type: No dummy

Mass: _____

Seat Position: _____



Geometry (inches)

A	<u>74</u>	E	<u>51.5</u>	J	<u>41</u>	N	<u>62.5</u>	R	<u>29.5</u>
B	<u>32</u>	F	<u>215.5</u>	K	<u>25</u>	O	<u>63.25</u>	S	<u>35.5</u>
C	<u>132</u>	G	<u>58.6</u>	L	<u>2.75</u>	P	<u>28.5</u>	T	<u>57.5</u>
D	<u>71.5</u>	H	_____	M	<u>16.25</u>	Q	<u>17.25</u>	U	<u>132.25</u>

Mass (lb)	<u>Curb</u>	<u>Test Inertial</u>	<u>Gross Static</u>
M ₁	<u>2725</u>	<u>2597</u>	_____
M ₂	<u>2268</u>	<u>2077</u>	_____
M _{Total}	<u>4993</u>	<u>4674</u>	_____

Mass Distribution (lb): LF: 1312 RF: 1285 LR: 999 RR: 1078

Figure B2. Vehicle properties for test 405160-3-2a.

Table B3. Exterior crush measurements for test 405160-3-2a.

VEHICLE CRUSH MEASUREMENT SHEET¹

Complete When Applicable	
End Damage	Side Damage
Undeformed end width _____ Corner shift: A1 _____ A2 _____ End shift at frame (CDC) (check one) < 4 inches _____ ≥ 4 inches _____	Bowing: B1 _____ X1 _____ B2 _____ X2 _____ Bowing constant $\frac{X1 + X2}{2} = \underline{\hspace{2cm}}$

Note: Measure C₁ to C₆ from Driver to Passenger side in Front or Rear impacts – Rear to Front in Side Impacts.

Specific Impact Number	Plane* of C-Measurements	Direct Damage		Field L**	C ₁	C ₂	C ₃	C ₄	C ₅	C ₆	±D
		Width** (CDC)	Max*** Crush								
1	Front plane at bumper ht		19.7	66.9	19.7	11.4	3.9	-0.8	-1.6	-2.4	0
2	Side plane at bumper ht		21.7	43.3	0.4	2.8	---	---	15	21.7	+69.7

¹Table taken from National Accident Sampling System (NASS).

*Identify the plane at which the C-measurements are taken (e.g., at bumper, above bumper, at sill, above sill, at beltline, etc.) or label adjustments (e.g., free space).

Free space value is defined as the distance between the baseline and the original body contour taken at the individual C locations. This may include the following: bumper lead, bumper taper, side protrusion, side taper, etc. Record the value for each C-measurement and maximum crush.

**Measure and document on the vehicle diagram the beginning or end of the direct damage width and field L (e.g., side damage with respect to undamaged axle).

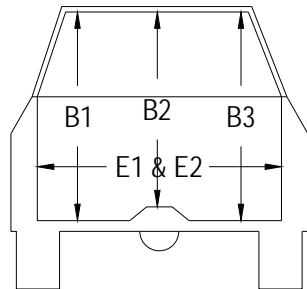
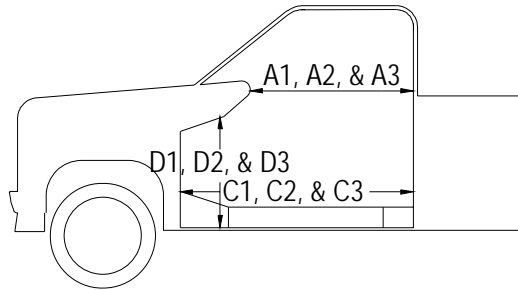
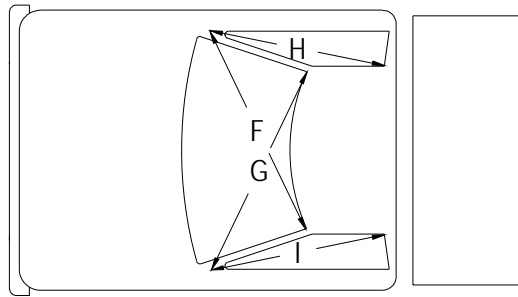
***Measure and document on the vehicle diagram the location of the maximum crush.

Note: Use as many lines/columns as necessary to describe each damage profile.

Table B4. Occupant compartment measurements for test 405160-3-2a.

Truck

Occupant Compartment Deformation



	BEFORE (inches)	AFTER (inches)
A1	34.3	34.1
A2	36.9	36.9
A3	36.8	36.8
B1	42.1	41.9
B2	37.1	37.1
B3	41.9	41.9
C1	54.0	54.0
C2	----	----
C3	54.0	54.0
D1	13.2	12.0
D2	5.9	5.5
D3	12.0	12.0
E1	62.4	62.4
E2	62.6	62.6
F	57.9	57.9
G	57.9	57.9
H	40.4	40.4
I	40.4	40.4
J*	60.0	59.6

*Lateral area across the cab from driver's side kickpanel to passenger's side kickpanel.

APPENDIX C. SEQUENTIAL PHOTOGRAPHS



0.000 s



0.171 s



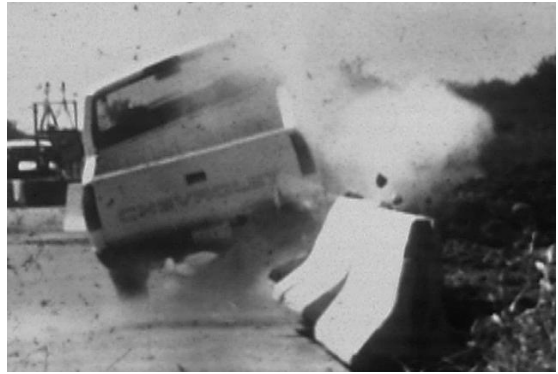
0.024 s



0.219 s



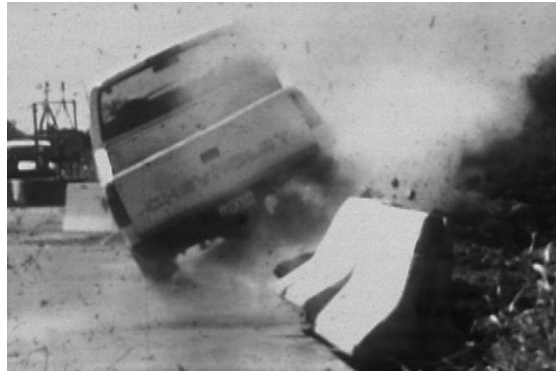
0.073 s



0.268 s



0.122 s



0.317 s

Figure C1. Sequential photographs for test 405160-3-1 (rear view).



0.000 s



0.024 s



0.073 s



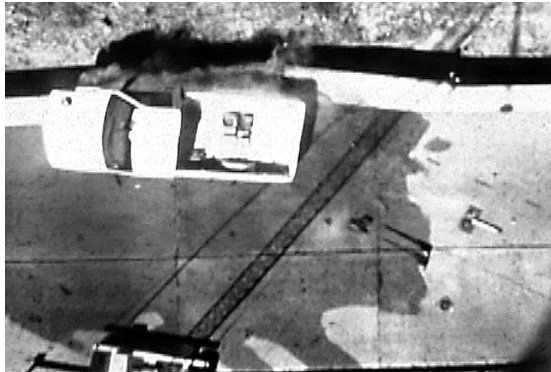
0.122 s



Figure C2. Sequential photographs for test 405160-3-1 (overhead and frontal views).



0.171 s



0.219 s



0.268 s



0.317 s



Figure C2. Sequential photographs for test 405160-3-1 (overhead and frontal views) (continued).



0.000 s



0.061 s



0.122 s



0.183 s



Figure C3. Sequential photographs for test 405160-3-2a (overhead and frontal views).



0.244 s



0.305 s



0.366 s



0.427 s



Figure C3. Sequential photographs for test 405160-3-2a (overhead and frontal views) (continued).



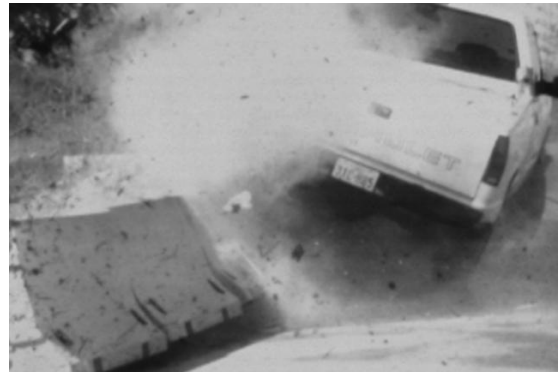
0.000 s



0.244 s



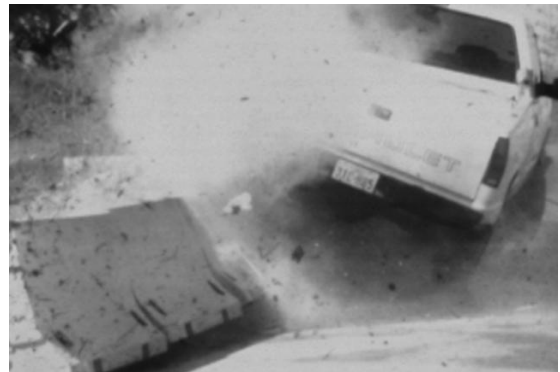
0.061 s



0.305 s



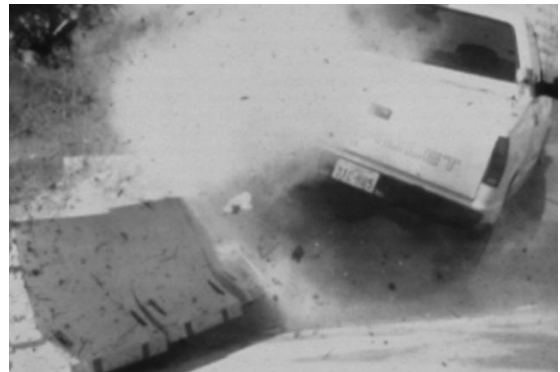
0.122 s



0.366 s



0.183 s



0.427 s

Figure C4. Sequential photographs for test 405160-3-2a (rear view).

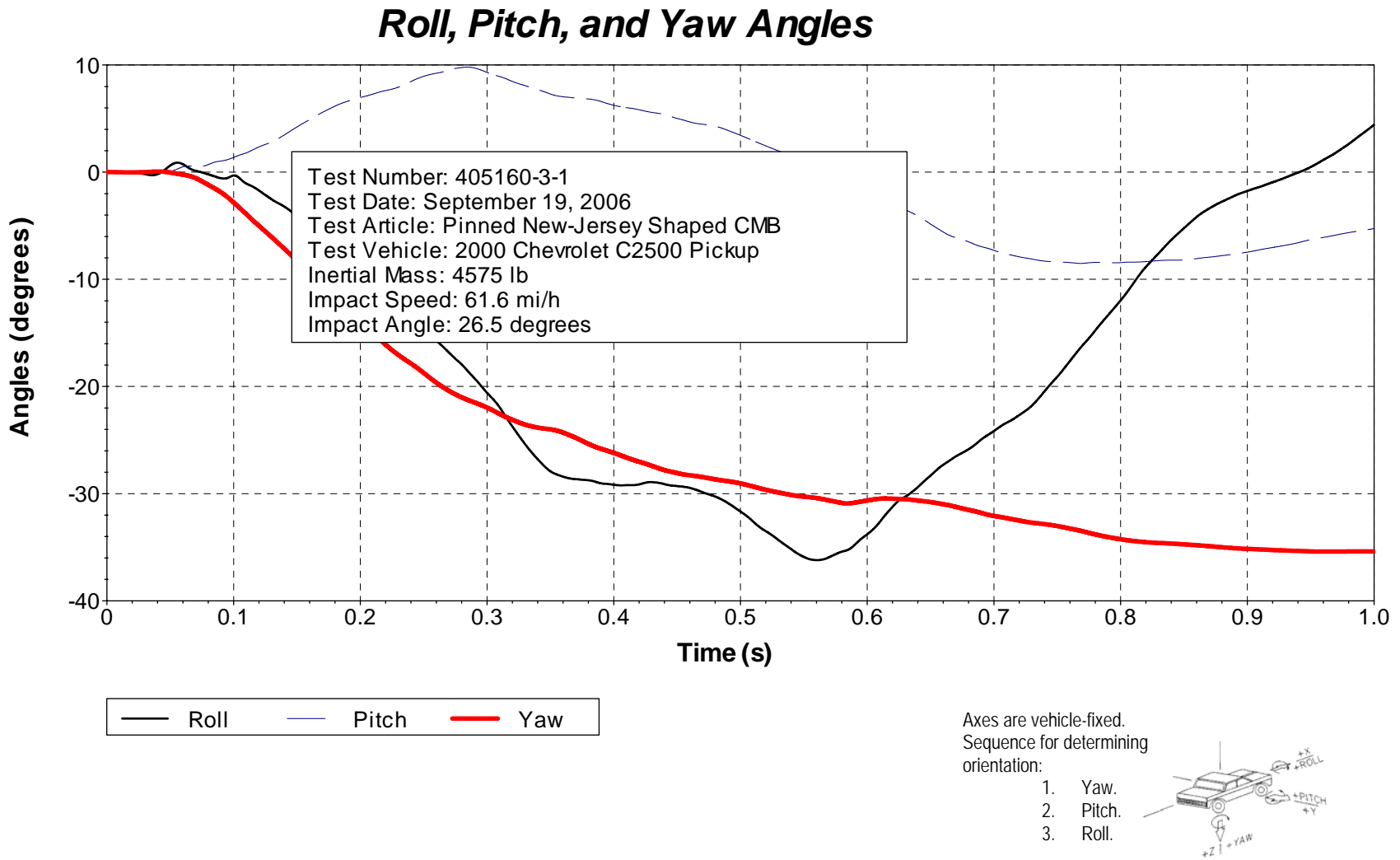


Figure D1. Vehicle angular displacements for test 405160-3-1.

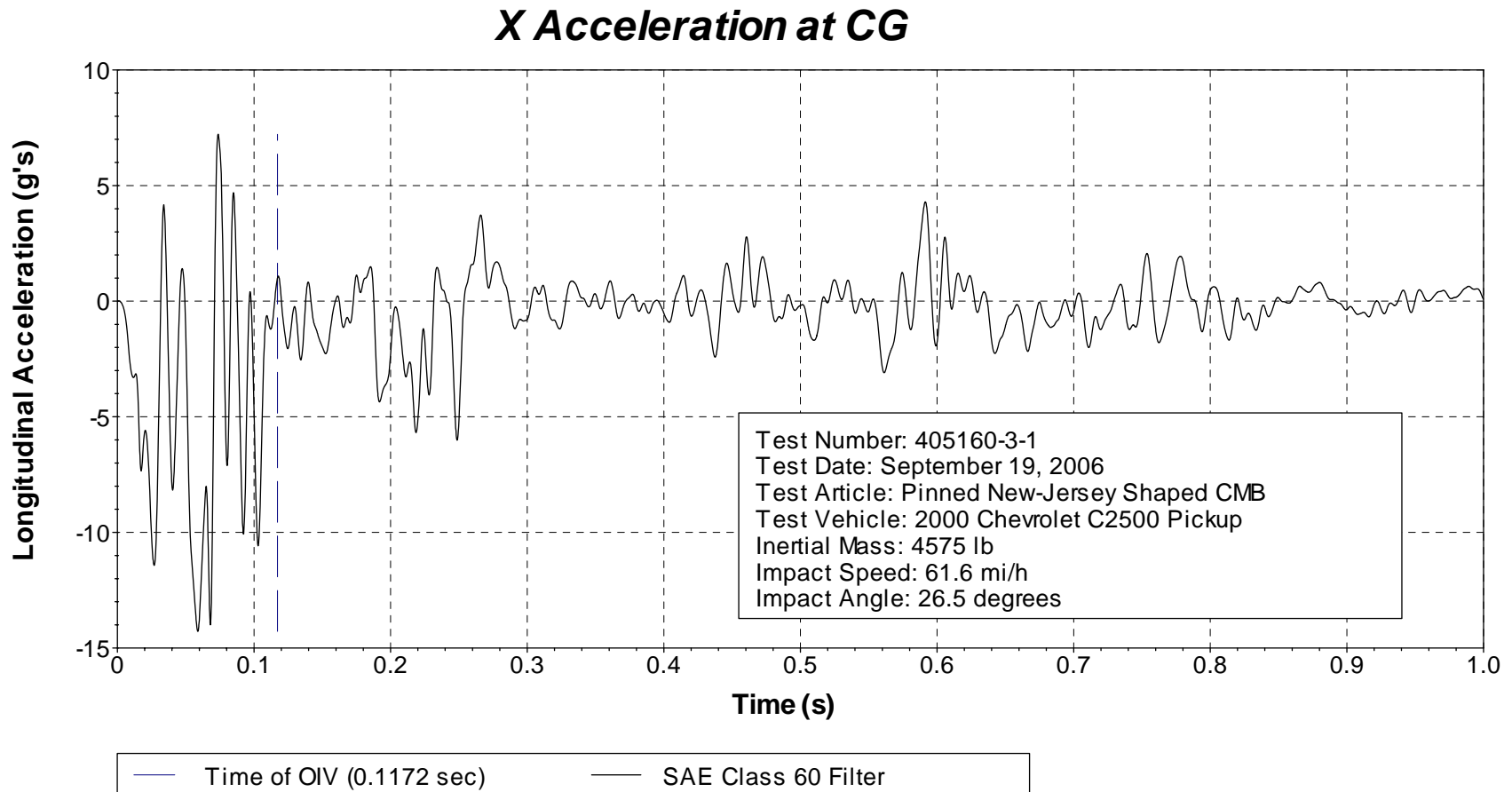


Figure D2. Vehicle longitudinal accelerometer trace for test 405160-3-1 (accelerometer located at center of gravity).

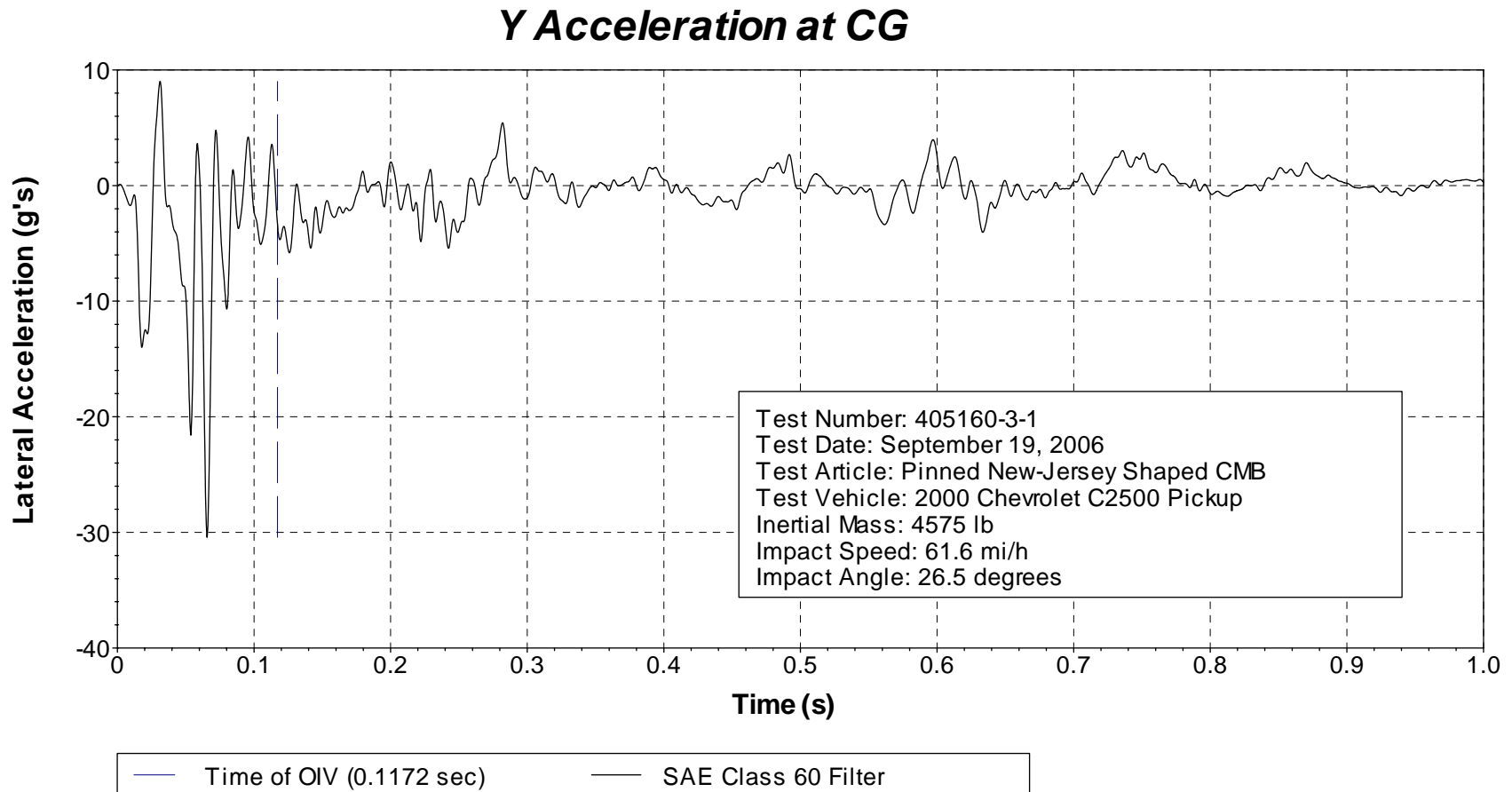


Figure D3. Vehicle lateral accelerometer trace for test 405160-3-1 (accelerometer located at center of gravity).

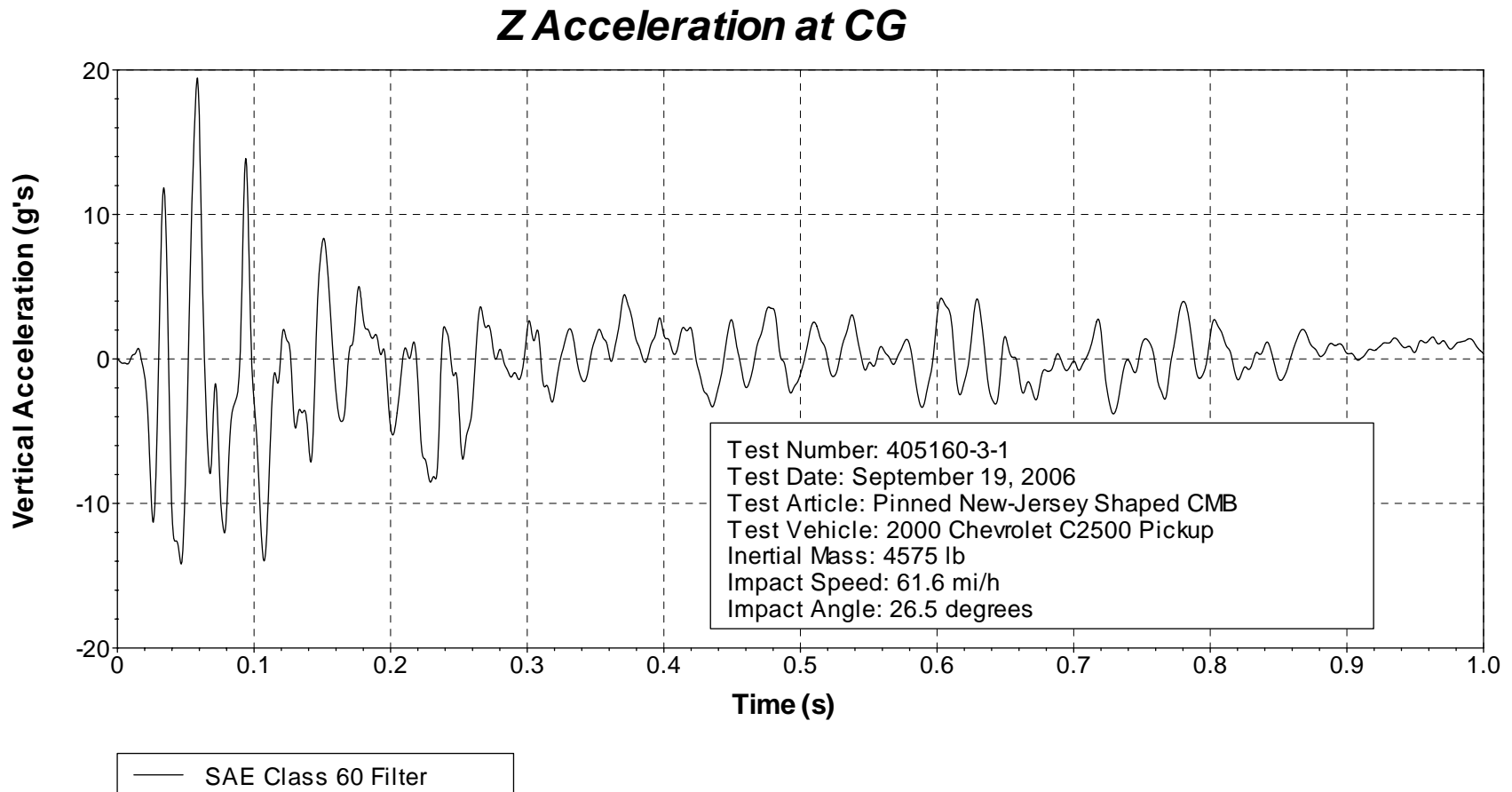


Figure D4. Vehicle vertical accelerometer trace for test 405160-3-1 (accelerometer located at center of gravity).

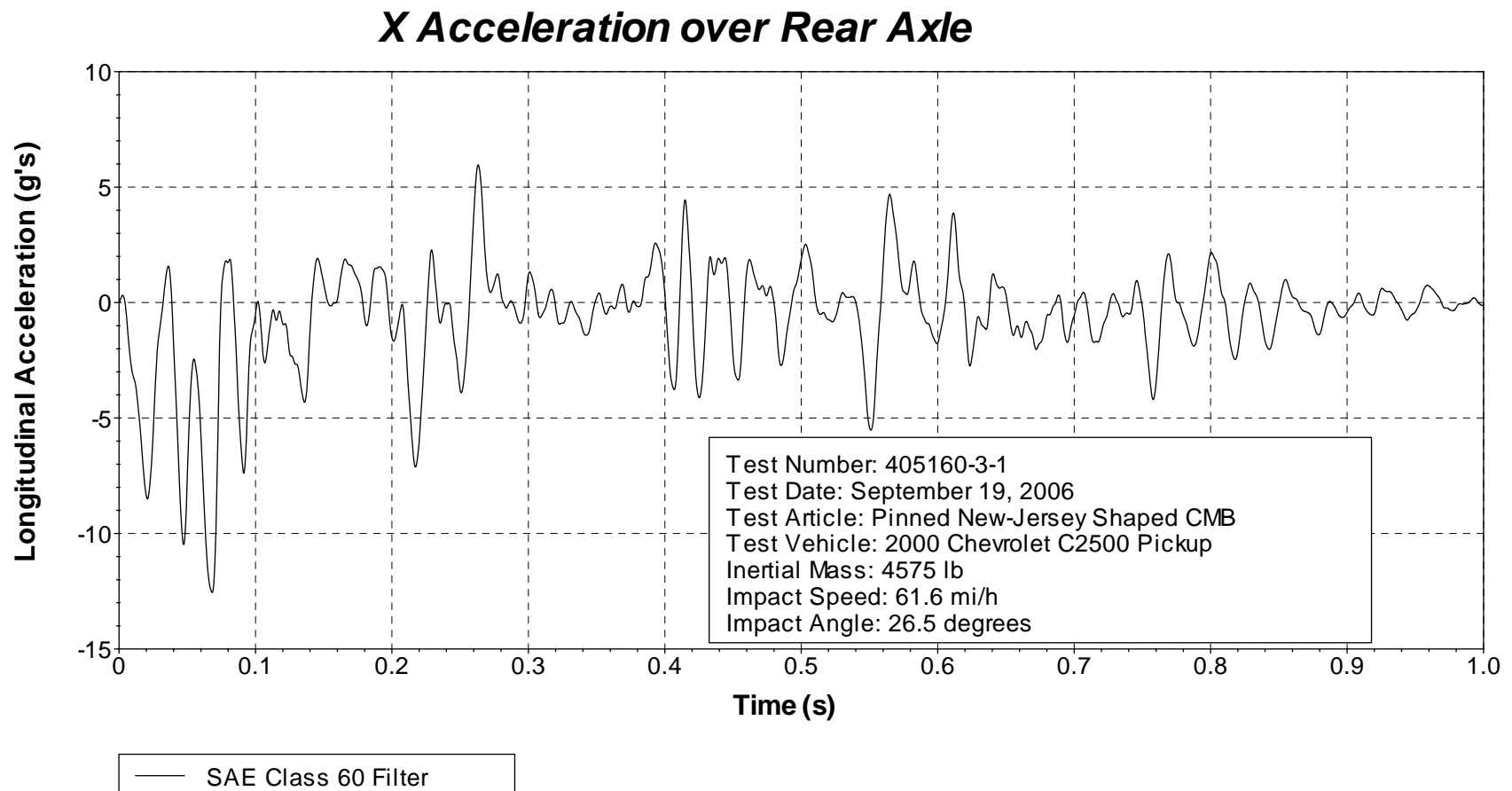


Figure D5. Vehicle longitudinal accelerometer trace for test 405160-3-1
(accelerometer located over rear axle).

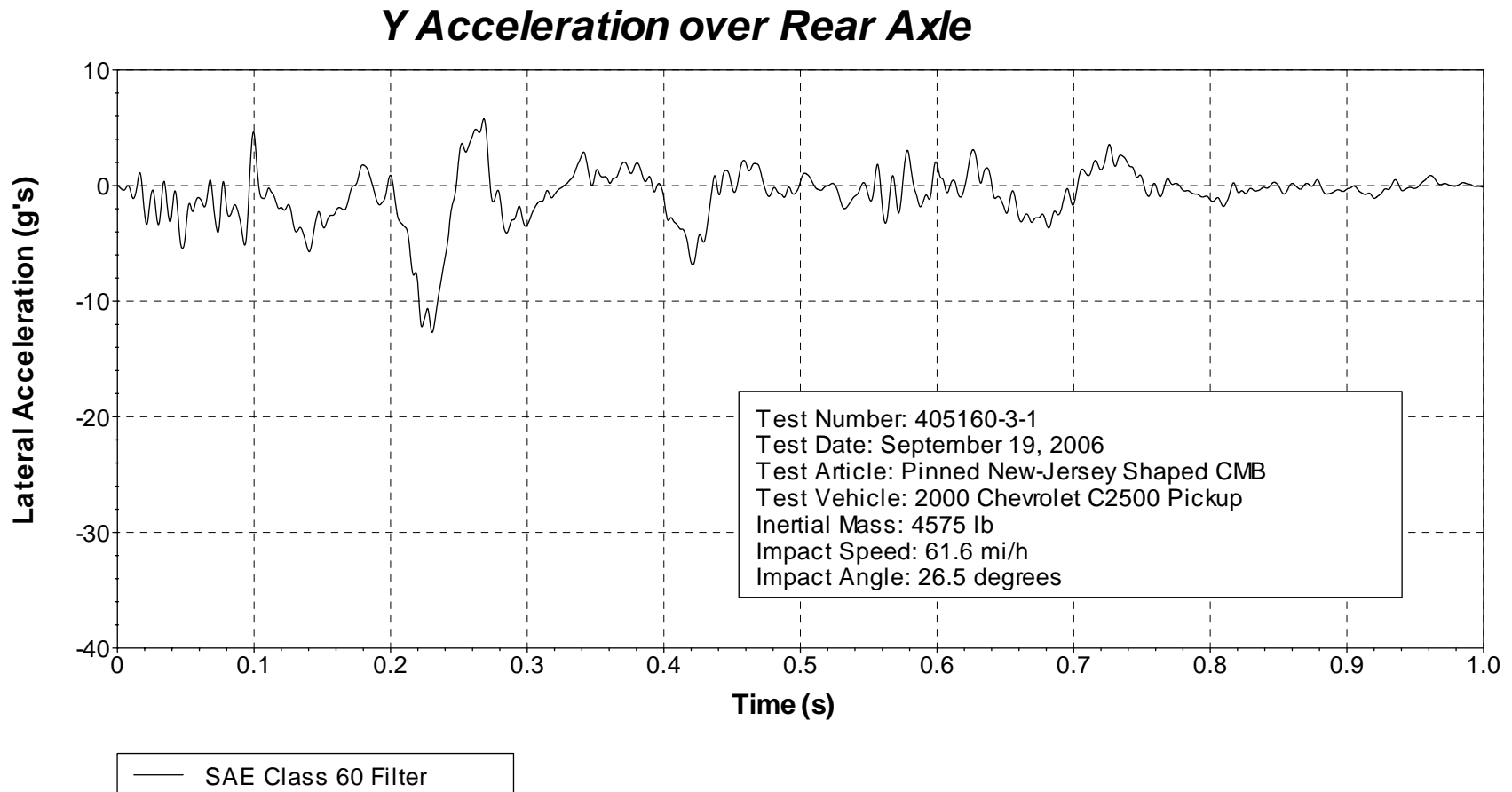


Figure D6. Vehicle lateral accelerometer trace for test 405160-3-1 (accelerometer located over rear axle).

Z Acceleration over Rear Axle

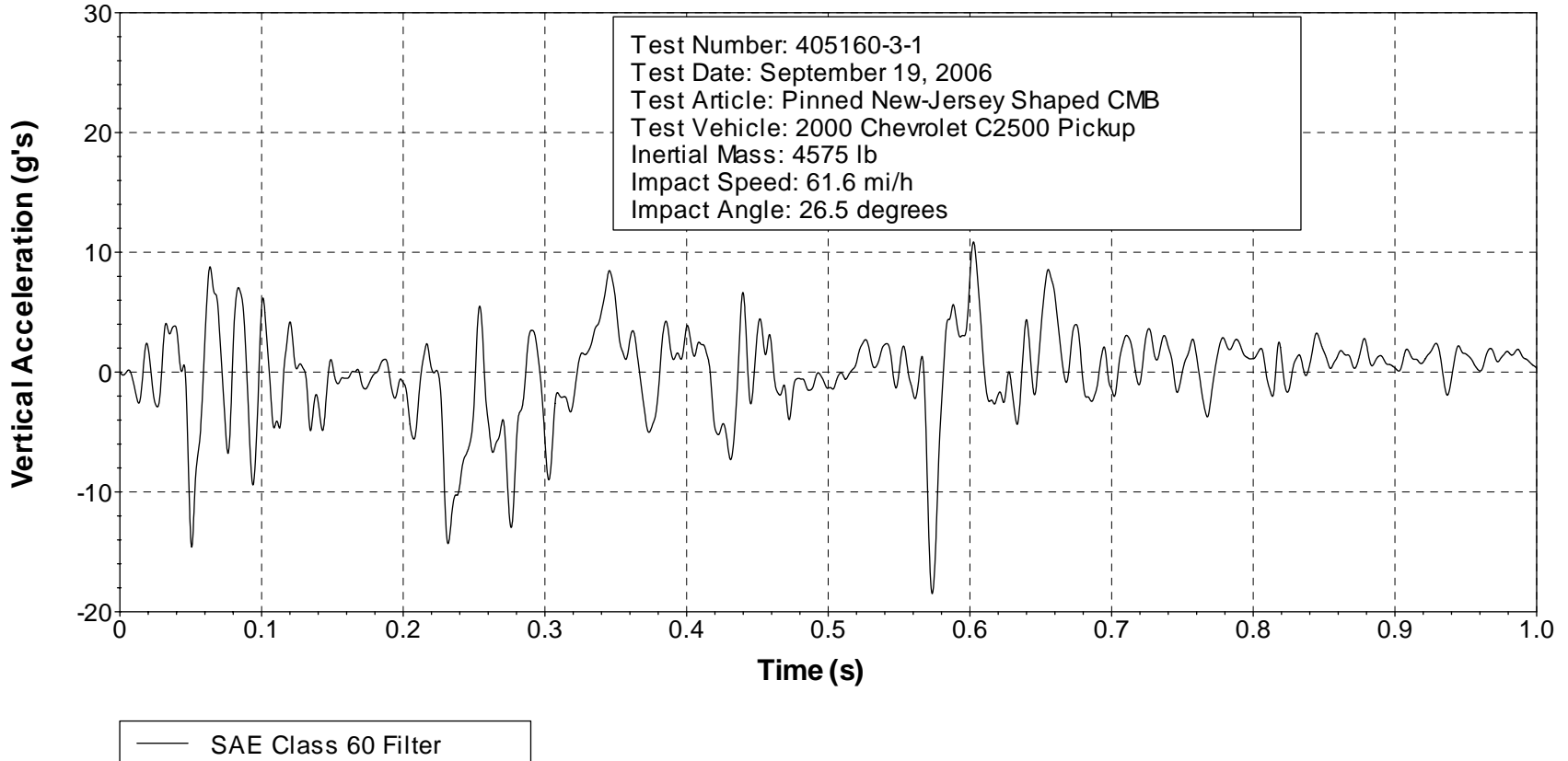
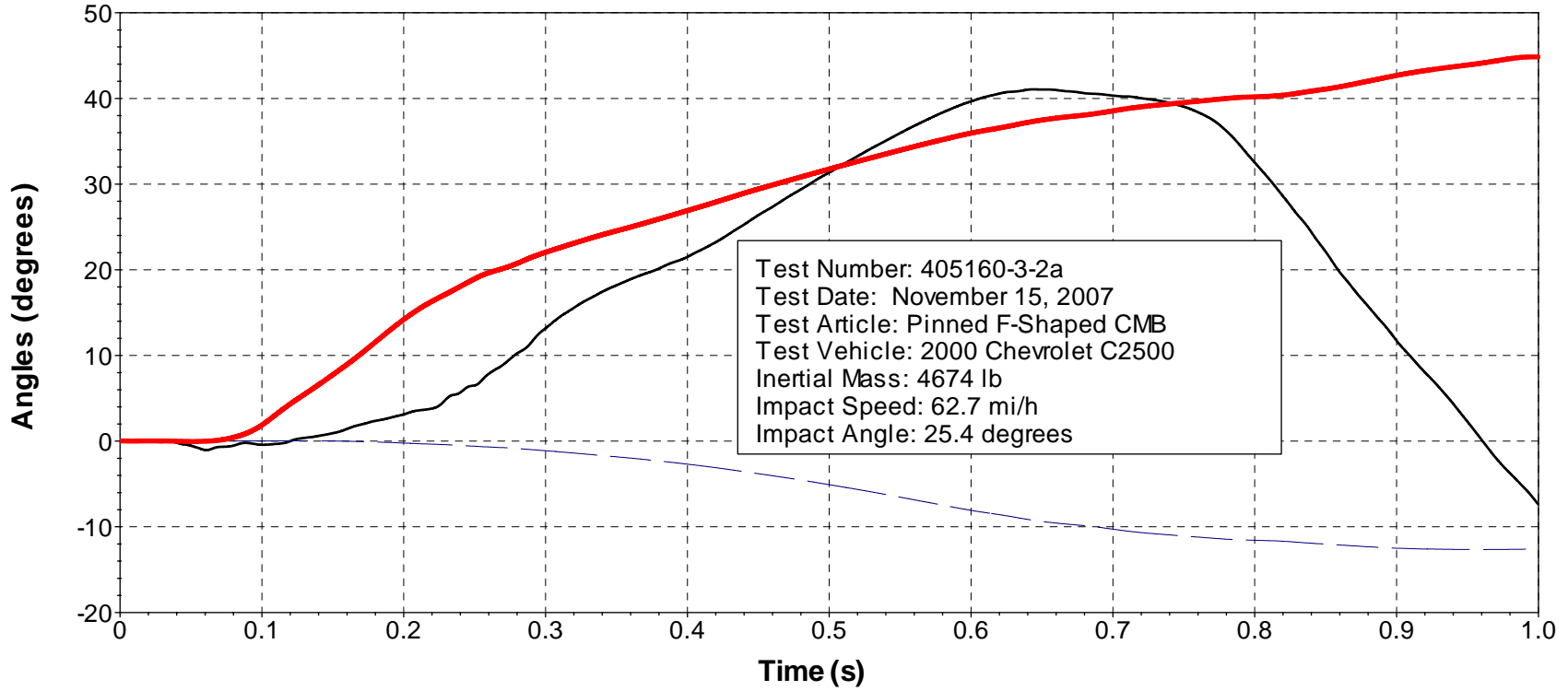


Figure D7. Vehicle vertical accelerometer trace for test 405160-3-1 (accelerometer located over rear axle).

Roll, Pitch, and Yaw Angles



Test Number: 405160-3-2a
 Test Date: November 15, 2007
 Test Article: Pinned F-Shaped CMB
 Test Vehicle: 2000 Chevrolet C2500
 Inertial Mass: 4674 lb
 Impact Speed: 62.7 mi/h
 Impact Angle: 25.4 degrees

— Roll - - - Pitch — Yaw

Axes are vehicle-fixed.
 Sequence for determining orientation:

4. Yaw.
5. Pitch.
6. Roll.

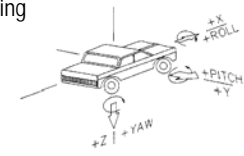


Figure D8. Vehicle angular displacements for test 405160-3-2a.

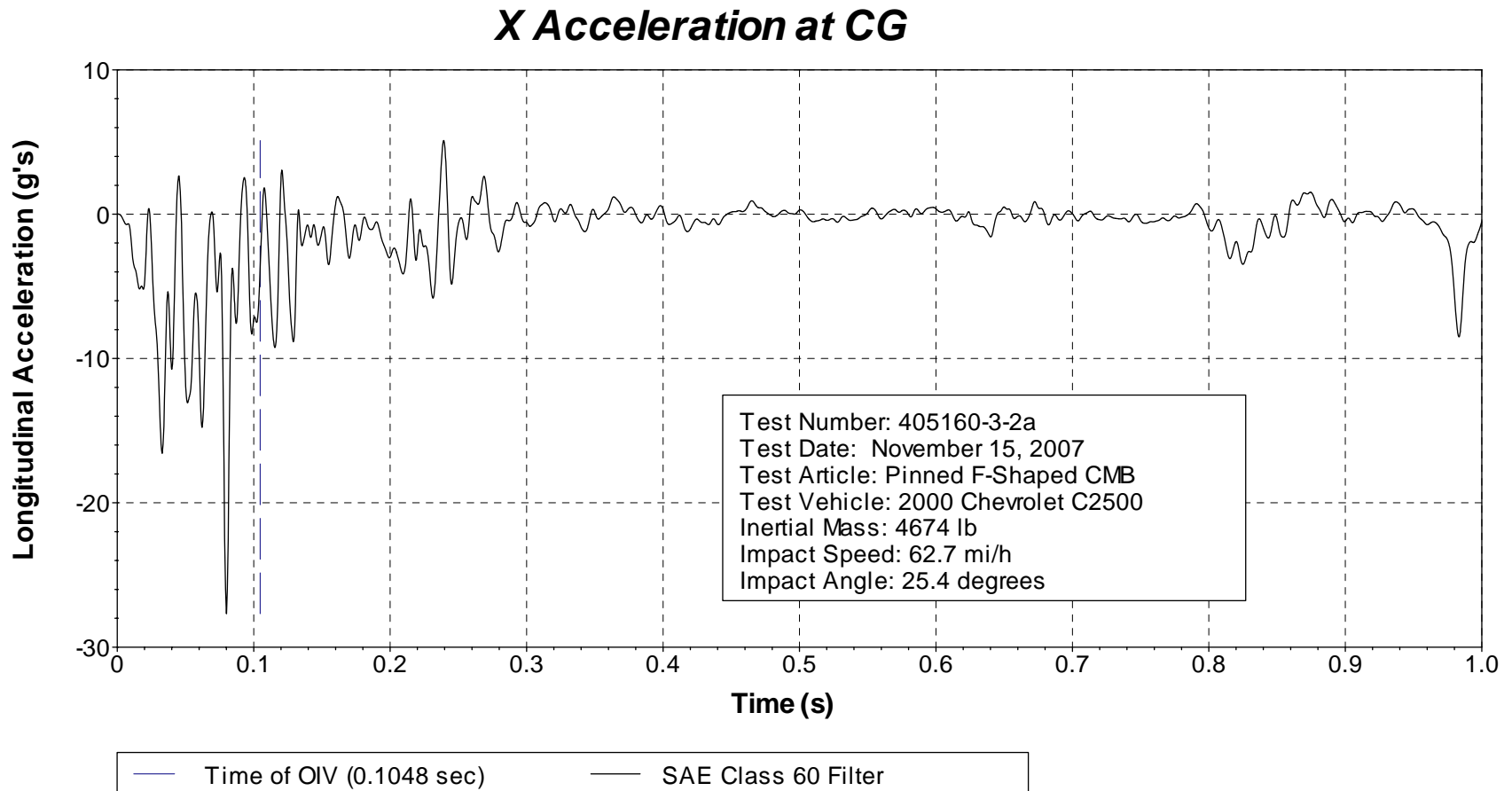


Figure D9. Vehicle longitudinal accelerometer trace for test 405160-3-2a (accelerometer located at center of gravity).

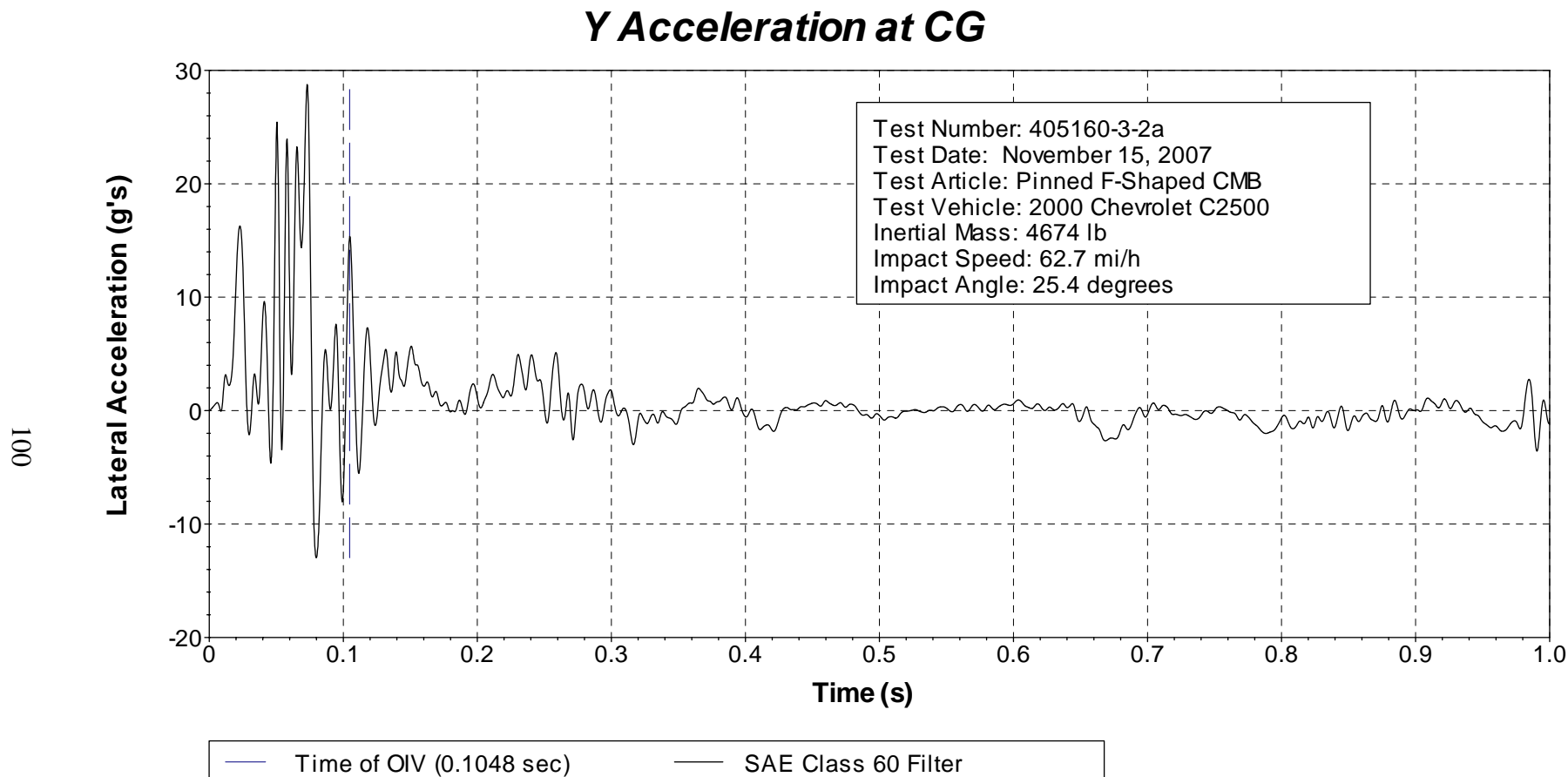


Figure D10. Vehicle lateral accelerometer trace for test 405160-3-2a (accelerometer located at center of gravity).

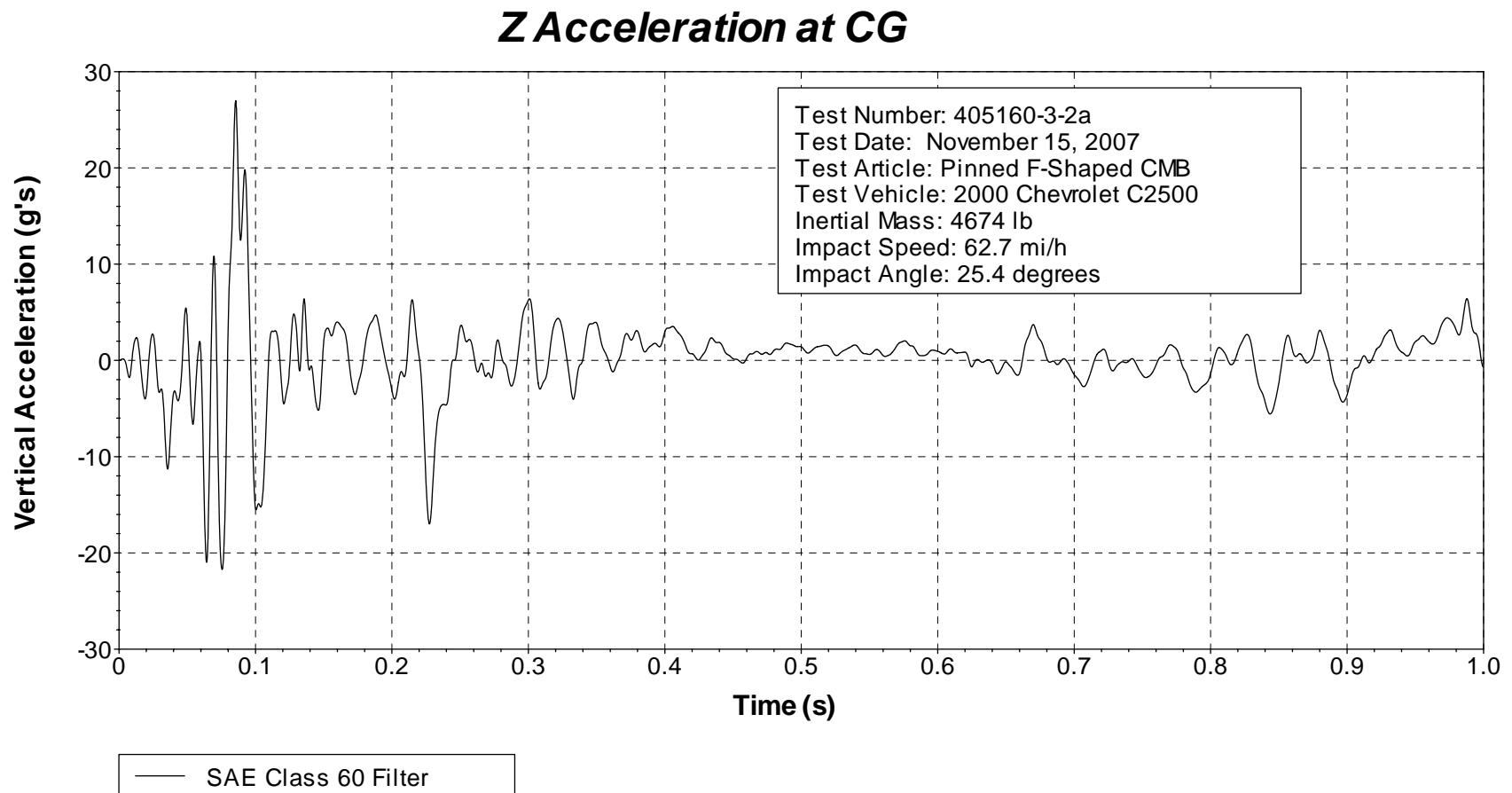


Figure D11. Vehicle vertical accelerometer trace for test 405160-3-2a (accelerometer located at center of gravity).

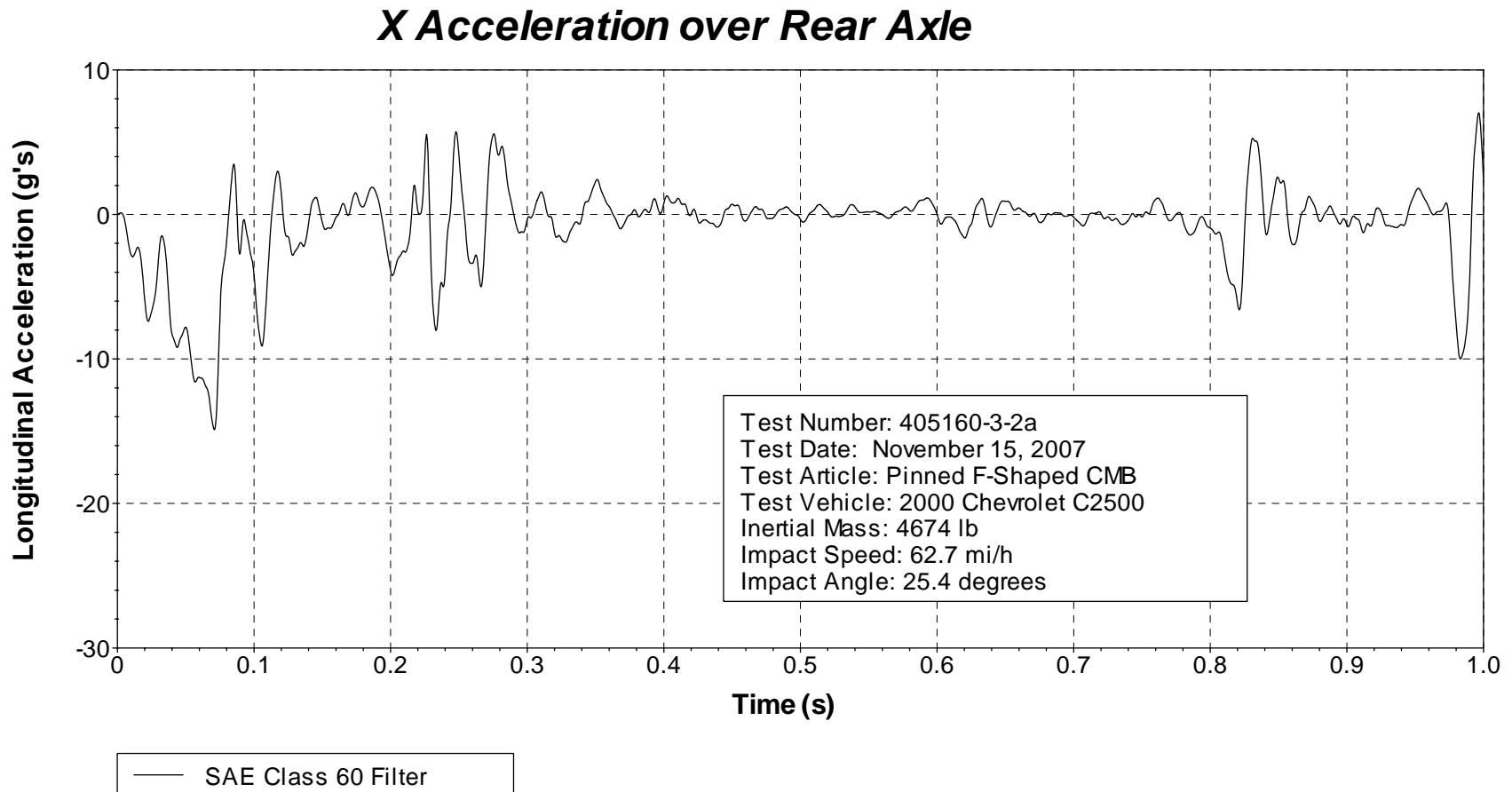


Figure D12. Vehicle longitudinal accelerometer trace for test 405160-3-2a
(accelerometer located over rear axle).

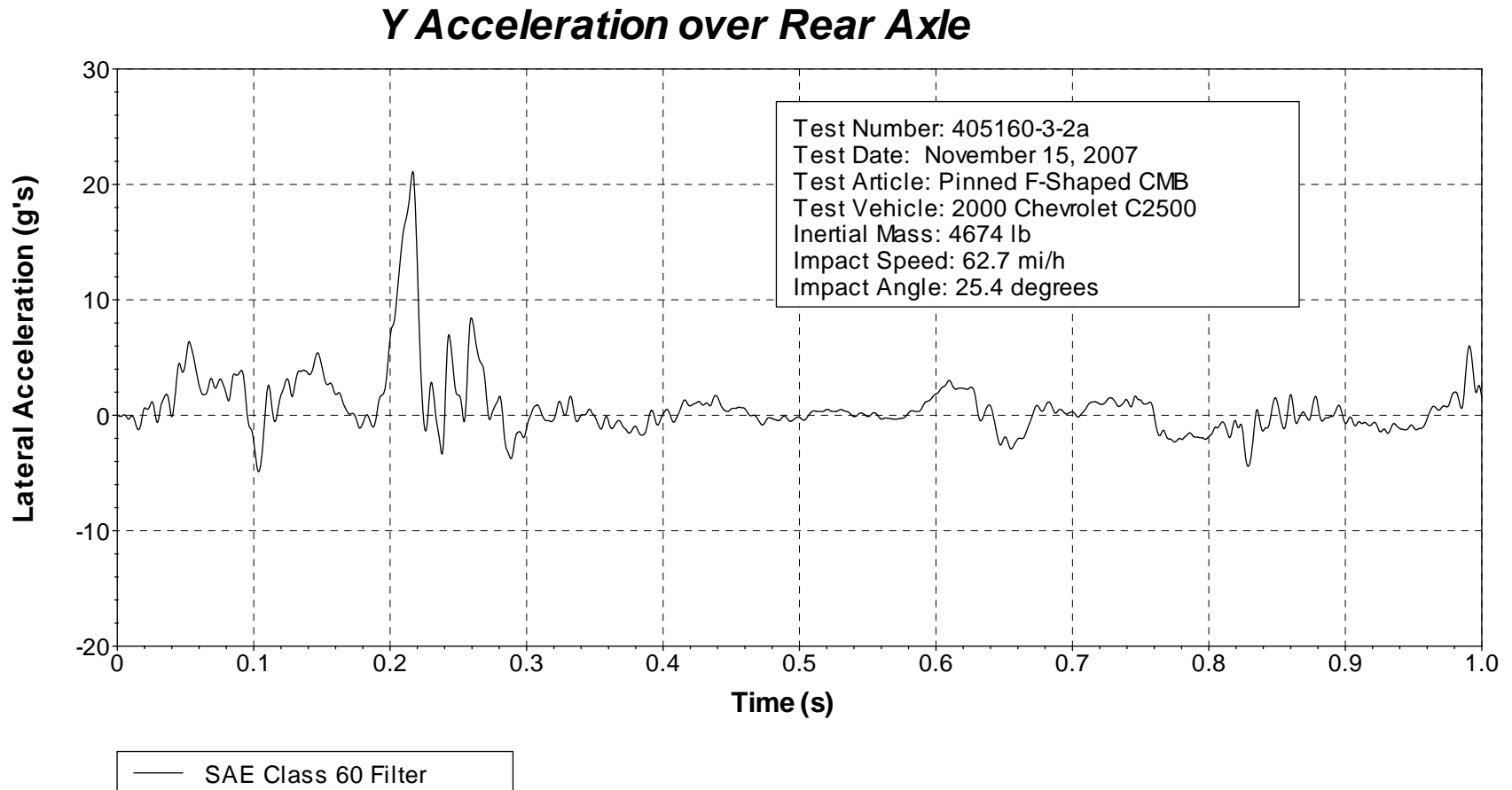


Figure D13. Vehicle lateral accelerometer trace for test 405160-3-2a (accelerometer located over rear axle).

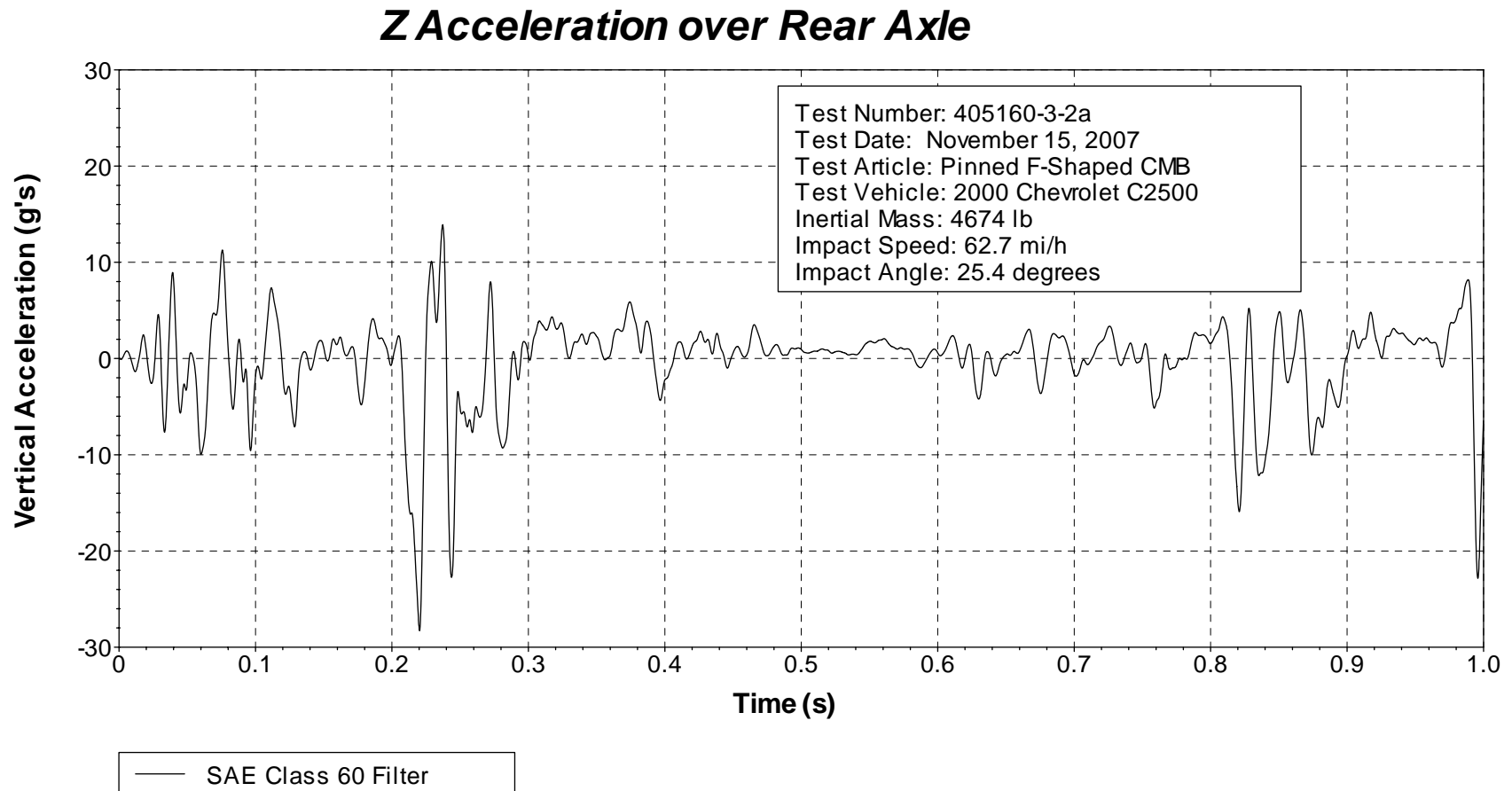


Figure D14. Vehicle vertical accelerometer trace for test 405160-3-2a (accelerometer located over rear axle).